Proposals for realization and signatures of anyons

Todorić, Marija

Doctoral thesis / Disertacija

2021

Degree Grantor / Ustanova koja je dodijelila akademski / stručni stupanj: **University of Zagreb, Faculty of Science / Sveučilište u Zagrebu, Prirodoslovno-matematički fakultet**

Permanent link / Trajna poveznica: https://urn.nsk.hr/urn:nbn:hr:217:895920

Rights / Prava: In copyright/Zaštićeno autorskim pravom.

Download date / Datum preuzimanja: **2024-07-16**

FACULTY OF SCIENCE
DEPARTMENT OF PHYSICS

Marija Todorić

PROPOSALS FOR REALIZATION AND SIGNATURES OF ANYONS

DOCTORAL DISSERTATION

Zagreb, 2021

FACULTY OF SCIENCE
DEPARTMENT OF PHYSICS

Marija Todorić

PROPOSALS FOR REALIZATION AND SIGNATURES OF ANYONS

DOCTORAL DISSERTATION

Supervisors:
prof. dr. sc. Hrvoje Buljan
doc. dr. sc. Dario Jukić

Zagreb, 2021

University of Zagreb

PRIRODOSLOVNO-MATEMATIČKI FAKULTET
FIZIČKI ODSJEK

Marija Todorić

PRIJEDLOZI REALIZACIJE I POTPISA ANYONA

DOKTORSKI RAD

Mentori:
prof. dr. sc. Hrvoje Buljan
doc. dr. sc. Dario Jukić

Zagreb, 2021.

Acknowledgements

Summary

Keywords: anyons, fractional statistics, integer quantum Hall effect, metamaterials, synthetic gauge fields, ultracold atoms, geometric phases, topological phases, Bose gases, hard-core bosons.

In three spatial dimensions, particles are classified into bosons and fermions. Bosons have integer spin and obey Bose-Einstein statistics, while fermions have half-integer spin and obey Fermi-Dirac statistics. In two-dimensional systems, particles with properties continuously interpolating from bosons to fermions are theoretically allowed to exist and they are called anyons. Anyons are characterized by a fractional spin, or more generally, by fractional quantum numbers. Apart from the fundamental interest, the main motivation for studying anyons comes from their potential importance in fault-tolerant topological quantum computing.

The work presented in this thesis contributes to the study of less traditional schemes for realization and manipulation of anyons. The first part focuses on new mechanisms for the realization and signatures of anyons in non-interacting systems. We propose an experimental realization of the original Wilczek's model for Abelian anyons. This proposal is implemented in two-dimensional electron gas placed in a perpendicular magnetic field which gives rise to the integer quantum Hall effect. Then we present exact solutions of a model for synthetic anyons in a non-interacting quantum many-body system. The model is represented by the Hamiltonian for non-interacting electrons in two dimensions, in a uniform magnetic field, pierced with specially tailored localized probes, solenoids with a magnetic flux that is a fraction of the flux quantum. Here we show that synthetic anyons cannot be considered as emergent quasiparticles. The second part of the thesis concentrates on a system of one-dimensional bosons coupled to synthetic gauge fields. In particular, we investigate a system of strongly interacting bosons placed on a one-dimensional ring pierced by a synthetic magnetic flux tube. An external localized delta-function potential barrier is placed on the ring and we explore the Berry phase associated to its adiabatic motion. The barrier produces a cusp in the density, where we show that the corresponding missing charge cannot be identified as a quasihole. This result is associated with the previous studies of synthetic anyons in non-interacting systems.

Contents

Chapter 1

Introduction

1.1   Introduction to fractional statistics

Quantum statistics has a fundamental theoretical importance in the quantum mechanical view of the world. Namely, the physical behaviour of collections of identical particles is governed not only by interactions but also by the particle statistics. Identical particles are those particles whose Hamiltonian is symmetric under exchange of one particle with the other, assuming they have identical intrinsic properties [1]. Contrary to classical physics, where we can always follow each particle at any time, in quantum mechanics there is no trajectory. Since one is not able to track identical particles separately, they are considered to be indistinguishable. This fact imposes definite symmetry requirements on the many-body wave function describing a system of many identical particles under interchange of any two particles. In three dimensions [(3+1)D] only two symmetries are possible and particles are classified into bosons and fermions depending on the statistics they obey. Bosons follow the Bose-Einstein and fermions the Fermi-Dirac statistics [1]. While Fermi and Bose formulated their theories in terms of the occupation number, i.e., the number of particles which may occupy the same energetic level, Dirac reformulated this problem in terms of the structure of the many-body wave functions. The wave functions turn out to be symmetric under permutations of identical bosons, and antisymmetric under permutations of identical fermions. The symmetry requirements are closely connected with the spin of the particles. According to the spin-statistics connection, bosons are particles with integer spin and fermions with half-integer spin. This connection can be proved by relativistic arguments [2], but in the frame of nonrelativistic quantum mechanics, it is accepted as an empirical postulate.

For a long time, bosons and fermions have been considered to be the only reasonable possibilities. This is true when particles move in at least three dimensions (3D), but in two dimensions (2D) the situation becomes more intriguing. Namely, the quantum statistics turns out to be a continuous interpolation between Bose-Einstein and Fermi-Dirac statistics. Particles which obey any fractional statistics in between are called *anyons* [3–5]. This doctoral thesis deals with

anyons. If one incorporates the concept of the spin-statistics connection, it may be assumed that anyons are represented by a fractional spin, i.e., by fractional quantum numbers. These special cases for spin and statistics were understood in the 1970s, when Leinaas and Myrheim explained that the root of the concept of fractional statistics lies in the special topological properties of the configuration space of collections of identical particles [6]. Most of the great interest that anyons have attracted recently derives from the fact that non-Abelian anyonic quasiparticles of topological states of matter could become the building blocks of fault-tolerant topological quantum computers [7, 8].

1.1.1 Exchange statistics

The concept of exchange statistics refers to the phase that a many-body wave function describing identical particles acquires when any two particles are adiabatically transported giving rise to the exchange [9]. The wave function of two identical hard-core particles with definite angular momentum is given as $\psi(\mathbf{r}_1, \mathbf{r}_2)$. Hard-core condition implies that two or more particles cannot occupy the same point in space. When one particle is moved around another by an azimuthal angle $\Delta\varphi$, as shown in Fig. 1.1, the wave function transforms in the following way:

$$\psi(\mathbf{r}_1, \mathbf{r}_2) \to \psi'(\mathbf{r}_1, \mathbf{r}_2) = e^{i\theta\Delta\varphi}\psi(\mathbf{r}_1, \mathbf{r}_2). \tag{1.1}$$
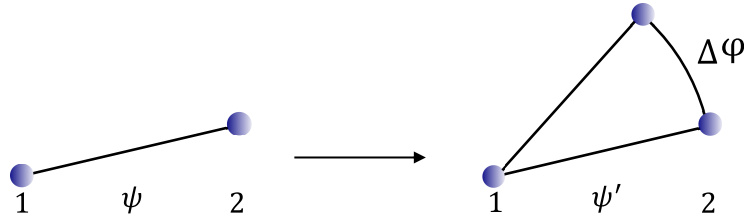
Figure 1.1: Particle 2 moves around particle 1 by an angle $\Delta\varphi$.

The parameter θ denotes the statistics of the particles. The definition where exchange statistics is associated with the phase acquired by the wave function under permutation of the particles, i.e., when all the quantum numbers of the particles are exchanged, is equivalent to the first one in 3D, but in 2D these definitions are different.

1.1.2 Path integrals

The problem of quantum statistics and quantum motion can be studied from the perspective of path integrals in quantum mechanics [10]. The probability amplitude for the system which evolves from the configuration c at time t to the configuration c' at time t' is represented by the propagator [11]

$$P(c', t'; c, t) = \int_{c(t)=c; c(t')=c'} \mathscr{D}c \, e^{\frac{i}{\hbar}\int_t^{t'} d\tau \mathscr{L}[c(\tau), \dot{c}(\tau)]} = \sum_{all\,paths} e^{\frac{i}{\hbar}\int_t^{t'} d\tau \mathscr{L}[c(\tau), \dot{c}(\tau)]}. \tag{1.2}$$

$\int_{c(t)=c;c(t')=c'} \mathscr{D}c$ denotes the sum over all potential paths connecting space-time points c at time t to c' at time t' and $\mathscr{L}(c,\dot{c})$ the Lagrangian density for the $N-$particle system. M_N^d is the configuration space of N identical hard-core particles moving in d dimensions. Then the propagator $P(c',t';c,t)$ evolves the single-valued wave function $\psi(c,t)$ as

$$\psi(c',t') = \int_{M_N^d} dc \langle c',t'|c,t \rangle \langle c,t|\psi \rangle = \int_{M_N^d} dc P(c',t';c,t) \psi(c,t).$$

1.1.3 Quantum statistics

We continue to study the statistics by following [12]. Two points in M_N^d are c and c'. One may select $c = c'$ and define loops in M_N^d. If a continuous deformation converts one loop into the other one, these two loops are homotopic or equivalent. One class consists of all homotopic loops, while the set of all such classes forms the fundamental group π_1. In the set π_1, if α_1 and α_2 refer to two classes with representatives c_1 and c_2, then a product $\alpha_1 \cdot \alpha_2$ denotes the class with the representative loop $c_1 c_2$. If one denotes the homotopic classes by $\alpha \in \pi_1(M_N^d)$, the amplitude $P(c,t';c,t)$ in Eq. (1.2) can be decomposed into a sum of subamplitudes $P_\alpha(c,t';c,t)$, which consists of contributions of homotopic loops, i.e., the amplitude is split into contributions from homotopically inequivalent path sectors labeled by elements on $\pi_1(M_N^d)$. Specifically, the amplitude takes the form [11]

$$P(c,t';c,t) = \sum_{\alpha \in \pi_1(M_N^d)} \chi(\alpha) C_\alpha(c,t';c,t), \tag{1.3}$$

where $\chi(\alpha)$ represent complex weight factors. In order to have the usual rule for combining probabilities

$$P(c'',t'';c,t) = \int_{M_N^d} dc' \langle c'',t''|c',t' \rangle \langle c',t'|c,t \rangle = \int_{M_N^d} dc' P(c'',t'';c',t') P(c',t';c,t),$$

the weights $\chi(\alpha)$ should satisfy for any α_1 and α_2

$$\chi(\alpha_1)\chi(\alpha_2) = \chi(\alpha_1 \cdot \alpha_2), \quad \text{with} \quad |\chi(\alpha_1)| = 1.$$

Interpretation of this statement is that the weight factors of partial amplitudes $\chi(\alpha)$ form a one-dimensional unitary representation of the fundamental group $\pi_1(M_N^d)$ [11].

Therefore, we want to determine M_N^d and its fundamental group [12]. We consider a system of N identical hard-core particles in the Euclidean d-dimensional space $\mathbb{R}^d$. Cartesian product of the one-particle spaces $(\mathbb{R}^d)^N$ specifies a configuration of a system. Hard-core requirement implies that the generalized diagonal has to be eliminated

$$D = \{(\mathbf{r}_1, \ldots \mathbf{r}_N) \in (\mathbb{R}^d)^N : \mathbf{r}_J = \mathbf{r}_K \quad \text{for some} \quad J \neq K\}. \tag{1.4}$$

Moreover, one should identify configurations which are different only in the ordering of the particles because the particles are identical and indistinguishable. Therefore, we divide the configuration space by the permutation group S_N for N identical particles and arrive at the configuration space of our system

$$M_N^d = \frac{(\mathbb{R}^d)^N - D}{S_N}. \tag{1.5}$$

The fundamental group of this space is [13, 14]

$$\pi_1(M_N^d) = \begin{cases} S_N, & \text{if } d \geq 3 \\ B_N, & \text{if } d = 2. \end{cases} \tag{1.6}$$

B_N is Artin's braid group of N objects and the permutation group S_N is a finite subgroup [15, 16] of B_N.

In order to have a better understanding of this result, we limit our discussion to the case of a two-particle system [6]. First we consider particles confined in two dimensions. The centre-of-mass coordinate is $\mathbf{R} = \frac{1}{2}(\mathbf{r}_1 + \mathbf{r}_2) \in \mathbb{R}^2$, and the relative coordinate $\mathbf{r} = \mathbf{r}_1 - \mathbf{r}_2 \in \mathbb{R}^2 - \{\mathbf{0}\}$, where $\mathbf{r}_1$ and $\mathbf{r}_2$ represent the coordinates of two particles. We exclude the singular point $\mathbf{0}$ due to the hard-core condition. The configuration space M_2^2 can be decomposed into a Cartesian product

$$M_2^2 = \mathbb{R}^2 \times r_2^2,$$

of the center of mass space and relative space r_2^2 defining the two degrees of freedom of the relative motion of the two particles. Now we look more closely at the topology of the configuration space r_2^2. If the difference of two configurations is only the ordering of the particle indices, these configurations are indistinguishable. Therefore, the relative space r_2^2 is the plane $\mathbb{R}^2$ where the points $\mathbf{r}$ and $-\mathbf{r}$ are identified. This identification can be achieved if one cuts the plane along a line s from the origin O and then fold it into a cone of half-angle $\pi/6$. The relative space r_2^2 is shown on Fig. 1.2.

In agreement with Eq. (1.1.3), one may categorize loops in M_2^2 by the number of times they wind around the cone r_2^2. If two loops c and c' differ in winding numbers, they are homotopically inequivalent. Namely, since the tip of the cone is removed, one cannot continuously deform one loop into the other. The spaces r_2^2 and $\mathbb{R}^2 \times r_2^2$ are infinitely connected, and

$$\pi_1(M_2^2) = \mathbb{Z} \cong B_2,$$

where $\mathbb{Z}$ is the group of integers under addition. B_2 allows a whole variety of 1D representations and this represents the root of fractional statistics.

Now we put into a consideration the case of two particles in 3D. We introduce the center-of-mass coordinate $\mathbf{R} \in \mathbb{R}^3$ and the relative coordinate $\mathbf{r} \in r_2^3$, where $\mathbf{r}$ and $-\mathbf{r}$ are identified. For
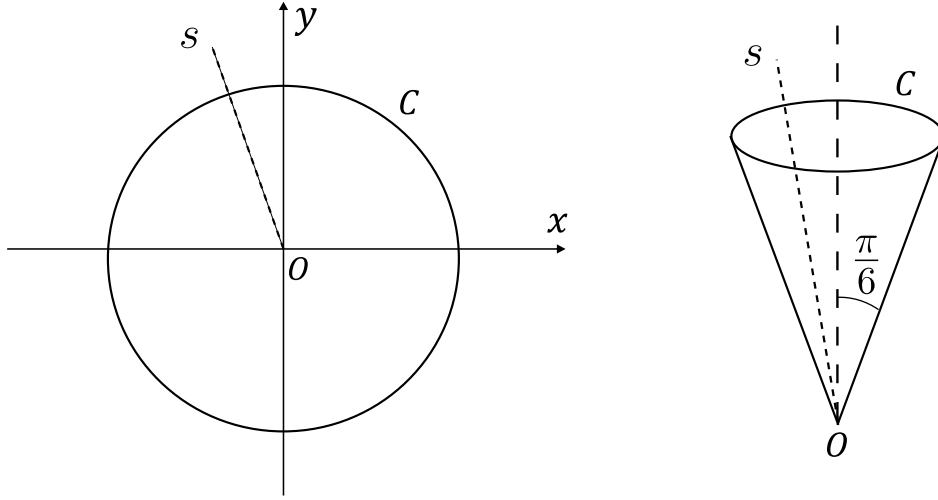
Figure 1.2: The manifold r_2^2 describing the relative coordinate of two identical particles in two dimensions.

the configuration space M_2^3 we can write

$$M_2^3 = \mathbb{R}^3 \times r_2^3.$$

r_2^3 is the product of the semiinfinite line describing $|\mathbf{r}|$ and of the projective space $\mathscr{P}_2$, which defines the orientation of $\pm\mathbf{r}/|\mathbf{r}|$. $\mathscr{P}_2$ can be seen as the hemisphere where the opposite points on the equator are identified.
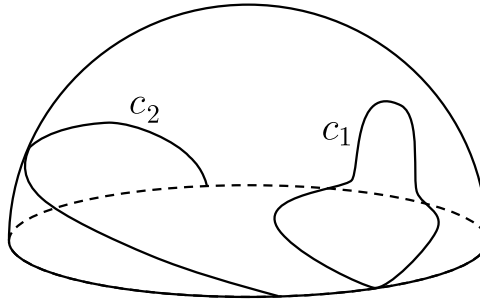
Figure 1.3: The projective space $\mathscr{P}_2$ with the examples of contractible (c_1) and non-contractible (c_2) loops.

$\mathscr{P}_2$ is doubly connected. There are loops (c_1) which can be contracted to a point by a continuous transformation and those which cannot (c_2), as shown in Fig. 1.3. Both curves c_1 and c_2 are closed loops since the two end points on the equator are identified. Since the square of a non-contractible loop is contractible, no other classes are possible. Therefore,

$$\pi_1(M_2^3) = \pi_1(\mathbb{R}^3 \times r_2^3) = \mathbb{Z}_2 \cong S_2,$$

where $\mathbb{Z}_2$ is the cyclic group of order 2, and one can only find bosons and fermions in 3D. Bosons correspond to contractible loops, while fermions correspond to non-contractible loops. As

we have presented, the core of anyonic statistics is the braid group B_N instead of the permutation group S_N. The following subsection will consider the braid group more closely.

1.1.4 Braid group

The braid group B_N on N strands, also known as the Artin's braid group, is an infinite group whose group operation is a composition of braids [15, 16]. It can be represented algebraically in terms of generators σ_i, with $1 \leq i \leq N-1$. Two defining relations satisfied by the generators σ_i of the braid group are

$$\sigma_i \sigma_{i+1} \sigma_i = \sigma_{i+1} \sigma_i \sigma_{i+1} \quad 1 \leq i \leq N-1, \tag{1.7}$$

and

$$\sigma_i \sigma_j = \sigma_j \sigma_i \quad |i-j| \geq 2.$$

σ_i^{-1} denotes the inverse of σ_i, and $\mathbb{1}$ is identity. In order to describe the generators σ_i, we represent the elements graphically. As shown in Fig. 1.4 (a), the generator σ_i acts on N ver-
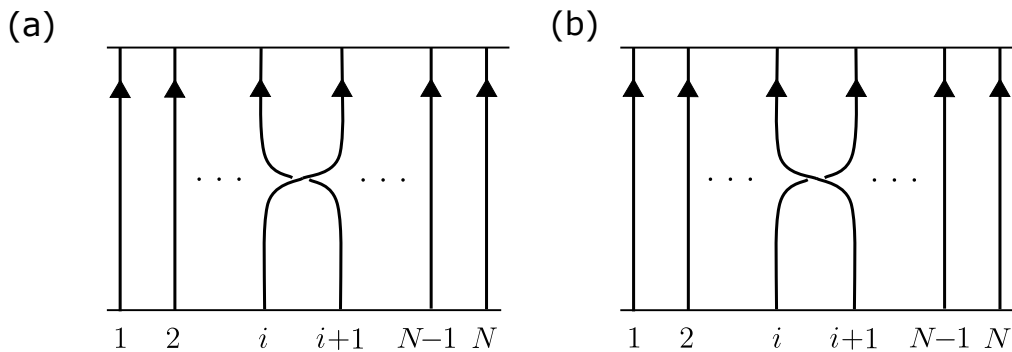
Figure 1.4: (a) Graphical representation of the elementary move σ_i. (b) Graphical representation of the inverse generator σ_i^{-1}.

tical strands by braiding the i-th strand around the $(i+1)$-st in a counterclockwise direction. Fig. 1.4 (b) shows the inverse σ_i^{-1} which acts in a clockwise direction, while Fig. 1.5 represents the braid relation in Eq. (1.7). We point out that generally $\sigma_i^2 \neq \mathbb{1}$. If the equality $\sigma_i^2 = \mathbb{1}$ holds for all i, then the braid group B_N becomes the permutation group S_N. This difference between S_N and B_N leads to the result that the permutation group is finite and the number of elements in the group is $|S_N| = N!$. On the contrary, the braid group is infinite.

1.1.5 Anyons

The braid group B_N is the group of inequivalent paths that arise in the adiabatic transport of N particles. Namely, the elements of the braid group B_N can be uniquely related to the topological classes of paths which take N particles from positions $r_1, \ldots, r_N$ at time t_0 to positions $r_1, \ldots, r_N$ at time t_1. Therefore, one can understand the diagrams of the braid group, such as diagrams in
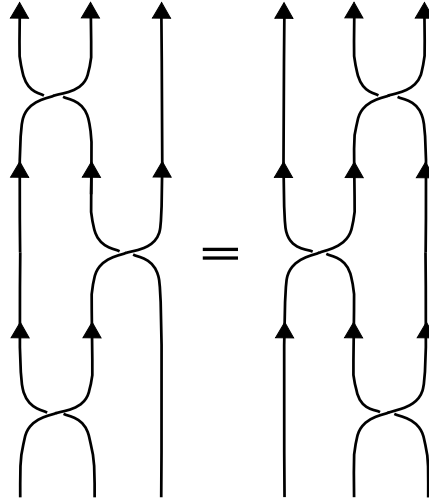
Figure 1.5: Graphical representation of the braid relation $\sigma_i\sigma_{i+1}\sigma_i = \sigma_{i+1}\sigma_i\sigma_{i+1}$.

Fig. 1.4 and Fig. 1.5, as they describe the time evolution of identical particles if one perceives the strands as world-lines which begin at initial positions and end at final positions. The initial time is at the bottom, while the final time is at the top. Generators of the braid group represent exchanges of neighbouring particles. With this, each set of trajectories of N particles becomes a braid. Group multiplication is defined as following one trajectory by another in time. We can understand that $\sigma_i\sigma_i^{-1} = \mathbb{1}$ and $\sigma_i^N \neq \mathbb{1}$, which is why any statistics is allowed in 2D.

Now we determine how the braid group operates on the states of the quantum system. A 1D representation is related to scalar quantum mechanics when the wave functions are one-component objects. The 1D representation of the braid group B_N is given by

$$\chi(\sigma_i) = e^{i\theta}$$

for any $i = 1,\dots,N-1$, where the phase θ is a real parameter defined mod 2. θ may be *any* arbitrary number because of $\sigma_i^2 \neq 1$. Therefore, particles with *any* exchange statistics governed by the braid group have been called *anyons* [3–5]. In the elementary move σ_i, the wave function accumulates the phase θ when the i-th particle is exchanged with the $(i+1)$-st in a counterclockwise manner. Specific cases of anyons with $\theta = 0$ and π correspond to bosons and fermions. We point out that these representations are Abelian.

Exchange statistics described by higher-dimensional irreducible representations of the braid group gives rise to non-Abelian anyons and non-Abelian braiding statistics [17]. Such representations appear when the wave functions are multiplets, i.e., when there is a degenerate set of l quantum states. The i-th element of the braid group is represented by a $(l \times l)$-dimensional unitary matrix $\rho(\sigma_i)$. Such matrix defines unitary transformation within the subspace of degenerate ground states. If two matrices $\rho(\sigma_i)$ and $\rho(\sigma_{i+1})$ do not commute, the particles obey non-Abelian braiding statistics, and the braiding of particles gives rise to nontrivial rotations in the degenerate Hilbert space.

1.1.6   Fusion of anyons

When N identical Abelian anyons with individual statistics θ are brought close together, they can be approximated as a single anyon with statistics $N^2\theta$. Namely, if two such composite anyons are rotated counterclockwise, there are N^2 pairs of individual anyons. Each pair contributes a phase $e^{i\theta}$. An analogous analysis applies to the fusion of different Abelian anyons. In general, since a system with anyonic particles provides various types of anyons, a complete characterization of such a system includes also other possible higher particle types. Abelian anyons composed by building successively larger composites of θ particles obey the fusion rule $n^2\theta \times m^2\theta = (n+m)^2\theta$. When considering non-Abelian anyons, different combinations of topological quantum numbers are possible, and they are named fusion channels. If $\times$ represents the fusion, we may formally write

$$\phi_a \times \phi_b = \sum_c M_{ab}^c \phi_c,$$

which means that, if a particle of type a fuses with the other of type b, the product may be a particle of type c when $M_{ab}^c \neq 0$. Here ϕ_c symbolizes all anyons in a representative set, while M_{ab}^c is called the fusion multiplicity of the occurence of anyon ϕ_c. The non-negative integers M_{ab}^c denote the fusion rules of the system. When considering Abelian anyons, the fusion multiplicities are $M_{ab}^c = 1$ for single value of c, while $M_{ab}^{c'} = 0$ for all other $c' \neq c$. In case of non-Abelian anyons, there is always at least one a, b so that various fusion channels c with $M_{ab}^c \neq 0$ arise. A broader review of fusion for non-Abelian anyons can be found in [7, 18]. In this thesis we focus on Abelian anyons.

1.2   Quantum mechanics of a charged particle in an electromagnetic field

1.2.1   Classical charged particle in an electromagnetic field

In the framework of classical electrodynamics, a charge q of mass m behaves in an electromagnetic field according to the spatial and temporal dependence of the electric $\mathbf{E}(\mathbf{r},t)$ and magnetic $\mathbf{B}(\mathbf{r},t)$ fields, which satisfy Maxwell equations. The fields $\mathbf{B}$ and $\mathbf{E}$ can be defined in terms of the vector potential $\mathbf{A}(\mathbf{r},t)$ and scalar potential $\phi(\mathbf{r},t)$ as [19]

$$\mathbf{B} = \nabla \times \mathbf{A} \tag{1.8}$$

$$\mathbf{E} = -\nabla\phi - \frac{\partial \mathbf{A}}{\partial t}. \tag{1.9}$$

The potentials are not uniquely defined by these equations. Namely, we are free to impose extra conditions on ϕ and $\mathbf{A}$ as long as $\mathbf{E}$ and $\mathbf{B}$ are unchanged. The fields $\mathbf{E}$ and $\mathbf{B}$ remain unchanged

if the potentials are transformed together using a scalar function $\chi(\mathbf{r},t)$,

$$\mathbf{A} \to \mathbf{A}' = \mathbf{A} + \nabla\chi \tag{1.10}$$

$$\phi \to \phi' = \phi - \frac{\partial\chi}{\partial t}. \tag{1.11}$$

This transformation is called a gauge transformation, and the invariance of the field under such transformations gauge invariance. Lagrangian for a charge in an electromagnetic field is

$$L(\mathbf{r},\dot{\mathbf{r}}) = \frac{1}{2}m\dot{\mathbf{r}}^2 - q\phi + q\dot{\mathbf{r}}\cdot\mathbf{A}. \tag{1.12}$$

Euler-Lagrange equations lead to an equation of motion which depends only on the fields $m\ddot{\mathbf{r}} = q(\mathbf{E}+\dot{\mathbf{r}}\times\mathbf{B})$. Lagrangian in Eq. (1.12) gives the canonical momentum $\mathbf{p}$,

$$\mathbf{p} = \nabla_{\dot{\mathbf{r}}}L = \pi + q\mathbf{A}, \tag{1.13}$$

where $\pi = m\dot{\mathbf{r}}$ represents the kinetic momentum. A Legendre transformation is used to obtain the Hamiltonian for a charged particle in an electric and magnetic field

$$H(\mathbf{r},\mathbf{p}) = \mathbf{p}\dot{\mathbf{r}} - L = \frac{1}{2}m(\mathbf{p}-q\mathbf{A})^2 + q\phi. \tag{1.14}$$

This equation proposes the principle of minimal substitution - the Hamiltonian for a charged particle of charge q in an external electromagnetic field and an external potential $V(\mathbf{r},t)$ can be derived from the Hamiltonian for an uncharged particle by using the substitutions

$$\mathbf{p} \to \mathbf{p} - q\mathbf{A}(\mathbf{r},t), \quad V(\mathbf{r},t) \to V(\mathbf{r},t) + q\phi(\mathbf{r},t). \tag{1.15}$$

1.2.2 Quantum charged particle in an electromagnetic field

In quantum mechanics, the position $\mathbf{r}$ and canonical momentum $\mathbf{p}$ are related to the operators $\hat{\mathbf{r}}$ and $\hat{\mathbf{p}}$. In order to make the transition to quantum mechanics, we perform the standard substitution $\hat{\mathbf{p}} = -i\hbar\nabla_{\mathbf{r}}$, so that the quantization rule

$$[\hat{r}_j, \hat{p}_k] = i\hbar\delta_{jk}, \tag{1.16}$$

holds for any $j,k \in \{x,y,z\}$ [1]. The Schrödinger equation for a charged particle in an electromagnetic field is

$$i\hbar\frac{\partial\psi}{\partial t} = \frac{1}{2m}[-i\hbar\nabla - q\mathbf{A}(\mathbf{r},t)]^2\psi + q\phi(\mathbf{r},t)\psi,$$

where $\psi(\mathbf{r},t)$ is the wave function, which is gauge dependent. Schrödinger equation is invariant if one simultaneously applies the gauge transformation of the potential as in Eq. (1.11) and the

local phase transformation of the wave function

$$\psi(\mathbf{r},t) \rightarrow \psi'(\mathbf{r},t) = e^{i\frac{q}{\hbar}\chi(\mathbf{r})}\psi(\mathbf{r},t). \tag{1.17}$$

1.2.3   Aharonov-Bohm phase

In classical electrodynamics, electromagnetic fields are the physical quantities affecting the motion of a particle, while potentials $\mathbf{A}$ and ϕ are considered as unphysical. However, potentials become basic parts of the physical formalism in quantum mechanics. In quantum mechanics their presence can be directly measured even if particles have never passed through the place of non-zero electromagnetic field.

This is the subject of the Aharonov-Bohm effect. Namely, if a quantum charged particle travels along a path $\mathscr{P}$, such that the magnetic field is zero $\mathbf{B} = \nabla \times \mathbf{A} = 0$ and the vector potential $\mathbf{A}$ is non-zero, the wave function obtains a phase [1]

$$\phi = \frac{q}{\hbar}\int_{\mathscr{P}} \mathbf{A} \cdot d\mathbf{r}.$$

Originally, Aharonov and Bohm considered two electronic wavepackets encircling a magnetic field that is confined to an inaccessible and infinitely long flux line of magnetic flux Φ [20]. By using Stoke's theorem, the wavepackets acquire a relative phase of

$$\phi_{AB} = \frac{q\Phi}{\hbar}, \tag{1.18}$$

and this phase, known as the Aharonov–Bohm phase, can be observed through interference effect when they close the loop. The Aharonov–Bohm phase is topological since it does not depend on the shape, or more generally, geometric characteristics of the path. Provided that the particle moves in a field-free region, it is determined only by its topological invariants. This phase emphasizes the unique role of electromagnetic potentials in quantum mechanics. It is a particular case of the Berry geometric phase acquired when a quantum system is adiabatically transported around a cyclic circuit in the parameter space, which we additionally address in Section 2.1.

1.3   Realizations of anyons

1.3.1   Wilczek's anyons

In this section we consider the prototype for anyons introduced by Frank Wilczek. He proposed a physical picture of a charged particle interacting with an infinitely long magnetic solenoid [3–5]. This system has been named a cyon [21]. In the following, it will be shown that Wilczek's anyon may obey fractional statistics. In the framework of non-relativistic quantum mechanics,

we consider a spinless particle of mass m and electric charge q. The particle is exposed to the magnetic field **B** of a cylindrically symmetric, infinitely long and thin solenoid placed at the origin and aligned along the z−axis where Φ is the magnetic flux through the solenoid. If one excludes the motion along the solenoid, the dynamics is confined to the xy-plane and the particle, with the position vector $\mathbf{r} = x\hat{x} + y\hat{y}$, orbits around the solenoid. In a symmetric gauge, the vector potential **A** of the solenoid is given by

$$\mathbf{A}(\mathbf{r}) = \frac{\Phi}{2\pi}\left(\frac{-y}{x^2+y^2}\hat{x} + \frac{x}{x^2+y^2}\hat{y}\right), \tag{1.19}$$

where $\hat{x}$ and $\hat{y}$ are the unit vectors. The magnetic field is $B = \Phi\delta^{(2)}(\mathbf{r})$. In order to find the orbital angular momentum of a particle, we use the following physical argument. When there is no current in the solenoid, the orbital angular momentum is quantized as an integer in units $l_z \in \mathbb{Z}$ [3]. According to the Faraday's law, when a current is slowly increased, the charged particle will be exposed to the electric field

$$\mathbf{E} = -\frac{\dot{\Phi}}{2\pi|\mathbf{r}|}\hat{z} \times \mathbf{r}.$$

This produces the change in angular momentum $\dot{l}_z = [\mathbf{r} \times (q\mathbf{E})]_z = -\frac{q}{2\pi}\dot{\Phi}$. Therefore, the total change in angular momentum is $\Delta l_z = -q\Phi/2\pi$. Accordingly, the quantized angular momenta l_z become

$$l_z = m - \frac{q\Phi}{2\pi}, \quad m \in \mathbb{Z}.$$

The same result can be obtained in a different way. Covariant angular momentum $l_z = -i\hbar\partial/\partial z - qA_\phi$ generates rotations around z-axis. The vector potential (1.19) expressed in cylindrical coordinates outside the solenoid is

$$A_\phi(r) = \frac{\Phi}{2\pi r},$$

and the azimuthal dependence of the electron wave function is $\psi_n \propto e^{in\phi}$, where $n \in \mathbb{Z}$ because of continuity. Then we have $l_z\psi_n = (n - q\Phi/2\pi)\psi_n$, confirming the previous conclusion.

When the distance between the charged particle and the solenoid is reduced to zero, one may consider this system as a single composite object - a charge-flux-tube composite, which can have any fractional angular momentum. This angular momentum is called the spin of the charge-flux-tube composite [3–5]. Assuming there is a generalized spin-statistics connection, we expect that these composites have fractional statistics due to the fractional angular momentum. In order to determine its statistical properties, now we study the quantum mechanics of two such composites. We assume that two such composites are described by a symmetric wave function ψ, and such wave function ψ is single-valued, i.e.,

$$H\psi = E\psi, \tag{1.20}$$

and
$$\psi(\mathbf{r}_1, \mathbf{r}_2) = \psi(\mathbf{r}_2, \mathbf{r}_1).$$

We suppose that the electrostatic forces are small and can be treated as a perturbation, i.e., we consider the limit $q \to 0$, where $q\Phi$ is fixed. We neglect interactions between charges and interactions between vortices. Now we slowly move one composite around the other on the closed loop. According to Aharonov and Bohm [20], when the first particle moves around the second solenoid on a closed loop Γ, a phase acquired by the wave function is

$$\gamma = \exp\left(-i\frac{q}{\hbar}\int_\Gamma \mathbf{A} \cdot d\mathbf{r}\right) = \exp\left(-\frac{iq\Phi}{\hbar}\right).$$

However, when the particles are rotated around each other, the same phase arises from the motion of quantum-mechanical solenoid which orbits around a fixed charge. Therefore, the total phase acquired by the wave function $\psi(\mathbf{r}_1, \mathbf{r}_2)$ is

$$\exp\left(-\frac{2iq\Phi}{\hbar}\right). \tag{1.21}$$

Taking into account these assumptions and approximations, this system can be described by the following Hamiltonian

$$H = \frac{1}{2m}\sum_{i=1}^{2}\left[\mathbf{p}_i - 2q\sum_{j\neq i}^{2}\mathbf{A}(\mathbf{r}_i - \mathbf{r}_j)\right]^2, \tag{1.22}$$

where the vector potential is

$$\mathbf{A}(\mathbf{r}_i - \mathbf{r}_j) = \frac{\Phi}{2\pi}\frac{\hat{z}\times(\mathbf{r}_i - \mathbf{r}_j)}{|\mathbf{r}_i - \mathbf{r}_j|^2}.$$

From Eq. (1.21) and Eq. (1.1), one concludes that the statistics of the composite is

$$\nu = -\frac{2q\Phi}{h},$$

implying that Wilczek's composites behave as anyons. The statistics ν and the spin s of the composite are related as $\nu = 2s$, satisfying the usual spin-statistics connection.

Now we show that fractional statistics can be described by complicated boundary conditions which replace the effective interaction [22]. This is usually called the anyon gauge description of fractional statistics. To eliminate the long-range vector potential between anyons, we perform a singular gauge transformation so that

$$\mathbf{A} \to \mathbf{A}' = \mathbf{A} - \nabla\Lambda(r, \varphi), \quad \text{where} \quad \Lambda(r, \varphi) = \frac{\Phi}{2\pi}\varphi. \tag{1.23}$$

The gauge potential vanishes completely and the Hamiltonian (1.22) becomes

$$H = \sum_{i=1}^{2} \frac{1}{2m} \mathbf{p}_i^2.$$

The transformed wave function is

$$\psi' = e^{-iq\Phi\varphi_{12}/\pi\hbar}\psi, \tag{1.24}$$

where φ_{12} is the azimuthal angle of the relative vector $\mathbf{r}_1 - \mathbf{r}_2$. The wave function ψ' is multi-valued and satisfies the boundary condition

$$\psi'(\mathbf{r}_2, \mathbf{r}_1) = e^{-iq\Phi/\hbar}\psi'(\mathbf{r}_1, \mathbf{r}_2). \tag{1.25}$$

From Eq. (1.25) we see that ψ' carries an Abelian representation of the braid group, implying that ψ' is an anyonic wave function. In the system of N composites, the transformed wave function (1.24) becomes

$$\psi' = \prod_{i<j}^{N} e^{-iq\Phi\varphi_{ij}/\pi\hbar}\psi, \tag{1.26}$$

where φ_{ij} is the azimuthal angle of the relative vector $\mathbf{r}_i - \mathbf{r}_j$. This wave function may also be written in a way which is more practical for applications. For each particle we introduce the complex coordinates $z_I = x_I + iy_I$ and $\bar{z}_I = x_I - iy_I$. One can notice that $z_{IJ} = |z_I - z_J|e^{i\varphi_{IJ}}$, so Eq. (1.26) can be written as

$$\psi' = \prod_{I<J} (z_I - z_J)^{-q\Phi/\pi\hbar} f(z_I, \bar{z}_I), \tag{1.27}$$

where $f(z_I, \bar{z}_I) = \psi \prod_{I<J} |z_{IJ}|^{q\Phi/\pi\hbar}$ is a single-valued function of the particle positions. In case when all the fields describing the solenoid and charged particle are bosonic, $f(z_I, \bar{z}_I)$ is symmetric in the pairs $(z_I, \bar{z}_I)$. On the contrary, if charged particle is fermionic, $f(z_I, \bar{z}_I)$ is antisymmetric. The general form of the wave function in Eq. (1.27) is the rule for many-body wave functions following ν statistics.

1.3.2 Physical realizations of anyons

So far we have demonstrated that anyonic braiding statistics is theoretically possible in 2D. Now we present several candidates for physical realizations of particles with anyonic properties. The most important anyonic physical objects are the quasielectron and quasihole excitations of 2D systems of electrons in a strong magnetic field exhibiting the fractional quantum Hall effect (FQHE) [23–25]. The manifestation of the FQHE is a plateau in the Hall conductivity at $\sigma = \nu e^2/h$, where the filling factor ν is a fraction. These plateaus of quantized resistance

indicate where the 2D electron gas (2DEG) acts as an incompressible fluid, implying that all charged excitations have a finite energy gap. For a fractional filling $v = 1/m$ for m odd, the charge of the quasielectron or a quasihole turns out to be $e^* = \mp e/m$, while the statistics of these Abelian anyons is $\theta = 1/m$ [26–28].

According to the theoretical predictions, non-Abelian anyons arise in FQHE at specific filling fractions [29–40]. This was first discovered for the $v = 5/2$ state [29], while the following work anticipated non-Abelian anyons at other filling fractions such as $v = 12/5$ [30]. The braiding properties of the non-Abelian quasiparticles were derived for filling fractions $v = 5/2$ [36] and $v = 12/5$ [37]. This subject will be explained more thoroughly in the subsection 2.2.5.

Theoretical proposals of anyons based on emulating the FQHE have been reported in ultracold atomic gases [41, 42]. Moreover, it was shown that non-Abelian potentials which act on ultracold gases with two hyperfine levels can lead to ground states with non-Abelian anyonic excitations [43]. Different mechanisms to achieve FQH states of light have also been proposed [44, 45].

Apart from the systems inspired by the FQHE, there are other proposals of systems that may be able to host fractional braiding statistics. Most of them are based on surface codes for encoding quantum information in the collective state of interacting spins on a surface. Lattice models include Kitaev toric code model defined on a 2D spin lattice [8, 46] where the low energy excitations of the Hamiltonian can be Abelian or non-Abelian quasiparticles. This model is a platform to perform topological quantum computing employing non-Abelian anyons. Physical constructions of this model were proposed using atomic [47–49] and molecular arrays [50]. The minimal variant of the model was experimentally achieved in ultracold atomic gases [51], and with trapped ions applying dissipative pumping processes [52]. Fractional statistics of anyonic excitations in the Kitaev toric model was demonstrated using a photonic quantum simulator [53, 54] and superconducting quantum circuits [55]. Anyons were observed in Kitaev paramagnetic state of the honeycomb magnet RuCl3 [56]. There are also other methods to construct spin lattice models, which encode the fusion rules of anyons [57, 58]. In one such model, known as the string-net model, Levin and Wen [59, 60] built an exactly solvable model of spins which is a non-Abelian generalization of Kitaev's toric code model. This model is a realization of a non-Abelian phase supporting Fibonacci anyons, which allows universal topological quantum computation. A simulation of this model by using nuclear magnetic resonance has been reported [61].

Another paradigm od anyonic systems includes Majorana zero modes. Non-abelian anyons called Ising anyons [62–64] appear as quasiparticles or defects supporting a Majorana zero mode in several model systems which could be implemented in real many-body systems. Their observation has been reported in solid state nanowire devices, as well as a proposal for their manipulation in solid state system and cold atom-molecular system (for a review see [64]).

In addition to the localised excitations of an interacting quantum Hamiltonian, anyons can arise as defects in an ordered system [65, 66]. Some of these less traditional schemes for real-

izing anyons in condensed matter experiments are worth mentioning [67–69]. It was proposed that anyons could be synthesized by coupling weakly interacting electrons to a topologically nontrivial background, or noninteracting electrons to topologically nontrivial external perturbations [67–69]. Another scheme is by using topological defects in graphene [70].

Anyons [71–79] in 1D have also stirred up interest, especially in 1D optical lattices [76–79]. In anyon-Hubbard model anyons emerge as low-energy elementary excitations [76–79] from occupation-dependent hopping amplitudes, which could be realized by using laser-assisted tunneling [76, 78], or Floquet modulation [79].

1.3.3   Topological quantum computing

In recent years there has been a surge of interest in anyons, driven by the possibility of using non-Abelian anyons as a resource for topological quantum computing [7, 62, 80]. Namely, Kitaev proposed the idea that the Hilbert space of non-Abelian anyons can be seen as the collection of qubits. In this perspective, the fusion and braiding operations of non-Abelian anyons are the unitary operations that act as quantum gates [8]. The unitary transformations are determined only by the topological class of the braid, and consequently, transformations are fault tolerant. This topological immunity is protected by an energy gap in the system and a length scale. In this scheme the information is not stored locally and the non-local state space is immune to local perturbations. As a result, the qubit encoded there is topologically protected from errors. It is immune to decoherence and other errors which damage calculations since this noise arises from local interactions. This approach to fault-tolerant quantum computation where the unitary quantum gates result from the braiding of non-Abelian anyons is known as topological quantum computation [7, 62, 80]. However, there is still a lot to be done until experiments will manage to precisely detect and manipulate anyons for fault tolerant quantum computation [7, 62]. As a consequence, it may be interesting to investigate some less conventional schemes for realization and manipulation of anyons, and this is the primary focus of this thesis.

1.4   Objectives and results

The objective of this research is to investigate new proposals for realization and signatures of anyons. In the first part of this thesis, we consider new mechanisms for the realization of anyons in 2D non-interacting systems exhibiting the integer quantum Hall effect (IQHE). We find that the original Wilczek's model for anyons can be achieved in 2D electron gas placed in a perpendicular magnetic field, which gives rise to the IQHE. Next, we present exact solutions of a model for synthetic anyons in a non-interacting quantum many-body system and show that these synthetic anyons cannot be considered as emergent quasiparticles. In the second part, we turn to the 1D quantum many-body system. The contribution of this part is twofold. This research explores the Berry phase in 1D quantum many-body models coupled to gauge fields,

but also provides deeper understanding of synthetic anyons in non-interacting systems.

In Chapter 2, we explain the concept of the Berry phase and then we review the quantum Hall effect, both integer and fractional. We describe the quasiparticles emerging in FQHE which show anyonic behavior. In Chapter 3 we consider new mechanisms for the realization and signatures of anyons. We propose an experimental realization of the original Wilczek's model for Abelian anyons, composites formed from charged particles and magnetic flux tubes. This is proposed in a 2D electron system, exhibiting the IQHE, which is sandwiched between two blocks of the high-μ_r material. As the signature of Wilczek's anyons we propose a slight shift of the resistivity at the plateau of the IQHE. Then, we present exact solutions of a model for synthetic anyons in a non-interacting quantum many-body system. This model is represented by the Hamiltonian for non-interacting electrons in two dimensions, in a uniform magnetic field, pierced with solenoids with a magnetic flux that is a fraction of the flux quantum. We show that these synthetic anyons cannot be considered as emergent quasiparticles. Chapter 4 deals with a system of 1D bosons coupled to synthetic gauge fields. We review the physics of 1D interacting bosonic systems. We investigate a particular system of strongly interacting bosons placed on a 1D ring pierced by a synthetic magnetic flux tube. An external localized delta-function potential barrier is placed on the ring. We study the Berry phase associated to the adiabatic motion of the delta-function barrier around the ring as a function of the strength of the potential and the number of particles. We show that the barrier produces a cusp in the density to which one can associate a missing fractional charge, and this missing charge cannot be identified as a quasihole. Finally, in Chapter 5 we summarize.

Chapter 2

Anyons and the quantum Hall effect

2.1 Berry phase

Berry phase is a subject which should be reviewed before we describe anyons in the quantum Hall effect. The cyclic evolution of external parameters in physical system generates a phase which depends only on the geometry of the path taken in parameter space, i.e., the phase does not depend on the velocity at which different parts of the path are traversed. This phase is called the geometric phase [81–83]. Geometric phase was predicted in different fields of physics [84], and the most remarkable example comes from classical electromagnetism where Pancharatnam studied consecutive changes in the polarization of a light beam transmitted through a sequence of crystal plates [85]. The geometric phase was independently discovered by Longuet-Higgins in the framework of molecular electronic degeneracies [86].

The idea of quantum geometric phase was generalized by Michael Berry in 1984 [87]. In quantum system where the external parameters are slowly changing and which is exposed to a cyclic adiabatic evolution, there is a nontrivial geometric phase that depends on the details of the evolution path. This phase is called the Berry phase. It is an Abelian geometric phase, and it refers to the adiabatic cyclic evolution of non-degenerate quantum states. In the following years, the subject of geometric phase was further generalized. Namely, Wilczek and Zee removed the restriction to non-degenerate states by studying a cycle which includes a set of N states that are degenerate for all points on the cycle, yielding non-Abelian phases [88]. Furthermore, Aharonov and Anandan removed the restriction to slow cycles by rephrasing the geometric phase in terms of a circuit in the projective quantum Hilbert space of states, rather than of the space of the Hamiltonian's parameters [89]. Next step was a research explaining that the evolution of the quantum system has to be neither cyclic nor unitary [90].

A classical analogue of the geometric phase is the Hannay angle [91]. Hannay studied the case of non-chaotic dynamics, where motion for fixed parameters is oscillatory and described by angles. When the parameters in the system are slowly cycled, final angle is different from the one acquired when calculated from the instantaneous frequency. This difference is called

the Hannay angle and it depends on the geometry of the cycle. An example of the Hannay angle is the precession of a Foucault pendulum.

2.1.1 Derivation of the Berry phase

In the following, we will derive a general expression for a Berry phase in an adiabatic process. First, let us consider a quantum system described by a Hamiltonian $H = H(\mathbf{x}, \mathbf{R})$, which depends on two different kinds of variables [83, 87]. The $\mathbf{x}$ are degrees of freedom of the system, while $\mathbf{R} = (R_1, R_2, ...)$ represents the set of parameters describing the environment. We want to solve the time-dependent Schrödinger equation

$$i\hbar \frac{\partial}{\partial t} |\Psi\rangle = H(\mathbf{R})|\Psi\rangle, \tag{2.1}$$

with the initial condition $|\Psi\rangle = |\Psi_0\rangle$ for $t = 0$. For a fixed t, the Hamiltonian can be diagonalized as

$$H(\mathbf{R})|\psi_n(\mathbf{R})\rangle = E_n(\mathbf{R})|\psi_n(\mathbf{R})\rangle, \tag{2.2}$$

where we obtain $\mathbf{R}$-dependent orthonormal stationary states and energies, and we assume that the spectrum is non-degenerate for all times. A system governed by cyclic adiabatic evolution is characterized by a time-dependent set of parameters $\mathbf{R}(t)$, which move adiabatically slowly on the closed path C in the space of parameters. In the adiabatic assumption, the initial state is a non-degenerate energy eigenstate of the Hamiltonian, i.e.,

$$|\Psi_0\rangle = e^{i\phi_0}|\psi_n(\mathbf{R}(0))\rangle, \tag{2.3}$$

where ϕ_0 is some phase. According to the adiabatic theorem, if the parameters are varied sufficiently slowly, the system will remain in the instantaneous eigenstate, i.e.,

$$|\Psi(t)\rangle \approx e^{i\phi(t)}|\psi_n(\mathbf{R}(t))\rangle. \tag{2.4}$$

From the time-dependent Schrödinger equation, it follows that the instantaneous eigenstate will accumulate the phase during such evolution,

$$\phi(t) = \phi_0 - \int_0^t \frac{E_n(\mathbf{R}(t'))dt'}{\hbar} + i \int_{\mathbf{R}(0)}^{\mathbf{R}(t)} \langle \psi_n(\mathbf{R})|\nabla_{\mathbf{R}}\psi_n(\mathbf{R})\rangle \cdot d\mathbf{R}.$$

The second term represents the dynamical phase. The third term is characterized by the Berry connection, which is defined as

$$\mathscr{A}^n(\mathbf{R}) = i\langle \psi_n(\mathbf{R})|\frac{\partial}{\partial \mathbf{R}}|\psi_n(\mathbf{R})\rangle.$$

Now we calculate the overlap of the state $|\Psi(t)\rangle$ with the initial state $|\Psi_0\rangle$. We have

$$\langle\Psi_0|\Psi(t)\rangle = e^{i(\phi(t)-\phi_0)}\langle\psi_n(\mathbf{R}(0))|\psi_n(\mathbf{R}(t))\rangle. \tag{2.5}$$

If we write $\langle\psi_n(\mathbf{R}(0))|\psi_n(\mathbf{R}(t))\rangle = r(t)e^{i\delta_n(t)}$ and $\langle\Psi_0|\Psi(t)\rangle = r(t)e^{i\Phi_n(t)}$ for the phase of overlap, we obtain

$$\Phi_n(t) = \delta_n(t) - \int_0^t \frac{E_n(\mathbf{R}(t'))}{\hbar}dt' + i\int_{\mathbf{R}(0)}^{\mathbf{R}(t)}\langle\psi_n(\mathbf{R})|\nabla_{\mathbf{R}}\psi_n(\mathbf{R})\rangle\cdot d\mathbf{R}. \tag{2.6}$$

Now we assume that there exists a time $t = \tau$ for which the Hamiltonian is the same as the initial Hamiltonian, $H(\mathbf{R}(\tau)) = H(\mathbf{R}(0))$. This means that the system has returned to its initial state. We allow that the initial and final parameters differ $\mathbf{R}(\tau) \neq \mathbf{R}(0)$. The stationary states will differ in these two times, but only by a phase, since they represent the same system,

$$|\psi_n(\mathbf{R}(\tau))\rangle = e^{i\Delta_n}|\psi_n(\mathbf{R}(0))\rangle,$$

with $\Delta_n = \delta_n(\tau)$ and $r(\tau) = 1$. Consequentially, we will also have

$$|\Psi(\tau)\rangle = e^{i(\gamma_n+\phi_d(\tau))}|\Psi_0\rangle,$$

with $\phi_d(\tau) = -\int_0^\tau \frac{E_n(\mathbf{R}(t))}{\hbar}dt$ being dynamical phase and

$$\gamma_n = \Delta_n + i\int_{\mathbf{R}(0)}^{\mathbf{R}(\tau)}\langle\psi_n(\mathbf{R})|\nabla_{\mathbf{R}}\psi_n(\mathbf{R})\rangle\cdot d\mathbf{R}, \tag{2.7}$$

which is called the geometric phase.

2.1.2 Invariance of the geometric phase

This geometric phase is invariant under the time reparameterization $\mathbf{R}(t) \to \mathbf{R}(f(t))$, meaning that it does not depend on the velocity we go around the closed path, as long as the adiabatic approximation holds. Moreover, it is invariant under arbitrary phase transformation of the stationary states. Let us use some other basis, which may or may not be single-valued in $\mathbf{R}$,

$$|\psi'_n(\mathbf{R})\rangle = e^{i\lambda(\mathbf{R})}|\psi_n(\mathbf{R})\rangle. \tag{2.8}$$

Since

$$\Delta'_n = \Delta_n + \lambda(\mathbf{R}(\tau)) - \lambda(\mathbf{R}(0)), \tag{2.9}$$

and

$$\langle \psi_n'(\mathbf{R})|\nabla_{\mathbf{R}}\psi_n'(\mathbf{R})\rangle = \langle \psi_n(\mathbf{R})|\nabla_{\mathbf{R}}\psi_n(\mathbf{R})\rangle + i\nabla_{\mathbf{R}}\lambda(\mathbf{R}), \tag{2.10}$$

the two extra contributions cancel in the expression (2.7) for γ_n' and the geometric phase remains the same, i.e., $\gamma_n' = \gamma_n$. Therefore, the Berry phase angle γ_n is gauge invariant. It must be noted that the Berry connection is a gauge-dependent quantity, and consequently does not correspond to an observable. However, the gauge invariant Berry phase angle represents a physical observable [83].

2.1.3 Aharonov-Bohm phase

Previously mentioned Aharonov-Bohm effect shows that in quantum mechanics vector potentials are physically relevant [20]. In the original paper by Aharonov and Bohm, this result was obtained by solving the Schrödinger's equation exactly for scattering in the flux line's vector potential [20]. However, Berry gave an alternative interpretation of the Aharonov-Bohm effect [87]. Aharonov-Bohm phase can be seen as a manifestation of Berry's geometric phase accumulated when a particle of charge q confined to a box is transported around a line of magnetic flux Φ.

The box is placed at position $\mathbf{r} = \mathbf{R}$ and the flux line does not pass through it. When there is no flux, i.e., $\mathbf{A} = 0$, Hamiltonian of the particle is

$$\hat{H} = H(\hat{\mathbf{p}}, \hat{\mathbf{r}} - \mathbf{R}), \tag{2.11}$$

where $\hat{\mathbf{r}}$ is a position and $\hat{\mathbf{p}}$ a conjugate momentum. The wave functions of states $|n(\mathbf{R})\rangle$ localised around $\mathbf{R}$ are $\psi_n(\mathbf{r} - \mathbf{R})$, while energies E_n are independent of $\mathbf{R}$. In the presence of flux, states $|n(\mathbf{R})\rangle$ are solutions of the Schrödinger equation

$$H(\mathbf{p} - q\mathbf{A}(\hat{\mathbf{r}}), \mathbf{r} - \mathbf{R})|n(\mathbf{R})\rangle = E_n|n(\mathbf{R})\rangle. \tag{2.12}$$

It is easy to prove that this equation can be solved exactly if ψ_n is multiplied by Dirac phase factor

$$\psi_n'(\mathbf{r} - \mathbf{R}) = \langle \mathbf{r}|n(\mathbf{R})\rangle = \exp\left(\frac{iq}{\hbar}\int_{\mathbf{r}'=\mathbf{R}}^{\mathbf{r}'=\mathbf{r}} \mathbf{A}(\mathbf{r}')\cdot d\mathbf{r}'\right)\psi_n(\mathbf{r} - \mathbf{R}). \tag{2.13}$$

Next we move the box around a circuit $\mathscr{P}$ which encloses the flux line and calculate the Berry connection

$$\mathscr{A}^n(\mathbf{R}) = i\langle \psi_n'(\mathbf{R})|\frac{\partial}{\partial \mathbf{R}}|\psi_n'(\mathbf{R})\rangle = q\mathbf{A}(\mathbf{R})/\hbar. \tag{2.14}$$

In this case, the Berry connection is identified with the electromagnetic vector potential. This

gives rise to the Berry phase, i.e., the Aharonov-Bohm phase,

$$\gamma_n(C) = \frac{q}{\hbar} \oint_{\mathscr{P}} \mathbf{A}(\mathbf{R}) \cdot d\mathbf{R} = q\Phi/\hbar. \tag{2.15}$$

Here we recognize that the Aharonov-Bohm phase is topological because it does not depend on the geometric properties of the path. It depends only on its topological invariants as long as the particle moves in a region of zero field.

2.1.4 Berry phase as a holonomy

There is a strong connection between geometric phases and the topological structure made by a Hilbert space $\mathscr{H}$ of the quantum system and the space of its parameters $\mathbf{R}$. The name of this topological structure is a vector bundle and it includes the manifold P, which denotes some region of parameter space [92], contained within the space $P \times \mathscr{H}$. Bundle specifies the group of the Hilbert spaces defined for particular values of $\mathbf{R}$, where every space is related to the parameter space P by the wave functions $\psi(\mathbf{R})$ [92, 93]. In geometry, a parallel transport of a tangent vector refers to the transport of the vector along the closed loop in the plane tangent to the surface of the closed surface, where the vector is not allowed to rotate with respect to the normal [93]. An example is the dynamical evolution of the Foucault pendulum, where the tangent vector giving the direction of swinging of the pendulum undergoes a parallel transport along the circle. A connection is an operation describing the way of transporting data such as vectors along a curve in a parallel and consistent manner [93]. When the vector completes a full cycle, it may happen that the vector points in a direction different from its original one. A name of this phenomenon is a holonomy of the connection [93]. The geometric Berry phase precisely corresponds to the holonomy in the Hermitian line bundle over the parameter space [92]. Connections provide a particular way of parallel transport of the wave functions $\psi(\mathbf{R})$ within a vector bundle, i.e., from one Hilbert space in $P \times \mathscr{H}$ to another. The process of parallel transport is possible if a smooth path between both spaces γ is specified, and in quantum mechanics, γ is smooth because of the adiabatic theorem. Parallel transport on a closed path maps a state $\psi(\mathbf{R})$ to $H(\gamma, D)\psi(\mathbf{R})$, where D is a connection and a linear map $H(\gamma, D)$ is the holonomy of the path. The holonomy is the geometric phase acquired by $\psi(\mathbf{R})$. Therefore, the Berry's phase represents an important example of holonomy identified in quantum mechanics [92].

2.2 The quantum Hall effect and anyons

This research is strongly related to the quantum Hall effect (QHE), and here we provide a short review of some important concepts. The FQHE is the most relevant example of anyonic systems [23–25]. Namely, the quasiparticle and quasihole excitations of 2D systems of electrons exhibiting the FQHE are the physical objects which may be described as anyons. In the follow-

ing, we will focus on the application of anyons to the theory of the FQHE (for a review of the QHE, see e.g. [94, 95]).
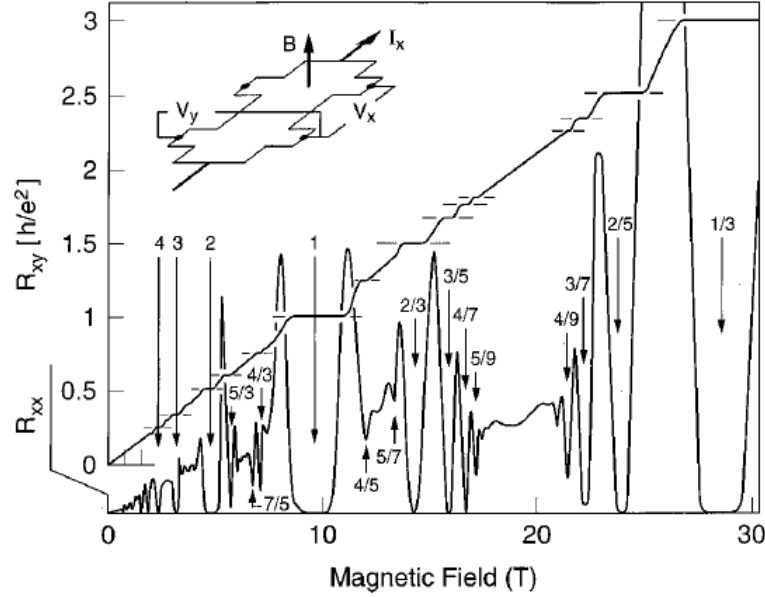
Figure 2.1: The dependence of the Hall resistance $R_{xy} = V_y/I_x$ and the magnetoresistance $R_{xx} = V_x/I_x$ of a 2D electron gas on the magnetic field ($n = 52.333 \times 10^{11} \text{cm}^{-2}, T = 85 \text{mK}$). The filling factors ν are identified for the most important quantum Hall states. R_{xy} shows plateaus quantized to $h/(\nu e^2)$ which are connected with the minima of vanishing R_{xx}. From [J. P. Eisenstein, H. L. Stormer, Science **248**, 1510 (1990) [96]]. Reprinted with permission from AAAS.

The IQHE [97, 98] and the FQHE [23, 25] were discovered in the specific context of semiconductor heterostructures (IQHE in Si MOSFET [97] and FQHE in GaAs-AlGaAs [23] heterojunction), subjected to very strong magnetic fields (~ 10T or even more) while held at millikelvin temperatures ($\sim$ mK). In this effect, a layer of electrons may be trapped at the interface between two semiconductors, known as a heterojunction, or between a semiconductor and an insulator. Conditions of the strong magnetic field and the low temperature block the motion along the direction perpendicular to the layer and restrict dynamics to the plane. Electrons in this layer can be described as a 2D gas with Coulomb repulsion.

The QHE shows that when the magnetic field varies at fixed electron density, the Hall resistance $R_{xy} = V_y/I_x$ does not vary smoothly, as semiclassical theory predicts, but rather remains constant over finite intervals as presented in Fig. 2.1. There are continuous intervals between the plateaus. The Hall conductance σ_{xy} on the plateaus is

$$\sigma_{xy} = \nu \frac{e^2}{h}, \tag{2.16}$$

where the quantum number ν is an integer for the IQHE [97, 98] or a rational number with odd denominator for the FQHE [23, 25]. At the plateaus, the conductance tensor is off-diagonal,

implying that a dissipationless transverse current flows in response to an applied electric field. The Hall coefficient is expressed in terms of fundamental physical quantities, where it can be shown that the quantization rule of the QHE is a topological quantization [99–102]. This relation is experimentally observed with extremely high accuracy at the National Institute of Standards and Technology with relative uncertainty of one part in 10^{10} [103]. The ratio h/e^2 is known as the fundamental unit of resistance, called the von Klitzing constant (R_K) [104].

2.2.1 Landau levels

In order to understand the QHE, we recall the elementary quantum mechanics of charged particles in a constant magnetic field. The Hamiltonian for a single electron of charge e confined to 2D plane in a perpendicular magnetic field is given by

$$H = \frac{1}{2m_b}[\mathbf{p} - e\mathbf{A}(\mathbf{r})]^2.$$

The vector potential $\mathbf{A}$ is given by $\nabla \times \mathbf{A} = \mathbf{B} = B\hat{z}$ and m_b denotes the band mass of the electron. In the presence of a magnetic field, the continuous spectrum of a free particle breaks up into discretely and equally spaced, highly degenerate levels known as Landau levels [1]. The eigenenergies are $E_n = \hbar\omega_c(n+1/2)$, where $\omega_c = eB/m_b$ denotes the cyclotron frequency, and $n = 0, 1, \dots$ the index of the Landau level.

In a symmetric gauge, $\mathbf{A}(\mathbf{r}) = \frac{1}{2}\mathbf{B} \times \mathbf{r}$, a basis of single-particle wave functions in the lowest Landau level (LLL) is

$$\varphi_m(z) = f(z)e^{-\frac{|z|^2}{4l_B^2}},$$

where $z = x + iy$ is a complex coordinate for the electron, and $f(z)$ any holomorphic function. An unnormalized basis of LLL wave functions expressed in terms of monomials is

$$\psi_{LLL,m} = z^m e^{-\frac{|z|^2}{4l_B^2}}, \quad m = 0, 1, 2, \dots \tag{2.17}$$

These states are also the eigenstates of angular momentum. For samples of finite area A pierced by magnetic flux BA, the number of states in each Landau level is

$$\mathcal{N} = \frac{eBA}{2\pi\hbar} = \frac{BA}{\Phi_0} = \frac{A}{2\pi l_B^2},$$

where $\Phi_0 = 2\pi\hbar/e$ is called the quantum of flux and $l_B = \sqrt{\hbar/eB}$ the magnetic length. In the absence of disorder, the single-particle states are degenerate. If one considers many independent electrons, the ground state is obtained by filling up the lowest energy single particle orbitals, with the condition that no orbital is occupied by more than one electron as required by the Pauli principle. The number of filled Landau levels is called the filling factor ν and it plays a central

role in the QHE. It is defined as

$$\nu = \frac{N}{\mathcal{N}} = 2\pi l_B^2 n,\tag{2.18}$$

where $n = N/A$ is the electron density. One can prove that the filling factor is the quantum number appearing in Eq. (6.3), using a rigorous derivation as in [94]. Since all combinations of electrons in the highest partially filled Landau level have the same energy, the many-particle ground state is infinitely degenerate. The special case is at an integral filling factor $\nu = n$, with unique ground state which has a gap to excitations.

2.2.2 Integer quantum Hall effect

In 1980 von Klitzing discovered the IQHE [97]. This phenomenon emerges when ν is integer, i.e., an integer number of Landau levels is completely filled [97, 98]. If the chemical potential lies between the ν-th and $(\nu + 1)$-th Landau levels, the Hall conductivity takes the quantized value $\sigma_{xy} = \nu e^2/h$ while $\sigma_{xx} = 0$. The IQHE can be explained in the context of an independent electron model and it becomes a manifestation of the previously explained Landau quantization for non-interacting electrons in a magnetic field. In the absence of disorder, the single-particle states in Landau levels are degenerate. The many-particle ground state is unique, the system is incompressible and develops a gap to excitations. The many-particle wave function for non-interacting electrons is built as a Slater determinant, antisymmetrized product of N single particle states $\psi_i(x)$, with $i = 1, \ldots, N$ [1]. When electrons are placed in the states of the lowest Landau level $\psi_{LLL,m}$ in Eq. (2.17), the resulting Slater determinant produces an unnormalized state

$$\psi(z_1, \ldots z_N) = \begin{vmatrix} z_1^0 & z_2^0 & \cdots & z_N^0 \\ z_1 & z_2 & \cdots & z_N \\ \vdots & \vdots & \ddots & \vdots \\ z_1^{N-1} & z_2^{N-1} & \cdots & z_N^{N-1} \end{vmatrix} \exp\left(-\sum_{i=1}^{N} \frac{|z_i|^2}{4l_B^2}\right) = \prod_{1 \le i < j \le N}(z_i - z_j)\exp\left(-\sum_{i=1}^{N} \frac{|z_i|^2}{4l_B^2}\right).$$

$$\tag{2.19}$$

The fully antisymmetric polynomial product factor is known as the Vandermonde determinant. In this way, one can obtain the wave function for a completely filled LLL. Although the origin of the IQHE is the opening of a gap, a periodic potential or a finite amount of disorder is needed to build the plateaus. Namely, in the absence of disorder, the calculation of the current gives the classical value of the Hall conductivity $\sigma = ne/B$ with no plateaus [18]. In the presence of a periodic potential or disorder, Landau levels broaden into bands. There are extended states at the centers of bands and localized states at all other places [94]. When the Fermi energy is placed in the region of localized states, a change of the number of electrons only increases or decreases the number of localized states which carry no current. The magnitude of the current is frozen at the value corresponding to the full Landau level, as we can understand by introducing

the impurities continuously from zero. Provided that no extended states cross the Fermi energy when the impurity potentials are introduced, the current stays at the value when the impurities are not present. Laughlin gave a more accurate explanation of the plateau. He demonstrated that the Hall conductivity is quantized at $\sigma_H = ne^2/h$ when the Fermi level lies in the localized states, where n is the number of extended bands under the Fermi level [98]. Thus, when the chemical potential lies in the region of localized states between the centers of the v-th and $(v+1)$-th Landau bands, the Hall conductance has the value $\sigma_{xy} = ve^2/h$, while $\sigma_{xx} = 0$.

2.2.3 Fractional Quantum Hall Effect

In 1982 Tsui, Stormer and Gossard discovered FQHE by observing a plateau at $\sigma = e^2/3h$ [23]. Plateaus at new fractions r of quantum conductance were later observed in the neighborhood of filling factor $v \approx r$. Observed plateaus occur in the following series of fractions

$$r = \frac{n}{2pn \pm 1}.$$

In addition to these fractions, the FQHE has also been detected at $r = 5/2$. According to the IQHE, the plateau at $\sigma = re^2/h$ with fraction r arises because of the opening of a gap at $v = r$. Therefore, there is a motivation to explain why the gaps emerge in a partially filled Landau level, and why they emerge at certain series of odd-denominator fractions. When an integer number of Landau levels is filled and the energy splitting between Landau levels $\hbar\omega_B$ much larger than the scale of the Coulomb energy e^2/l_B, the neglect of Coulomb interactions is justified. However, when the electron density is such that the Landau level is only partially filled, Coulomb interactions become important. While IQHE is achievable with independent electrons, gaps at fractional filling factors are created because of interactions. Therefore, one should consider a more complete problem of interacting electrons. In the absence of interaction, the ground state of each partially filled Landau level is macroscopically degenerate. This degeneracy is broken by Coulomb interaction between electrons, resulting in a spectrum of states with gaps at the filling fractions where quantum Hall states are observed [94].

Laughlin made the first approach to the FQHE at filling fraction $v = 1/m$ in 1983 [25]. When electrons interact through Coulomb repulsion, the ground state can be described precisely by Laughlin's variational wave function for $v = 1/m$

$$\psi_m = \prod_{i<j}(z_i - z_j)^m \exp\left(-\sum_{i=1}^{N} |z_i|^2/4l_B^2\right),$$

up to normalization. Laughlin wave function is known to be an exact ground state for a repulsive ultra-short-ranged model interaction [94].

Here m is an odd integer, and therefore, ψ_m is totally antisymmetric describing ordinary fermions. If m is an even integer, this state can be considered as a quantum Hall state for

bosons. The prefactor $\sum_{i<j}(z_i - z_j)^m$ is analytic, implying that all particles are in the LLL. It has a zero of order m when the points coincide $(z_I = z_J)$, indicating that electrons favor to repel each other in a way that is suitable to minimize the Coulomb interaction. These ground states exist even when there is a disorder that is weak enough compared to the gap to excited states, i.e., $\hbar\omega_B \gg E_{\text{Coulomb}} \gg V_{\text{disorder}}$. It is important to note that Laughlin wave function represents an incompressible quantum liquid, what is the essence of the FQHE [94].

Measurements of many fractions different from $1/m$ implied the presence of a more general structure. In 1989 Jain suggested a theory of composite fermions [105]. A term composite fermion refers to the bound state of an electron and an even number of the flux quanta. In this theory, flux quanta, i.e., vortices, are absorbed by strongly interacting electrons in LLL, transforming electrons into weakly interacting composite fermions in a reduced magnetic field. Therefore, the fractional Hall conductivity is described as a manifestation of the IQHE of such composite fermions [105–108].

2.2.4 Plasma analogy

The approach of plasma analogy gives numerous phenomenological results of the Laughlin wave function [18, 25]. In this approach quantum probability density $|\psi_m|^2$ is understood as a Boltzmann distribution with potential energy U_m,

$$|\psi_m|^2 = e^{-\beta U_m},$$

where

$$\beta U_m = -2m \sum_{i<j}^{N} \log\left(\frac{|z_i - z_j|}{l_B}\right) + \frac{1}{2l_B^2} \sum_{i=1}^{N} |z_i|^2. \tag{2.20}$$

One can recognize that the prefactor of ψ_m leads to the logarithmic terms of U_m, and the exponential to the last term. Potential of a 2D one-component plasma of particles with charge q which move in a neutralizing background of density n_0 is

$$U_{plasma} = -q^2 \sum_{i<j} \log\left(\frac{|z_i - z_j|}{l_B}\right) + \frac{1}{2}\pi n_0 q^2 \sum_{i} |z_i|^2. \tag{2.21}$$

Coulomb interaction in two dimensions between two particles of charge q is expressed in the first term. The second term describes the interaction of the particles with the neutralizing background of constant density n_0.

In the statistical mechanics β is inverse temperature. If in Eq. (2.20) we take β to take

particular value of $\beta = 2/m$, the potential is then

$$U_m = -m^2 \sum_{i<j} \log\left(\frac{|z_i - z_j|}{l_B}\right) + \frac{m}{4l_B^2} \sum_{i=1}^{N} |z_i|^2. \tag{2.22}$$

Since the forms of equations (2.21) and (2.22) are the same, we may look at U_m as the potential of plasma of particles with charge $q = m$ in a neutralizing background of charge density

$$\rho_0 = \frac{1}{2\pi l_B^2}. \tag{2.23}$$

In order to minimise the energy, the plasma tries to neutralize the background charge density. The compensating density of particles n should be $mn = \rho_0$, i.e.,

$$n = \frac{1}{2\pi l_B^2 m}. \tag{2.24}$$

For a state at filling fraction $\nu = 1/m$, this corresponds to the expected density, and it is constant. Laughlin state $m = 1$ agrees with the wave function for a completely filled LLL in Eq. (2.19). Therefore, by employing plasma analogy, we obtain the density in the $\nu = 1$ IQHE, $n = 1/2\pi l_B^2$.

2.2.5 Quasiparticles in the FQH state

Electrons in the FQH regime build an incompressible fluid state which allows localized excitations [25]. In the FQH regime, electrons form an incompressible fluid state that supports localized excitations [25]. Deviations from the density in Eq. (2.24) lead to the creation of localized quasiparticles, quasiholes and quasielectrons, with a gap in the spectrum that is related to the energy cost of a quasiparticle. It can be shown that these excitations have fractional charge and fractional statistics, implying that they are anyons.

In the simplest case, they can be obtained if we insert an infinitesimally thin flux-tube in a nondegenerate state at a point z_0 and then adiabatically increase flux ϕ from zero to one unit, $\phi = 0 \rightarrow \phi = \pm\phi_0 = \pm h/e$, so that the system continues to be an instantaneous eigenstate of the varying Hamiltonian [25]. This creates a vortex or an antivortex. Namely, because of the Faraday law, the change of the flux results in a circular electric field around the point z_0. Depending on the sign of ϕ, the particles will move outwards or inwards, and negative or positive charge will gather around z_0. A gauge transformation can take care of the variation of flux by one quantum ϕ_0, implying that the final state may be regarded as an excited state of the initial Hamiltonian. Originally, it was shown that in the incompressible fluid at filling $\nu = 1/m$ described by ψ_m, the excitation is a quasihole or a quasielectron with charge $e^* = \mp\nu e = \mp e/m$ [25]. More generally, at $\nu = n/(2pn \pm 1)$, the value of the charge is $|e^*| = \nu e = e/(2pn \pm 1)$ [94, 106].

The wave function describing a quasihole excitation above the ground state ψ_m at filling

$\nu = 1/m$ with a quasihole at the point z_0 is given by

$$\psi_m^{h,z_0} = \mathcal{N}_h \prod_i (z_i - z_0) \psi_m, \tag{2.25}$$

where $\mathcal{N}_h$ is a normalization factor [25]. On the other hand, the wave function for the state at $\nu = 1/m$ with a quasielectron at z_0 is

$$\psi_m^{e,z_0} = \mathcal{N}_e \prod_i \left(2l_B^2 \frac{\partial}{\partial z_i} - \bar{z}_0 \right) \psi_m. \tag{2.26}$$

The charge of the excitations of the FQHE can be obtained by applying the plasma analogy directly to Eq. (2.25) and Eq. (2.26) [25]. For the quasihole wave function ψ_m^{h,z_0}, the plasma potential energy is

$$U_{m,h} = -m^2 \sum_{i<j} \log\left(\frac{|z_i - z_j|}{l_B} \right) + \frac{m}{4l_B^2} \sum_{i=1}^N |z_i|^2 - m \sum_i \log\left(\frac{|z_i - z_0|}{l_B} \right).$$

In comparison with Eq. (2.22), we recognize an additional term. This term may be interpreted as interaction of plasma with an impurity having charge 1. Since the charge of an electron in plasma is $q = m$, one concludes that the impurity carries $1/m$ of the charge of electron. In order to preserve the charge neutrality in the system, mobile charges in plasma repel from the impurity (or equivalently, we can define mobile hole charges in plasma which are attracted to the impurity). Consequentially, the effects of the impurity cannot be observed at far distances and this effect is called screening. The free energy of the plasma does not depend on the positions of the impurities. In plasma with particles of charge m, the screening cloud will have a depletion of $1/m$ particles, i.e., the compensating charge is $-1/m$. Therefore, each z_0 corresponds to a quasihole with charge $e^* = -e/m$ [109].

The same result can be obtained by applying the concept of Berry phase in a method which was proposed by Arovas, Schrieffer and Wilczek in 1984 [27]. This method computes also the statistics of the quasiparticles. In this approach the charge of the quasihole is found by calculating the Berry phase of the wave function ψ_m^{h,z_0} as the quasihole position z_0 adiabatically traverses a closed loop, and thereby encloses a flux ϕ. When this phase is identified with the Aharonov-Bohm phase, one can determine the charge of the quasihole.

This approach is also a method to determine the statistics of the quasiparticles. We examine the state with a quasihole at the point z_0 and a quasihole at the point z_1. The wave function is then given as

$$\psi_m^{h,z_0,z_1} = \mathcal{N}_{0,1} \prod_i (z_i - z_0)(z_i - z_1) \psi_m.$$

We consider the case where the quasihole at z_0 adiabatically undergoes a closed loop and the quasihole at z_1 remains fixed. First, one calculates the Berry phase if in its motion z_0 does not encircle z_1. Then, the Berry phase is found if the quasihole at z_1 is contained in the loop.

The difference between these two phases may be interpreted as the statistical effect, where the two quasiholes are exchanged twice. The statistics turns out to be $1/m$, confirming that the quasiparticles and quasiholes are Abelian anyons of fractional statistics $v = 1/m$. As may be seen, the statistics is directly associated with the fraction of electrons composing a quasihole or a quasielectron. The measurement of the fractional charge of quasiparticles in the $v = \frac{1}{3}$ Laughlin state was performed in resonant tunneling experiments [110], and in shot noise experiments [111]. The measurement of the fractional braiding statistics has been reported [28, 110].

2.2.6 Non-Abelian anyons in FQHE

Now we review very briefly more complicated case of non-Abelian anyons in FQHE. The state of $v = 5/2$ Hall plateau is the first FQHE state assumed to be non-Abelian [29]. In 1991 Moore and Read constructed the trial wave function for the state at $v = 5/2$ using a conformal field theory [29]. This construction was generalized by Read and Rezayi to a sequence of non-Abelian states, the sequence of spin polarized states at filling factors $v = 2 + k/(k+2)$ [30], and to other non-Abelian states, which include spin-singlets states [31–33]. It was shown numerically that $v = 5/2$ and $v = 12/5$ ground states have a very good overlap with the exact ground states obtained from the numerical diagonalization of small systems [34, 35]. The braiding behavior of quasiholes of the $v = 5/2$ and $v = 12/5$ states was studied in depth in [36], as well as the behavior of other states in the Read-Rezayi series in [37]. Since the Moore-Read state can be mapped onto a p-wave superconductor of composite fermions [38], this enabled alternative explicit calculations of the non-Abelian exchange statistics of quasiparticles in this state in the context of unpaired, zero-energy Majorana modes related to the vortex cores [39, 40].

Chapter 3

Proposals for realization of anyons

The work presented in this chapter has been published in the following papers:

- M. Todorić, D. Jukić, D. Radić, M. Soljačić, and H. Buljan, *Quantum Hall Effect with Composites of Magnetic Flux Tubes and Charged Particles*, Phys. Rev. Lett. **120**, 267201 (2018).

- F. Lunić, M. Todorić, B. Klajn, T. Dubček, D. Jukić, H. Buljan, *Exact solutions of a model for synthetic anyons in noninteracting systems*, Phys. Rev. B **101**, 115139 (2020).

In the search for the physical realization of anyons, quasiparticle excitations in 2D interacting many-body systems play a major role [7]. A paradigm of quasiparticles with fractional statistics are excitations in the FQHE [23–28]. As explained in subsection 2.2, the manifestation of both the IQHE and FQHE is a plateau in the Hall conductivity at $\nu e^2/h$, where the filling factor ν is an integer for the IQHE, and a fraction for the FQHE. The key ingredients in the FQHE are 2D electrons in a strong uniform magnetic field [23] and Coulomb interactions [24, 25]. In contrast, Coulomb interactions are not needed to explain the IQHE [97, 98]. Subsection 2.2 provides an overview of proposals for the realization of anyons. Some more recent examples for realizing anyons include spin systems [8, 46, 51, 56] and Majorana zero modes [62, 63]. We emphasise a few examples of the condensed matter experiments for realizing and manipulating anyons in a weakly interacting or noninteracting system [67–69]. However, there is still a long way to go before experiments will be able to efficiently detect and manipulate anyons, especially for fault tolerant quantum computing [7, 62]. Thus, there is an interest to explore some less traditional schemes for realizing and manipulating anyons.

Motivated by the IQHE, in this chapter we consider new mechanisms for the realization and signatures of anyons in non-interacting systems. In Section 6.3.1 we propose an experimental realization of the original Wilczek's model for anyons in 2D electron gas placed in a perpendicular magnetic field, which gives rise to the IQHE. We show that the signature of anyons

is a slight shift of the Hall resistance. In Section 3.2 we present exact solutions of a model for synthetic anyons in a noninteracting quantum many-body system, which was considered in [67, 68]. Synthetic anyons occur when the noninteracting system is perturbed with specially tailored localized probes. We show that the ground state is anyonic in the coordinates of the probes.

3.1 Quantum Hall effect with composites of magnetic flux tubes and charged particles

In this section we propose an experimental realization of the original Wilczek's model for (Abelian) anyons, composites formed from charged particles and magnetic flux tubes [3–5]. First, we propose a scheme for realizing charged flux tubes, in which a charged object with an intrinsic magnetic dipole moment is placed between two semi-infinite blocks of a high-permeability (μ_r) material, and the images of the magnetic moment create an effective flux tube. This scheme is used in a particular system to develop a proposal for a realization of Wilczek's anyons. A 2D electron gas (2DEG) is placed in a perpendicular uniform magnetic field, which gives rise to the IQHE [97, 98]. Suppose that we sandwich the 2DEG between two semi-infinite blocks of high-μ_r material, assumed to have a fast temporal response (in the cyclotron and Larmor frequency range). The electron spins (i.e., magnetic dipole moments) will be aligned due to the Zeeman effect, while the high-μ_r material will induce a flux tube attached to each electron. For this system, we exploit the exact many-body wave function. We find a signature of the presence of anyons in this system - the Hall conductance. The Hall resistance at the plateau of the IQHE, which serves as a standard of electrical resistance [97, 103, 104], would be slightly shifted. We discuss possible implementations of the proposed system, the obstacles, and possible ways to overcome them. The quest for high-μ_r materials at high frequencies, which is underway in the field of metamaterials, and the quest for anyons, are here found to be on the same avenue.

3.1.1 Scheme for creating Wilczek's composites

Our scheme for creating charged flux tubes involves two semi-infinite blocks of a high permeability (high-μ_r) material ($\mu_r \gg 1$), which are separated by some distance d, and a charged object with an intrinsic magnetic dipole moment. The object is located in the center of the slab between the high-μ_r materials, and its magnetic dipole moment is perpendicular to the surface of the blocks. Method of images was first introduced in the 19th century by Lord Kelvin in the course of solving electrostatic problems. The application of the method of images is later extended to numerous problems in magnetostatics. Here we use the method of current images to calculate the magnetic field of the magnetic dipole moment in the presence of high-permeability

material.
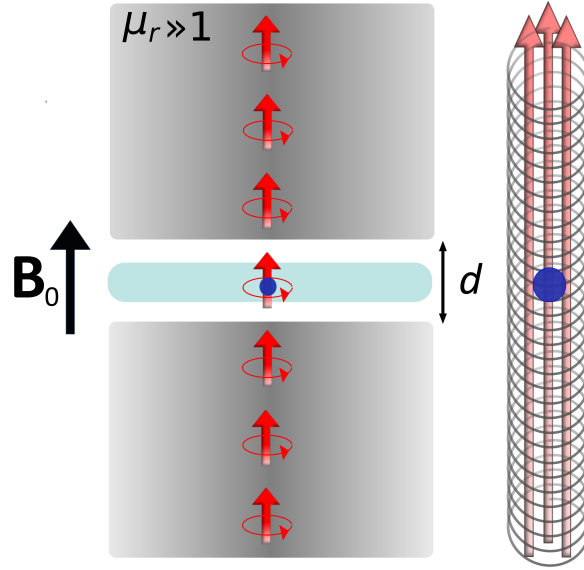
Figure 3.1: The scheme which gives rise to Wilczek's flux-tube-charge composites. A charged object with an intrinsic magnetic dipole (blue circle with a red arrow) induces an array of image magnetic dipole moments within high-μ_r blocks (shaded gray), which can be interpreted as a flux-tube-charge composite.

The image potential of one such magnetic moment, arising from the high-μ_r material, creates an effective flux tube, thereby realizing a flux-tube-charge composite, as illustrated in Fig. 3.1. The object could, for example, relate to an electron or a trapped ion, which have intrinsic magnetic moments.

3.1.2 Realization of Wilczek's anyons

We use this scheme in a particular system to develop a proposal for a realization of Wilczek's anyons. We propose to convert electrons into anyons by introducing an electron-electron $(e-e)$ vector potential mediated by the high-μ_r material. Our starting point is a 2DEG (in the $z=0$ plane) in a magnetic field $\mathbf{B}_0 = B_0\hat{z}$ $(B_0 < 0)$ exhibiting IQHE. We assume that the electrons populate only the lowest Landau level; i.e., the filling factor is $\nu = 1$. The two semi-infinite blocks of high-μ_r material with $\mu_r \gg 1$ are then introduced in the region $|z| > d/2$, see Fig. 3.2. The method of current images from classical electrodynamics models the influence of high-μ_r blocks on electrons and allows one to calculate the magnetic vector potential $\mathbf{A}(\mathbf{r})$ in the $|z| < d/2$ slab due to the magnetic dipole moment of a single electron [19]. For a stationary magnetic dipole $\mathbf{m} = m\hat{z}$ located at the origin, in the limit $\mu_r \to \infty$, $\mathbf{A}(\mathbf{r})$ is identical to that of an infinite array of magnetic moments deep within semi-infinite blocks. These virtual images are equal in magnitude and direction to the original magnetic moment, and equally spaced by d, as illustrated in Fig. 3.1. Thus, for $r = |\mathbf{r}|$ sufficiently larger than d, an array of magnetic moments

can be viewed as a flux tube with $\mathbf{A}(\mathbf{r}) \approx \Phi/2\pi r \hat{\phi}$, where the flux is $\Phi = \mu_0 m/d$. For a finite value of μ_r, the vector potential in the $z = 0$ plane is given by

$$\mathbf{A}(\mathbf{r}) = \frac{\Phi r d}{4\pi} \sum_{n \in \mathbb{Z}} \left(\frac{\mu_r - 1}{\mu_r + 1} \right)^{|n|} \frac{1}{(r^2 + n^2 d^2)^{\frac{3}{2}}} \hat{\phi}.$$

In order to estimate the validity of the approximation $\mathbf{A}(\mathbf{r}) \approx \Phi/2\pi r \hat{\phi}$, in Fig. 3.3 we plot $\Delta = \frac{e}{\pi \hbar} \oint \mathbf{A} \cdot \mathbf{dl}$ as a function of r and μ_r ($e < 0$); the integral is taken around the circle of radius r centered at the origin. Evidently, for $\mu_r = \infty$, Δ is essentially a constant independent of r (except for $r < d$), verifying that the flux $\Phi = \oint \mathbf{A} \cdot \mathbf{dl}$ is concentrated close to the origin, and the approximation is excellent. For finite values of $\mu_r = 10^4 - 10^5$, Δ changes very slowly over a large span of values of r from d up to the mean free path $l_{m.f.p.}$ in standard QHE samples [118], which underpins the approximation in realistic circumstances. For concreteness, we plot Fig. 3.3 for $d = 10$ nm, and $-\Delta$ is plotted up to 10000 nm, but similar results are obtained for a span of values $d = 10 - 100$ nm. We assume that the medium has sufficiently fast response, so that this picture is valid for a moving electron as well. This gives rise to the vector potential interactions between the electrons. The viability of the proposal and approximations are discussed below.
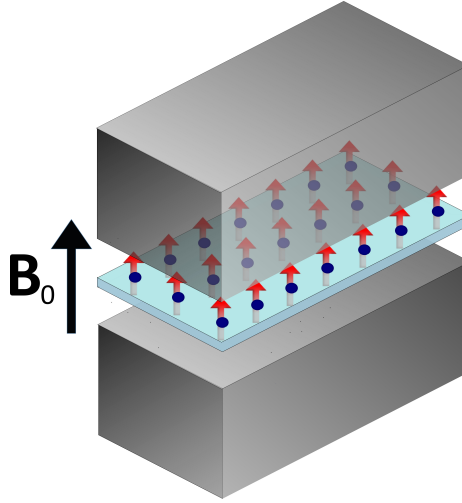
Figure 3.2: A 2DEG in a uniform magnetic field $\mathbf{B}_0$ (in the IQHE state) is sandwiched between two blocks of high-μ_r material (shaded grey). Dipole magnetic moments of the electrons (illustrated as red arrows) are aligned with $\mathbf{B}_0$ and behave as Wilczek's flux-tube-charge composites.

If an electron encircles a fixed solenoid of flux Φ, its wave function accumulates the Aharonov-Bohm phase $\exp(ie\Phi/\hbar)$, but the same phase arises also from a quantum-mechanical solenoid orbiting around a fixed charge. Thus, the $e-e$ vector potential mediated by the high-μ_r material is equivalent to that of a charge interacting with twice the flux in one flux tube [21, 119], that is, the interaction is $2e\mathbf{A}(\mathbf{r}_i - \mathbf{r}_j)$, where

$$\mathbf{A}(\mathbf{r}_i - \mathbf{r}_j) = \frac{\Phi}{2\pi} \frac{\hat{z} \times (\mathbf{r}_i - \mathbf{r}_j)}{|\mathbf{r}_i - \mathbf{r}_j|^2}. \tag{3.1}$$

In the presence of a magnetic field, the electron energies of the up and down spins split due to the Zeeman effect. In large magnetic fields, large energies are needed to flip the spin; restricting to low energies, we can neglect electrons with magnetic moments opposite to that of the magnetic field. Under the assumptions and approximations stated above, the system is described by the Hamiltonian

$$H = \sum_{i=1}^{n} \frac{1}{2m} \left[\mathbf{p} - e\mathbf{A}_0(\mathbf{r}_i) - 2e \sum_{j \neq i} \mathbf{A}(\mathbf{r}_i - \mathbf{r}_j) \right]^2, \tag{3.2}$$

with the symmetric gauge vector potential $\mathbf{A}_0 = \frac{1}{2}\mathbf{B}_0 \times \mathbf{r}$ for the constant magnetic field.
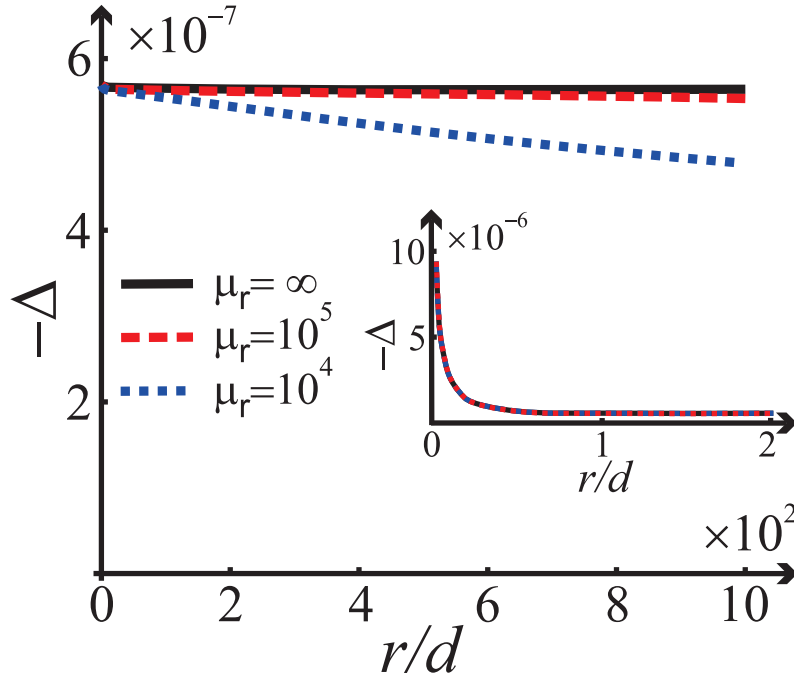
Figure 3.3: Parameter $-\Delta = -e\pi^{-1}\hbar^{-1}\oint \mathbf{A} \cdot \mathbf{dl}$ as a function r/d, for three values of μ_r; $d=10$ nm.

Electron-electron vector potential in Eq. (3.2) is eliminated by a singular gauge transformation,

$$\psi'(\mathbf{r}_1, ..., \mathbf{r}_n) = \prod_{i<j} e^{-i\phi_{ij}\Delta} \psi(\mathbf{r}_1, ..., \mathbf{r}_n), \tag{3.3}$$

where ϕ_{ij} is the azimuthal angle of the relative vector $\mathbf{r}_i - \mathbf{r}_j$ and $\psi(\{\mathbf{r_i}\})$ is the fermionic wave function in the regular gauge. The ground state of the Hamiltonian (3.2), in the singular gauge is [113, 115–117]

$$\psi'(\{z_i\}\{z_i^*\}) = \prod_{i<j} (z_i - z_j)^{\alpha} \exp(-\frac{1}{4l_B^2} \sum_l |z_l|^2), \tag{3.4}$$

where we have introduced complex coordinates $z_i = x_i - iy_i$, the magnetic length $l_B = \sqrt{-\hbar/eB_0}$, and the statistical parameter $\alpha = 1 + \Delta$. The energy of this state is $E = n\hbar\omega_c/2$, where $\omega_c = -eB_0/m$ is the cyclotron frequency. Here we assumed that the electrons in the initial IQHE system, which we started with, populate only the LLL.

3.1.3 Signature of anyons

In the following, we demonstrate that the Hall conductance for this state is

$$\sigma_H = \frac{1}{\alpha}\frac{e^2}{h}. \tag{3.5}$$

To calculate the Hall conductance in this system, we use the Laughlin pumping argument in the Corbino ring geometry [18, 98]. Suppose that we introduce an infinitely thin solenoid at $z = 0$, and adiabatically increase the flux from 0 up to $\Phi_0 = -2\pi\hbar/e$ (one flux quantum). The state (3.4) adiabatically evolves into

$$\psi'_{z_0}(\{z_i\}\{z_i^*\}) = \prod_i (z_i - z_0)\,\psi'(\{z_i\}\{z_i^*\}), \tag{3.6}$$

which is an eigenstate of the system with the same energy. In this process, charge q^* is pumped from the solenoid (at $z = 0$) to the edge of the ring. It can be calculated from the single particle densities, ρ_α for the state in Eq. (3.4), and $\rho_{\alpha,0}$ for the state in Eq. (3.6). The calculation is performed analytically in the thermodynamic limit $N \to \infty$ by using the plasma analogy, first introduced by Laughlin [25] (see Refs. [120, 121] for details),

$$\rho_\alpha(x,y) = \frac{1}{2\pi\alpha l_B^2}$$

and

$$\rho_{\alpha,0}(x,y) = \frac{1}{\alpha}\left(\frac{1}{2\pi l_B^2} - \delta(x)\delta(y)\right).$$

Evidently, the missing charge at $z = 0$ is $q^* = e/\alpha$, which yields

$$\sigma_H = q^*\frac{e}{h} = \frac{1}{\alpha}\frac{e^2}{h}$$

for the Hall conductivity. Thus, before we place the two high-μ_r blocks in the system, the initial value of the Hall conductivity is $\nu e^2/h$ with $\nu = 1$ by assumption. After placing the blocks, which induce the $e-e$ vector potential, the Hall conductivity at the plateau shifts from $\nu = 1$ to $1/\alpha = 1/(1+\Delta) \approx 1 - \Delta$. The shift $-\Delta$ is plotted in Fig. 3.3, and it has the value $10^{-7} - 10^{-6}$. Despite the fact that the shift is small, $\Delta\sigma_H \sim 10^{-7} \times e^2/h$, measurements indicate that the value of the quantized Hall resistance can be reproduced within a relative uncertainty of one part in 10^{10} [103], meaning that the shift in the Hall conductance could be detectable as the signature of Wilczek's anyons. In addition, we note that as the $e-e$ vector potential is introduced (a flux tube with flux Φ is adiabatically attached to every electron), according to the adiabatic principle developed by Greiter and Wilczek [114], the system remains gapped; i.e., incompressible quantum Hall states remain incompressible.

3.1.4 Implementation of the system

Now we discuss possible implementations of this system, the obstacles, and possible routes to overcome them. We have assumed that the $e - e$ vector potential picture is valid also for electrons moving in the 2DEG, even though it was derived for static electrons. In the classical picture, electrons exhibiting the Hall effect move in circular orbits with the cyclotron frequency, giving rise to oscillating fields that material should respond to. In the quantum picture, electrons are in the Landau level states. Recent experiments [122] have demonstrated that the currents corresponding to electrons promoted in Landau level states oscillate at cyclotron ($\omega_c = -eB/m^*$) and Larmor frequencies ($\Omega = -eB/2m^*$), depending on the particular state; here m^* is the effective mass of electrons. Therefore, we conclude that the demanded high-μ_r material should have a strong magnetic response in the frequency range corresponding to cyclotron motion. A typical system for the QHE is the interface of a GaAs/AlGaAs heterojunction where $m^* = 0.067 m_e$ [123], and the frequencies are in the terahertz range. Unfortunately, the magnetic response of most conventional materials is beginning to tail off in the gigahertz region [124]. A few natural magnetic materials that respond above microwave frequencies have been reported, but the magnetic effects in these materials are typically weak (see Ref. [125] and references therein).

These restrictions can in principle be overcome by using metamaterials, artificial structures which can be constructed to have a strong effective magnetic response $\mu_{eff}(\omega)$ at high frequencies (ranging from gigahertz to terahertz) [124–126]. Another advantage of using metamaterials in this context is that their response is usually not broadband. Therefore, a high-μ_r metamaterial at terahertz frequencies is likely to have low response (or none) at zero frequency (for example, see Ref. [127]) and would not be affected by the constant magnetic field used to create the IQHE state. One possible route for constructing a desirable metamaterial could be photonic doping, recently used to construct a material with effective $\mu_{eff} \to \infty$ [127] for polarization where the magnetic field is parallel to the surface (here we demand that the magnetic field be perpendicular to the surface). The characteristic scale of the building constituents of the metamaterial should be smaller than the magnetic length l_B, so that the concept of the effective macroscopic permeability remains valid. Another possibility to overcome the obstacle of fast material response is to reduce the Fermi velocity and thereby the cyclotron frequency by involving heavy fermion materials, in which electrons have a large enough effective mass. The cyclotron frequency scales as $1/m^*$; thus, to bring the cyclotron frequency down to the gigahertz range, by using typical numbers from above, the effective mass of the electrons should be $m^* \sim 10^2 m_e$.

An important parameter, which should be tuned to get the desired effect, is the distance between the high-μ_r materials d. The flux tube approximation $\mathbf{A}(\mathbf{r}) \approx \Phi/2\pi r \hat{\phi}$ for the vector potential of an electron, which is illustrated in Fig. 3.3, is excellent already for $r > d$. We find that for values of $\mu_r \sim 10^4$ and larger, it is excellent up to $r \sim l_{m.f.p.}$ and more (this depends on μ_r). It gives rise to the $e - e$ interactions in Eq. (3.1). Hence, the average separation between

electrons should be greater than d for Eq. (3.1) to apply. In standard IQHE experiments, the electron density is $10^{11} - 10^{12}$ so that the average separation is of the order of 20 nm, but in principle it could be larger. For larger values of d (say $d \sim$30-60 nm), the flux tube approximation is even better at scales from d to $l_{m.f.p.}$. However, the shift in the Hall conductivity $\Delta \sigma_H$, which is the signature of the effect, scales as $1/d$. Thus, we must find an appropriate value for d smaller than the average separation between electrons, and small enough for the effect to be measurable, but large enough to be possible to sandwich a thin material with IQHE between two blocks of high-μ_r material. This is a viable task according to the parameters used in Fig. 3.2. Moreover, assuming one could tune d in an experiment, a measurement yielding $\Delta \sigma_H \sim 1/d$ would be a clear evidence of Wilczek's anyons in this system. Since the area of the IQHE sample is finite and $\nabla \cdot \mathbf{B} = 0$, when $r \to \infty$, $-\Delta \to 0$. Thus, the high-μ_r materials should have a large aspect ratio (height much larger than the square root of the area) to properly steer the magnetic streamlines.

We note that a promising possibility to observe Wilczek's flux tubes is to engineer 2D materials [128]. To this end, we propose to intercalate a metallic monolayer between two layers of hexagonal boron nitride (h-BN); this could be Li, K, Na or some other metallic monolayer [129, 130]. The density-functional theory calculations for an h-BN–Li–h-BN monolayer show structural stability and a parabolic band dispersion [131]. The principle of intercalation is here very similar to such intercalation in graphite, which has been extensively studied [132]. The h-BN–metallic monolayer–h-BN structure can in principle be sandwiched between two blocks of the high-μ_r material, thus constituting a candidate for observing anyons according to our scheme. Another route could be to grow a metallic monolayer on the film of a semiconductor as in Ref [133], and to place it between the high-μ_r blocks (the semiconductor should be sufficiently pure not to conduct). Viable paths could also be conceived with layered dichalcogenides [128].

For concreteness, our theoretical analysis above is based on the QHE with electrons in a 2D parabolic band. The most famous 2D material—graphene—has a conical band structure [134–136]. However, graphene sandwiched between two blocks of high-μ_r material could also be a candidate for exploring (Wilczek-Dirac type) anyons according to the present proposal. Although the quantum Hall effect in graphene is distinctive, as it occurs at half-integer filling factors [134, 135], the Landau-level wave functions for low-energy electrons in graphene have the same mathematical structure as in the 2DEG (up to the coefficients that enter these wave functions [136]). Thus, we conjecture that the signature of Wilczek's flux tubes in this system would also be a small shift of the resistance at the plateau. Graphene also has the possibility to be strained [137] and induce effective gauge fields, which is an additional useful degree of freedom when tinkering with this system.

$\sim$

In conclusion, we have proposed a scheme for creating flux-tube-charge composites, which employs a material with high magnetic permeability μ_r. Thus, advances in developing high-μ_r metamaterials could lead to novel ways for creating anyons. We have calculated the Hall conductivity for a 2DEG in the IQHE regime, sandwiched between two semi-infinite blocks of high-μ_r metamaterial with a fast temporal response, and found that the Hall resistance at the plateau would exhibit a small but detectable shift, which is to some extent a striking consequence because it serves as a standard of electrical resistance [97,103,104]. Finally, we would like to note that the quest for anyons is of broad interest and underway in many systems including ultracold atomic gases [41,43,51], photonic lattices [138] and quantum spin liquids [56]. Our scheme for creating charged flux tubes has potential to be used in other systems such as trapped ions. Here we have addressed Abelian anyons. We believe that further studies inspired by this proposal could yield schemes for realizing non-Abelian anyons for topological quantum computing [7].

3.2 Exact solutions of a model for synthetic anyons in a non-interacting system

In the context of some less traditional schemes for realizing and manipulating anyons, let us mention a few examples of the condensed matter experiments for realizing and manipulating anyons in weakly (or noninteracting) system. It was proposed that anyons could be synthesized by coupling weakly interacting (or noninteracting) electrons to a topologically nontrivial background (or topologically nontrivial external perturbations) [67–69]. In Refs. [67, 68], anyons are proposed in a system of an artificially structured type-II superconducting film, adjacent to a two-dimensional electron gas (2DEG) in the IQHE with unit filling fraction [67, 68]. A periodic array of pinning sites imprinted on the superconductor will structure an Abrikosov lattice of vortices [67]. Anyons are bound by vacancies (interstitials) in the vortex lattice, which carry a deficit (surplus) of one-half of a magnetic flux quantum [67]. In Ref. [69] anyons were proposed in integer QHE magnets [69]. Magnetic vortices in this system are topologically stable and have fractional electronic quantum numbers yielding anyonic statistics. Anyons were also proposed by using topological defects in graphene [70].

In this section we study a theoretical model for synthetic anyons in a noninteracting quantum many-body system. We present exact solutions of a model for synthetic anyons, which was considered in Refs. [67, 68]. Synthetic anyons can occur in a noninteracting system when it is perturbed with specially tailored localized probes, which supply the demanded nontrivial topology in the system. The model is represented by the Hamiltonian for noninteracting electrons in two dimensions, in a uniform magnetic field, pierced with solenoids with a magnetic flux that is a fraction of the flux quantum. In a potential experimental realization of the model, there should be a mechanism fixing the flux in all solenoid probes to an identical value for these perturbations to represent synthetic anyons. We find analytically the ground state of the model when only the lowest Landau-level states are occupied. We calculate the statistical parameter by using the Berry phase, and show that the ground state is anyonic in the coordinates of the probes. These results are confirmed numerically. We show that these synthetic anyons cannot be considered as emergent quasiparticles. The fusion rules are discussed for different microscopic realizations of the fusion process.

3.2.1 Ground-state wave function

In our theoretical model we consider N_e noninteracting spin-polarized electrons in 2D configuration space (in the xy plane), in a uniform magnetic field $\mathbf{B}_0 = \mathbf{\nabla} \times \mathbf{A}_0 = B_0 \hat{z}$, where $\mathbf{A}_0(\mathbf{r}) = \mathbf{B}_0 \times \mathbf{r}/2$ is the vector potential in the symmetric gauge ($B_0 > 0$). The system is perturbed with N very thin solenoids at locations $\boldsymbol{\eta}_k = \eta_{x,k}\hat{x} + \eta_{y,k}\hat{y}$. The vector potential of each

solenoid is

$$\mathbf{A}_k(\mathbf{r}) = \frac{\Phi}{2\pi} \frac{\hat{\mathbf{z}} \times (\mathbf{r} - \boldsymbol{\eta}_k)}{|\mathbf{r} - \boldsymbol{\eta}_k|^2}, \tag{3.7}$$

where Φ is the magnetic flux through a solenoid. The Hamiltonian representing the model is then

$$H = \sum_{j=1}^{N_e} \frac{1}{2m} \left(\mathbf{p}_j - q\mathbf{A}_0(\mathbf{r}_j) - q\sum_{k=1}^{N} \mathbf{A}_k(\mathbf{r}_j) \right)^2 + \sum_{j=1}^{N_e} V(\mathbf{r}_j), \tag{3.8}$$

where $V(\mathbf{r})$ is zero for $r < R_{max}$, and infinite otherwise; $q < 0$ (m) is the electron charge (mass, respectively). The system is illustrated in Fig. 3.4(a). We assume that the Fermi level is such that only the states from the lowest Landau level (LLL) of energy $\hbar\omega_B/2$ are populated ($\omega_B = -qB_0/m$), and we assume they are *all* populated. The many-body ground state of this system is denoted by $\psi(\{z_j\}, \{\bar{z}_j\}; \{\eta_k\}, \{\bar{\eta}_k\})$, where $z_j = x_j + iy_j$ and $\bar{z}_j = x_j - iy_j$ are the electron coordinates, and $\eta_k = \eta_{x,k} + i\eta_{y,k}$ and $\bar{\eta}_k = \eta_{x,k} - i\eta_{y,k}$ are the probe coordinates in complex notation.
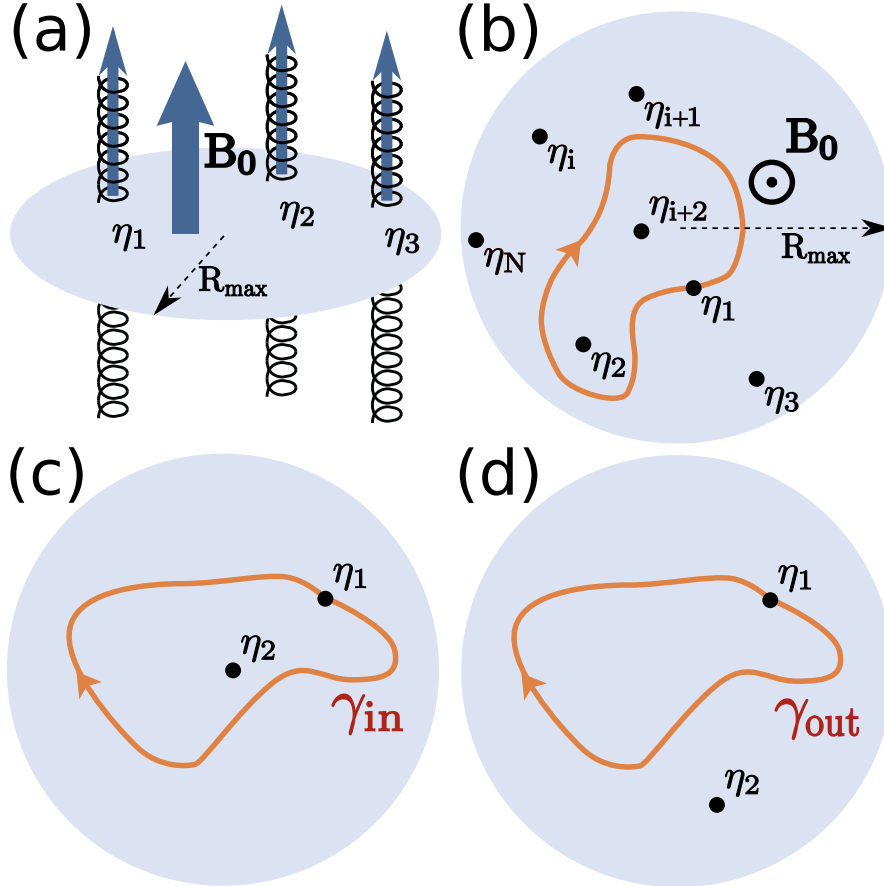
Figure 3.4: Sketch of the model. (a) We explore a 2DEG in a magnetic field $\mathbf{B}_0$, on a disc of radius R_{max}. The solenoid probes with flux Φ, pierce the 2DEG at positions η_j (coordinates are in complex notation). (b) The contour path of one probe, which adiabatically traverses a closed loop in space; we are interested in the Berry phase accumulated along such paths. Illustration of the contours corresponding to γ_{in} (c), and γ_{out} (d).

In this section we demonstrate that the ground state wave function with energy $N_e\hbar\omega_B/2$ is

given by

$$\psi = \frac{1}{\sqrt{Z(\{\eta_k\},\{\bar{\eta}_k\})}} \left[\prod_{j=1}^{N_e}\prod_{k=1}^{N} |z_j - \eta_k|^{-\alpha}\overline{z_j - \eta_k}\right]$$
$$\times \left[\prod_{i<j}^{N_e}(\bar{z}_i - \bar{z}_j)\right] \exp\left(-\sum_{i=1}^{N_e}\frac{|z_i|^2}{4l_B^2}\right), \tag{3.9}$$

where $l_B = \sqrt{-\hbar/B_0 q}$ is the magnetic length, $\alpha = \Phi/\Phi_0$, $\Phi_0 = -2\pi\hbar/q$ is the flux quantum, and $Z(\{\eta_k\},\{\bar{\eta}_k\})$ accounts for normalization. We consider $\alpha \in \langle 0,1\rangle$; results for fractional values outside of the $\langle 0,1\rangle$ interval are easily deduced.
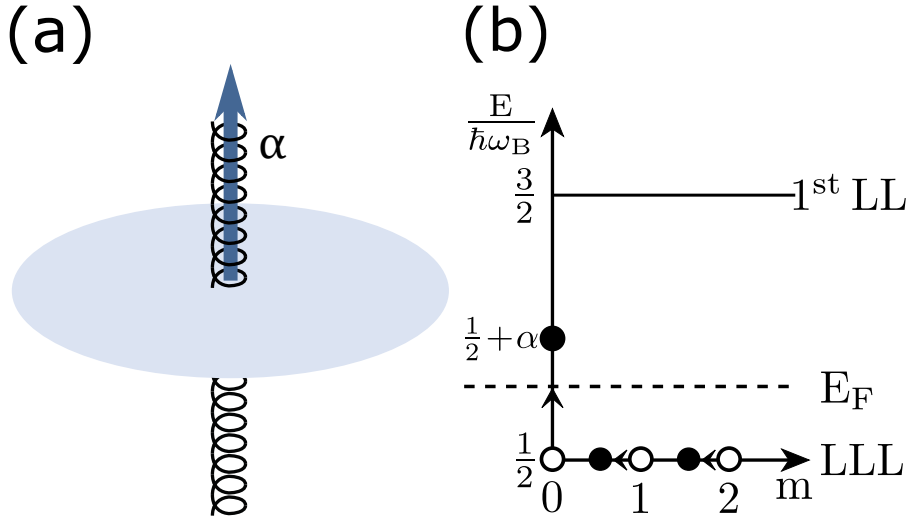
Figure 3.5: Sketch of the energy scales and the spectral flow for just one probe. (a) A probe is centered in the system, its flux is such that $0 \le \alpha = \Phi/\Phi_0 \le 1$. (b) As α is increased, there is a spectral flow as illustrated. The Fermi energy E_F is always set such that only the LLL states are populated.

For the clarity of the presentation, we first present what happens with the system when only one probe is placed in the system, and subsequently what happens when two probes are inserted. For a single probe, the single particle states of the system at the LLL energy are given by

$$\psi_m = |z - \eta|^{-\alpha}\overline{z - \eta}\bar{z}^m \exp\left(-\frac{|z|^2}{4l_B^2}\right), \quad m = 0,1,2,\ldots. \tag{3.10}$$

There is one state localized at the position of the probe, with energy $\hbar\omega_B(1+2\alpha)/2$ in between the LLL and the first excited Landau level:

$$\psi_{LS} = |z - \eta|^{\alpha} \exp\left(-\frac{|z - \eta|^2 + \bar{\eta}z - \eta\bar{z}}{4l_B^2}\right).$$

Suppose that one introduces the solenoid probe at some point in time, and adiabatically increases the flux through it. As α increases from zero to one, there is a spectral flow illustrated

in Fig. 3.5; one state from the LLL rises in energy and starts flowing towards the first Landau level. When $\alpha = 1$, this flux is just gauge, and the energies map back onto those at $\alpha = 0$. This scenario is well known from studies of the QHE [18]. Here we assume that the flux is fixed at some value α, and the Fermi energy is between LLL energy and $\hbar\omega_B(1 + 2\alpha)/2$; thus, this localized state is not populated. The many-body ground state is constructed by inserting all LLL states in a Slater determinant; it is given by Eq. (3.9) for $N = 1$.

For the case of two probes, the single particle states of the system at the LLL energy are

$$
\begin{aligned}
\psi_m &= |z - \eta_1|^{-\alpha}|z - \eta_2|^{-\alpha}\overline{z - \eta_1 z - \eta_2} \\
&\times \bar{z}^m \exp\left(-\frac{|z|^2}{4l_B^2}\right), m = 0, 1, 2, \ldots
\end{aligned}
\tag{3.11}
$$

Now there are two localized states in between the LLL and the first excited Landau level. We did not find analytical expressions for these states but they are visible in numerical calculations. The energies of these localized states are in the gap, between the LLL and the first excited LL. They increase with increasing alpha and join the first excited LL when $\alpha = 1$ as expected. The many-body ground state is given by Eq. (3.9) for $N = 2$.

Now we generalize our results for any number of the probes N. To this end, we employ the following singular gauge transformation:

$$
\psi' = \psi \prod_{1 \leq i \leq N_e} \prod_{1 \leq j \leq N} \exp(i\alpha\phi_{ij});
\tag{3.12}
$$

here ϕ_{ij} denotes the argument of $z_i - \eta_j = |z_i - \eta_j|\exp(i\phi_{ij})$. In this gauge, the vector potential of the probes is $\mathbf{A}'_k = \mathbf{0}$ everywhere except at the positions of the probes, and the Hamiltonian H' is given by Eq. (3.8) with $\mathbf{A}_k$ replaced by $\mathbf{A}'_k = \mathbf{0}$. It is straightforward to verify that ψ' is an eigenstate of H' with energy $N\omega_B/2$, and hence the ground state.

It should be pointed out that in the limit $\alpha \to 0$ the wave function 3.9 does not approach the IQHE ground state with all LLL states filled, but rather it becomes an IQHE state with N of the LLL states left empty. Namely, the localized states which appear at the position of the probes for $\alpha > 0$ are not included in the Slater determinant used to construct the ground state 3.9, as discussed above. For $\alpha = 0$ they enter the LLL, but since they were not used in constructing 3.9, the wave function 3.9 does not approach the IQHE ground state (with all LLL states filled) in the limit $\alpha \to 0$. Strictly speaking, Eq. 3.9 is the ground state for $\alpha \in \langle 0, 1 \rangle$, provided that only the LLL states are filled; it is not the ground state for $\alpha = 0$ and all LLL states filled.

In a potential experimental implementation of the proposed system, one should not populate the localized states such as ψ_{LS}. With this state populated, the ground state is no longer anyonic in the coordinates of the probes. For this state to remain empty, the temperature must be sufficiently low such that $kT \ll \hbar\omega_B\alpha$, which is difficult to obtain for small α. However, an additional localized repulsive scalar potential at the location of the probes (e.g., the delta

function potential), which may be present naturally depending on the realization, would lift the energies of the localized states to remedy this issue.
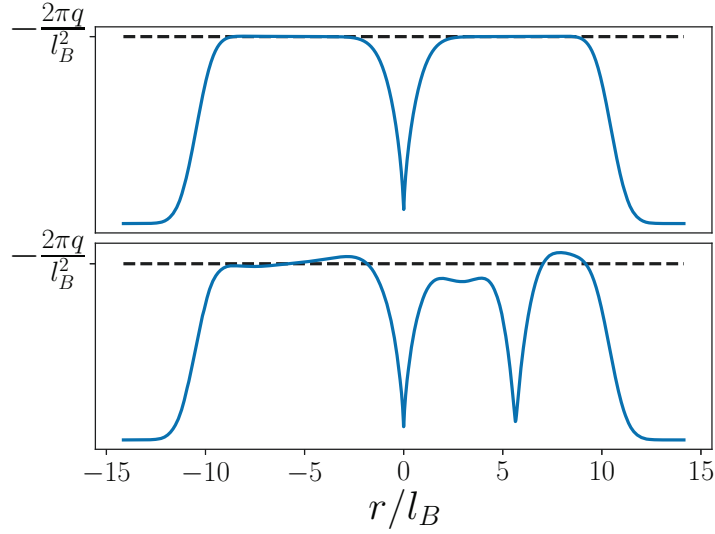
Figure 3.6: The single-particle densities (cross sections) of the ground states with one probe (at $r = 0$) and two probes (at $r = 0$ and $5.264l_B$). The flux through the probes is given by $\alpha = 0.7$. The horizontal dashed line depicts the density of an infinite system.

In Figure 3.6 we illustrate the single particle density (cross section) for the system with one and two probes. Clearly, the single particle density has a cusp-like dip at the position of a probe, i.e., a missing electron charge Δq. It is tempting to identify the composite of a missing electron charge Δq and the probe with flux Φ with Wilczek's charge-flux-composite anyons [139], however, a careful analysis of the Berry phase below shows that this is not the case.

To end this section, let us mention that when calculating the single-particle states of the LLL, which enter the Slater determinant used to construct the ground state (3.9), one encounters a spurious single particle state of the form

$$\psi_{\text{spur}} = |z|^{-\alpha} \exp\left(-\frac{|z|^2}{4l_B^2}\right), \tag{3.13}$$

which, although normalizable, has divergent density. The form (3.13) corresponds to a system with a single probe centered at the origin. A more careful analysis shows that this state is, in fact, not an eigenstate of the Hamiltonian and should not be used in the construction of the Slater determinant. If this state was physical and present in the ground state, the ground state would not be anyonic in the coordinates of the probes. In that case, however, the aforementioned additional localized repulsive scalar potential at the location of the probes could be used to lift it in energy and remove it from the ground state. We should note that in Ref. [67] this spurious state was used to construct the many-body ground state, and as a result the ground state from Ref. [67] is in fact not anyonic.

3.2.2 Anonic properties of the wavefunction - calculation of the Berry phase

Here we calculate the Berry phase as one of the probes undergoes adiabatically a closed loop in space as illustrated in Fig. 3.4(b). The Berry phase depends on how many other probes are contained in the loop. More specifically, following the calculation of Arovas et al. [27], we calculate the Berry phase when a single probe is within the loop (call it γ_{in}, see Fig. 3.4(c)), and when all of the other probes are outside of the loop (call it γ_{out}, see Fig. 3.4(d)). The difference between the two phases is the statistical phase, which we find to be $\gamma_S = \gamma_{in} - \gamma_{out} = 2\pi(\alpha - 1)$, where $\alpha = \Phi/\Phi_0$; this result means that in the coordinates of the external probes, the wavefunction ψ is anyonic when α is fractional.

1 Plasma analogy First we consider a normalized state with N probes given by (3.9). Using the plasma analogy, normalization factor $Z(\{\eta_k\}, \{\bar{\eta}_k\})$ can be interpreted as the partition function of the 2D one-component plasma (electrons) at $\{z_i\}$ at an inverse temperature $\beta = 2$, interacting with charged impurities (probes) at η_k [18, 25]. The potential energy for this system is given by

$$
U(z_i) = \frac{1}{4l_B^2} \sum_i^N |z_i|^2 - \sum_{k<l}^N \log\left(\frac{|z_k - z_l|}{l_B}\right)
$$
$$
- (1-\alpha) \sum_{i,j}^{N,2} \log\left(\frac{|z_i - \eta_j|}{l_B}\right).
$$
(3.14)

In the thermodynamical limit (large N), the partition function Z can be obtained by using the saddle-point technique, where the particles are driven into configuration which has the minimum energy [120, 121]. For $N \to \infty$, sum over particles becomes a continuous distribution, which equals the electron density. Minimizing the energy and using $\frac{\partial}{\partial \bar{z}} z^{-1} = \pi \delta^2(z)$, one obtains the density of particles

$$
\rho(z) = \frac{1}{2l_B^2 \pi} - (1-\alpha) \sum_{j=1}^2 \delta^2(z - \eta_j).
$$
(3.15)

We can recognize two contributions $\rho(z) = \rho_0 + \delta\rho(z)$. The first one is constant and corresponds to the density in the case of the IQHE, while the second one describes the charge depletion at positions of the probes. In the presence of impurities, the charges rearrange themselves to cluster around the impurity by accumulating an equal and opposite charge so that its effects cannot be noticed at far distances. In order to describe the plasma with impurities, one includes the energy cost between the impurities and the constant background charge, and the Coulomb energy between different impurities. Corrected potential energy and partition function should

be independent of the positions η_i. This leads us to the result for the normalization factor:

$$Z = C \exp\left(-(1-\alpha)^2 \sum_{k<l} \log \frac{|\eta_k - \eta_l|^2}{l_B^2} + \frac{1-\alpha}{2l_B^2} \sum_k |\eta_k|^2\right).$$

2   Berry phase   In order to find the statistics of the probes, we pick one of the probes, for example η_1, and move it on a closed path $C = \partial S$. After traversing the path, the wave function

$$\psi = \frac{1}{\sqrt{Z}}\chi$$

acquires a phase shift given by the Berry phase

$$e^{i\gamma} = \exp\left(-i\oint_C \mathscr{A}_{\eta_1} d\eta_1 + \mathscr{A}_{\bar\eta_1} d\bar\eta_1\right), \tag{3.16}$$

where $\mathscr{A}_{\eta_1}$ is holomorphic and $\mathscr{A}_{\bar\eta_1}$ anti-holomorphic Berry connection:

$$\mathscr{A}_\eta(\eta,\bar\eta) = -\frac{i}{Z}\langle\chi|\frac{\partial}{\partial\eta}|\chi\rangle + \frac{i}{2}\frac{\partial}{\partial\eta}(\log Z),$$

$$\mathscr{A}_{\bar\eta}(\eta,\bar\eta) = -\frac{i}{Z}\langle\chi|\frac{\partial}{\partial\bar\eta}|\chi\rangle + \frac{i}{2}\frac{\partial}{\partial\bar\eta}(\log Z).$$

Calculation of the Berry phase proceeds as in [27]. The braiding phase corresponds to the difference of the Berry phases for closed paths with and without another probe enclosed by it. When η_1 is taken around the closed path C, contributions from the normalization factors, i.e., partition function Z, cancel each other. Derivatives of the unnormalized wave function χ are given as

$$\frac{\partial\chi}{\partial\eta_1} = \frac{\alpha}{2}\chi\sum_{i=1}^N \frac{1}{z_i - \eta_1},$$

$$\frac{\partial\chi}{\partial\bar\eta_1} = \left(\frac{\alpha-2}{2}\right)\chi\sum_{i=1}^N \frac{1}{\bar z_i - \bar\eta_1}.$$

Taking the definition of the charge density

$$\rho(z) = \frac{1}{Z}\langle\chi|\sum_i \delta(z_i - z)|\chi\rangle, \tag{3.17}$$

one obtains

$$\gamma = i\frac{\alpha}{2}\int d^2z \oint_C d\eta_1 \frac{\rho(z)}{z - \eta_1} + i\frac{\alpha-2}{2}\int d^2z \oint_C d\bar\eta_1 \frac{\rho(z)}{\bar z - \bar\eta_1}.$$

If we denote the integral

$$\mathscr{I} = \oint_c d\eta_1 \int d^2z \frac{\rho(z)}{z - \eta_1}, \tag{3.18}$$

we have

$$\gamma = i(\alpha \text{Re} \mathscr{J} - \bar{\mathscr{J}}).$$

Concerning the contribution of ρ_0 in Eq. (3.18), if η_1 is integrated in anticlockwise direction, only values of z inside this loop ($z \in S$) contribute $-2\pi i$ to the integral. Then we can evaluate the surface integral, where we use the relationship between the charge and the magnetic flux Φ_S in S for the $\nu = 1$ IQH state. In order to find the contribution of the second term $\delta \rho(z)$, first we evaluate the surface integral and obtain a non-vanishing contribution from $\eta_j \neq \eta_1$. Contour integral then evaluates to $-2\pi i$ only if η_j is inside the closed path of η_1. This leads us to the result

$$\mathscr{J}_{out} = -2\pi i \frac{\Phi_s}{\Phi_0}$$
$$\mathscr{J}_{in} = -2\pi i \frac{\Phi_s}{\Phi_0} + 2\pi i(1-\alpha).$$

Let us denote the mean number of electrons inside the contour as $\langle n \rangle_C$. Thus, when η_1 traverses a path where it does not encircle any other probe the Berry phase is

$$\gamma_{out} = 2\pi \frac{\Phi_s}{\Phi_0} = 2\pi \langle n \rangle_{C,out}.$$

On the other hand, if another probe is inside the loop, the Berry phase sums up to

$$\gamma_{in} = 2\pi \frac{\Phi_s}{\Phi_0} - 2\pi(1-\alpha) = 2\pi \langle n \rangle_{C,in}.$$

The statistical phase is the difference between these two cases:

$$\gamma_S = 2\pi(\langle n \rangle_{C,in} - \langle n \rangle_{C,out}) = 2\pi(\alpha - 1).$$

Thus, γ_S mod 2π is equal to $2\pi\alpha$. Let us briefly comment on the fact that $\Delta q \to -q$ as $\alpha \to 0$, and $\Delta q \to 0$ as $\alpha \to 1$, which may seem awkward at first sight. This is related to our discussion in the previous section on the behavior of the wave function 3.9 as $\alpha \to 0$. When constructing the wave function 3.9, we do not populate the localized states which appear at the position of the probes for $\alpha > 0$. Therefore, as $\alpha > 0$, they are not in the Slater determinant, leaving a hole of charge $\Delta q = -q$ at the position of the probe. When $\alpha \to 1$, the localized states at the position of the probe enter the first LL (which is empty anyhow by assumption); however, the corresponding state in the LLL below is now filled, yielding $\Delta q = 0$, as the spectrum has flown back to itself when α flows from zero to one.
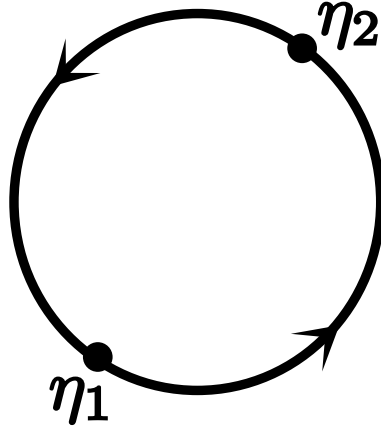
Figure 3.7: Two probes at opposite radii η_1 and η_2 are exchanged leading to an exchange phase $\pi(\alpha - 1)$.

From the viewpoint of the relative coordinate, when one of the probes encircles the other probe, this corresponds to a double exchange of the two probes illustrated in Fig. 3.7. Thus, we conclude that if we exchange two of the probes adiabatically along a path illustrated in Fig. 3.7 (with no other probes within the closed contour) the exchange phase accumulated by the wave function will be $\pi(\alpha - 1)$. This means that the wave function ψ is anyonic in the coordinates of the probes, with the statistical parameter given by $\theta = \pi(\alpha - 1)$.

3.2.3 Gauge invariance

We end this section by a note on the gauge invariance of the Berry phase calculated along the closed path C. The wave function ψ in Eq. (3.9) is a single-valued function of the positions of the external probes η_k, provided that the normalization $Z(\eta_k, \bar{\eta}_k)$ is also chosen to be a single-valued function of η_k. In contrast, the singular gauge wave function ψ in Eq. (3.12) is a multivalued function of η_k. Equation (3.16) for calculating the Berry phase yields different results when naively used for ψ and ψ'. However, the Berry phase calculated along a closed path must be independent of the gauge used. This issue is resolved by noting that Eq. (3.16) should be used only for single-valued wave functions (that is ψ in our case). If one wishes to calculate the Berry phase in the singular gauge by using the multivalued wave function ψ', there is an additional term that should be included in the Berry phase formula [see Eq. (5.12) in Ref. [141] which ensures gauge invariance. We note that our results differ from Refs. [67, 68], which have used multivalued wave functions and Eq. (3.16) to calculate the Berry phase.

3.2.4 Synthetic anyons are not emergent quasiparticles

From the illustration of the single-particle density in Fig. 3.6 we see that at the position of every solenoid probe there is a cusplike dip, i.e., a missing electron charge, which is found to be $\Delta q = -q(1 - \alpha)$ from the single-particle density. We have already noted that it is tempting to identify the composite of a missing electron charge Δq, and a solenoid with flux Φ with Wilczek's

charge-flux-composite anyon [4, 5]. Now we show that such an interpretation is erroneous. When a probe traverses a closed path C, the system acquires the Berry phase $\gamma = 2\pi\langle n\rangle_C$. Let us try to calculate the missing charge by a different route using the Aharonov-Bohm phase, and by assuming that we are dealing with a charge-flux-composite. To this end, let us denote the missing charge q^*, and check whether we obtain the same result as with the single-particle density. When the charge q^* traverses the path C, it will acquire the Aharonov-Bohm phase $q^*\Phi_C/\hbar$, where $\Phi_C = \langle n\rangle_C\Phi_0$ is the total magnetic flux within the path C (we have assumed unity filling of the LLL). To obtain the Berry phase, we should include the Aharonov-Bohm phase acquired by the solenoid with flux $\alpha\Phi_0$ that circulates around the charge $q\langle n\rangle_C$, which is equal to $q\langle n\rangle_C\alpha\Phi_0/\hbar$. By identifying

$$\gamma = 2\pi\langle n\rangle_C = \frac{q^*\Phi_C}{\hbar} + \frac{q\langle n\rangle_C\alpha\Phi_0}{\hbar},$$

we find

$$q^* = -q(1+\alpha) \neq \Delta q = -q(1-\alpha).$$

This difference may come as a surprise, because an equivalent calculation for anyons in the FQHE yields identical expressions for the missing charge from the single-particle density and from the Aharonov-Bohm calculation of q^*.

To understand the obtained result, first we note that the external solenoid probe acts as a ladle that stirs the electron sea around, and the Aharonov-Bohm phase depends on the movements of the electrons in the sea, and not of the missing charge. When the missing charge corresponds to the quasiparticle, as in the FQHE, then $q^* = \Delta q$ because the motion of (quasi)holes uniquely corresponds to the motion of the electron sea. However, the missing charge here is not a quasi-hole, and we cannot interpret the missing charge attached to the solenoid probe as Wilczek's charge-flux-tube composite. One way to understand this difference is to assume that the electron sea is a superfluid, and the Aharonov-Bohm phase acquired by stirring the ladle would be zero.

3.2.5 Fusion rules of synthetic anyons

The conclusion of the previous section has impact on the fusion rules of synthetic anyons. The fusion rule states that the exchange phase Γ_S of a particle formed by combining n identical anyons with exchange phase γ_S is $\Gamma_S = n^2\gamma_S$. The fusion rules depend on the physical microscopic process which corresponds to the fusion.

For example, suppose that we have $N = 4$ solenoid probes in the system with flux $\alpha\Phi_0$, i.e., we have two pairs of probes. Next, we slowly bring together (merge) two of the solenoids from each pair, thereby forming a system with $N = 2$ solenoid probes with flux $2\alpha\Phi_0$. This system is identical to the one we have explored with α replaced by 2α mod 1. Thus, the exchange phase changes from $\pi(\alpha - 1)$ to $\pi[(2\alpha\bmod1) - 1]$. This is not the exchange phase $2^2\pi(\alpha - 1)$

expected from fusing two anyons. This is related to the fact that we cannot interpret the missing charge attached to a solenoid probe as Wilczek's charge-flux-tube composite, because in that case the standard fusion rules would be applicable.

Let us now consider the fusion process as pairing the solenoids two by two in the following manner. Suppose that we have two pairs of probes, i.e., $N = 4$ solenoid probes, with flux $\alpha \Phi_0$ in the system located at $\{\eta_1, \eta_2, \eta_3, \eta_4\}$. The wave function ψ is given by (3.9). Two solenoids are paired so that they remain separated by a small constant vector. For each pair we use center-of-mass and relative coordinates

$$X_c = \frac{\eta_1 + \eta_2}{2}, \quad X_r = \frac{\eta_1 - \eta_2}{2}$$
$$Y_c = \frac{\eta_3 + \eta_4}{2}, \quad Y_r = \frac{\eta_3 - \eta_4}{2}.$$

If we encircle the first pair of solenoids at X_c along a circle of radius R around the second pair at Y_c, which is held static, this process can be described as

$$X_c'(\theta) = Y_c + Re^{i\theta} = Y_c + \lambda,$$

where λ is a complex coordinate which moves around the closed path $C = \partial S$, a circle of radius R. Then the coordinates of the first pair are moved according to

$$\eta_1' = Y_c + X_r + \lambda, \quad \eta_2' = Y_c - X_r + \lambda.$$

The Berry phase acquired in this process is given by

$$\Gamma = i \int_0^{2\pi} d\theta \langle \psi | \frac{\partial}{\partial \theta} \psi \rangle.$$

Since the normalization factor of the wave function is single-valued in θ, it does not contribute to the Berry phase for a closed path. Taking into account the expression for the charge density and the result

$$\frac{d\eta_{1,2}'}{d\theta} = \frac{d\lambda}{d\theta},$$

we obtain

$$\Gamma = i \oint_C d\lambda \frac{\alpha}{2} \int d^2z \left[\frac{\rho(z)}{z - \eta_1'} + \frac{\rho(z)}{z - \eta_2'} \right]$$
$$+ i \oint_C d\bar{\lambda} \left(\frac{\alpha - 2}{2} \right) \int d^2z \left[\frac{\rho(z)}{\bar{z} - \bar{\eta}_1'} + \frac{\rho(z)}{\bar{z} - \bar{\eta}_2'} \right].$$

Denoting

$$\mathscr{I} = \oint d\lambda \int d^2z \left[\frac{\rho(z)}{z - \eta_1'} + \frac{\rho(z)}{z - \eta_2'} \right], \tag{3.19}$$

the Berry phase is then

$$\Gamma = i(\alpha \mathrm{Re}\, \mathscr{J} - \bar{\mathscr{J}}).$$

Regarding the contribution of ρ_0 in Eq. (3.19), when λ is integrated anticlockwise, only values of z inside this path contribute $-4\pi i$ to the integral. After this, one calculates the surface integral and uses the relationship between the charge and the magnetic flux Φ_S for the $\nu = 1$ IQH state. Concerning the contribution of $\delta\rho(z)$, first the surface integral is evaluated. This gives us the result

$$\mathscr{J} = -4\pi i \frac{\Phi_s}{\Phi_0} - (1-\alpha) \oint d\lambda \left[\frac{1}{\eta_3 - \eta_1'} + \frac{1}{\eta_4 - \eta_1'} + \frac{1}{\eta_3 - \eta_2'} + \frac{1}{\eta_4 - \eta_2'} \right].$$

Evaluating the contour integral, we obtain

$$\mathscr{J} = -4\pi i \frac{\Phi_s}{\Phi_0} + 8\pi i (1 - \alpha),$$

and, finally, the Berry phase is

$$\Gamma = 4\pi \frac{\Phi_s}{\Phi_0} + 8\pi(\alpha - 1).$$

We can recognize the Aharonov-Bohm phase and the statistical phase $\Gamma_S = 8\pi(\alpha - 1)$ which confirms the fusion rule for anyons.

3.2.6 Experimental realization

It might be interesting to discuss a potential experimental realization, and pertinent challenges, of Hamiltonian (3.8) in ultracold atomic gases. Ultracold atomic gases have been experimentally realized in two dimensions [142,143], and a viable path (although not a simple one) for implementing IQHE states with ultracold atoms is to employ synthetic magnetic fields [144–147]. The missing ingredients are solenoid-like probes. The synthetic vector potential of a solenoid can in principle be achieved with vortex laser beams nonresonantly interacting with two-level atoms [148]. Namely, by exploring Eq. (7) in Sec. II of Ref. [145], one finds that a vortex beam interacting with a two-level atom can yield the Berry connection which corresponds to the vector potential of a solenoid. The vortex phase ensures proper direction of the vector potential; however, to obtain the proper $\sim 1/r$ dependence one must in addition properly adjust the detuning and the intensity of the laser. An additional challenge along this path would be to ensure that the synthetic magnetic flux through every solenoid is identical, so that an exchange of any of the two lasers would depend on the unique statistical parameter (otherwise localized perturbations at the probes could not be referred to as synthetic anyons). The advantages of

ultracold atomic systems are long coherence times and the possibility to relatively easily braid the laser probes.

$$\sim$$

In conclusion, we have presented exact solutions of a model for synthetic anyons in noninteracting many-body systems. The key ingredients in the model are specially tailored external potentials (that could correspond to some external localized probes), which supply the demanded nontrivial topology in the system. The Hamiltonian representing the model is that of noninteracting electrons in a uniform magnetic field (in the IQHE state), and the probes are solenoids with a magnetic flux that is a fraction of the flux quantum. The Fermi level is such that only the lowest Landau-level states are occupied; the localized states which appear at the position of every probe, with energy in the gap, are assumed to be empty. We have found the ground state of this system, and demonstrated that it is anyonic in the coordinates of the probes, when the flux through solenoids is a fraction of the flux quantum $\alpha\Phi_0$. The statistical parameter of synthetic anyons is $\theta = \pi(\alpha - 1)$. We have shown that these synthetic anyons cannot be considered as emergent quasiparticles, and that they cannot be interpreted as Wilczek's charge-flux-tube composites. This observation has consequences on the fusion rules of these synthetic anyons, which depend on the microscopic details of the fusion process.

Chapter 4

Berry phase for a Bose gas on a one-dimensional ring

The work presented in this chapter has been published in the paper:

- M. Todorić, B. Klajn, D. Jukić, and H. Buljan, *Berry phase for a Bose gas on a one-dimensional ring*, Phys. Rev. A **102**, 013322 (2020).

One-dimensional (1D) quantum many-body systems have intrigued mathematicians and physicists for almost a century. Bethe determined an exact solution to the 1D Heisenberg model of a spin-$\frac{1}{2}$ chain employing an ansatz for the wave function [149]. Many exact solutions to other theoretical 1D models accompanied this one, including solution introduced by Girardeau [150] which describes an impenetrable Bose gas. Simple 1D models whose solutions could not be found exactly were explored in detail by effective approaches particularly fitted for one dimension. An important example is the model introduced by Lieb and Liniger [151] which describes a system of identical Bose particles in 1D interacting via δ-function interactions of strength c.

These solutions were considered as nothing more than mathematical curiosities that are not of crucial importance for the real 3D world. However, recent technological progress in trapping ultracold atomic gases led to the experimental realization of many (quasi-)1D models and this revived the interest in studying the theoretical 1D models [152–155] (for a review see Ref. [156]). In experiments, ultracold atoms are loaded in tight, transversely confined, effectively 1D atomic waveguides, where transverse excitations are strongly suppressed [152–155]. These atomic gases are characterized by the Lieb-Liniger (LL) model [151] of contact interactions of arbitrary strength c. In the case of infinite interaction strength $(c \to \infty)$, such bosonic particles may be described by the Tonks-Girardeau (TG) model [150]. The TG regime has been experimentally achieved [153–155] with atoms at low temperatures and linear densities

and with strong effective interactions [157–159]. In the limit of weak interaction, LL model can be described by Gross-Pitaevskii (GP) theory [160].

In this chapter Section 4.1 introduces basic concepts needed to realize and describe 1D quantum many-body systems. In Section 4.2 we focus on a particular system of strongly interacting bosons placed on a 1D ring pierced by a synthetic magnetic flux tube. On the ring there is an external localized delta-function potential barrier. We study the Berry phase associated to the adiabatic motion of the delta-function barrier around the ring. This research is related to the research on synthetic anyons in a noninteracting system in Section 3.2. The barrier produces a cusp in the density and the corresponding missing charge (missing density) cannot be identified as a quasihole. This result confirms the result in Section 3.2 that synthetic anyons cannot be considered as emergent quasiparticles.

4.1 One dimensional bosons

4.1.1 Experimental techniques

We briefly present the experimental techniques for realization of low-dimensional models in ultracold atomic systems. The invention of the laser enabled the development of effective methods for cooling and trapping of atomic vapors. The methods have been developing for more than three decades and they are based on manipulating neutral atoms with various optical (laser) and magnetic fields [161]. Nowadays the gases can be cooled down even to the temperatures in the nano-kelvin regime. An important progress occured in 1995 with the achievement of Bose-Einstein condensates (BECs) in 3D systems of ultracold atoms [162–164].

A standard method to make the motion of the atoms effectively 1D or 2D is by creating an optical potential [165–168] that produces tight confinement by freezing out motion in one or two directions. Let us consider two oppositely directed laser beams, each with the same frequency. The interference of two beams produces the potential that has the form of a static standing wave, with the wave vector equal to the difference of the wave vectors of the two beams. Neutral atoms in an electric field gain dipole moments that are determined by their polarizability. Optical dipole traps depend on the interaction between an induced dipole moment in an atom and an external electric field. There is an interaction of atoms with a radiation field. One can show that the dipole force on atoms is attractive if the laser frequency is red-detuned and repulsive in the case of a blue-detuned laser. The interference between two counter-propagating beams will create an external periodic potential acting on the atom. When the intensity of the laser light field is strong enough, implying a large amplitude of the potential, so that the probability of hopping of atoms from one minimum to the neighbouring one is supressed, the 3D gas of atoms develops into a system of many decoupled 2D disk-like trapping potentials.

A 2D optical lattice can be created when two orthogonal standing waves are superimposed. Atoms are confined to an array of 1D potential tubes, in which the atoms can only move along

the weakly confining axis of the potential tube, thus realizing 1D quantum behaviour. The radial motion is totally eliminated for low-enough temperatures. A 3D optical lattice for atoms is produced by three orthogonal optical standing waves. Atoms can also be trapped by using atom chip traps [169, 170], where the magnetic fields trap atoms close to the surface. This trap is based on the magnetic potential, i.e., coupling of atoms with spin and the magnetic field. A magnetic field is created by a microfabricated structure of the chip, consisting of tiny wires carrying electric currents. If one superimposes an external uniform field perpendicular to the wire axis, this produces a local minimum of the total magnetic field along the line parallel to the wire. The field minimum traps atoms in states with spin antiparallel to the magnetic field, which are called low-field seeking spin states.

4.1.2 Interactions between atoms

Interaction between two neutral atoms at large separation is dominated by the van der Waals attraction, which is the result of electric dipole-dipole interaction between atoms [161]. The form of interaction is $-\alpha/r^6$, where r is the atomic separation. For small separations the interactions are dominated by a strong repulsive core due to the overlap of electron clouds. We introduce a model potential [161] describing this system which has van der Waals form $\sim 1/r^6$ at large distances, and is cut off at short distances by an infinitely hard core of radius r_c:

$$U(r) = \infty \quad \text{for} \quad r \leq r_c, \quad U(r) = -\frac{\alpha}{r^6} \quad \text{for} \quad r > r_c.$$

The core radius is not a realistic representation of the short-distance behaviour of the potential, but it can provide an insight into the main features of scattering of two neutral atoms at low energies. In general, collisions in ultracold regime occur in the channel with the lowest angular momentum, for bosons the scattering is of the s-wave ($l = 0$). In the low-energy limit, the two-body collision problem is totally determined by the s-wave 3D scattering length a, and the scattering amplitude $f(k) = -a/(1 + ika)$. It can be shown that this is the exact scattering amplitude at arbitrary values of k for the Huang's pseudopotential [157]

$$V(\mathbf{r})\psi(\mathbf{r}) = \frac{4\pi\hbar^2 a}{2M_r}\delta(\mathbf{r})\frac{\partial}{\partial r}(r\psi(\mathbf{r})), \tag{4.1}$$

where ψ is the wave function of the relative motion of two atoms and M_r their reduced mass. Therefore, at low temperatures, two-body interactions in ultracold gases may be described by a pseudopotential, where the scattering length a is usually taken as an experimentally found parameter. The interaction is repulsive for positive and attractive for negative scattering lengths a. Let us consider two-body collisions between cold atoms confined transversally by an atom waveguide or highly elongated "cigar"-shaped atomic trap [157]. The system can be described within the pseudopotential approximation and the waveguide potential is replaced by an axially

symmetric 2D harmonic potential of a frequency $\omega_\perp$. If $k_B T \ll \hbar\omega_\perp$ and $E_{int} \ll \hbar\omega_\perp$, where E_{int} is the interaction energy per particle, atoms are in the ground state of transversal potential and the system becomes effectively 1D. In this case it can be shown [157] that pseudopotential (4.1) leads to the effective contact interaction

$$V_{int}(x_i, x_j) = g_{1D}\delta(x_i - x_j), \tag{4.2}$$

where g_{1D} is the effective coupling strength:

$$g_{1D} = 2\hbar^2 a[ma_\perp^2(1 - Ca/\sqrt{2}a_\perp)]^{-1}.$$

Here $a_\perp = \sqrt{\hbar/m\omega_\perp}$ is the transverse oscillator width and $C = 1.4603$ [157]. Using the effect of Feshbach resonance, it is possible to tune the scattering length by varying the strength of an applied magnetic or electric field, and consequently change the atomic interactions [161]. Moreover, since the effective interaction depends also on the strength of transversal confinement, when the system is in a weakly interacting mean-field regime for some value of $\omega_\perp$, then by increasing $\omega_\perp$, the system may be brought to the strongly interacting Tonks-Girardeau regime ($g_{1D} \to \infty$) [157]. Different regimes of 1D bosonic gases are usually characterized by a non-dimensional parameter $\gamma = mg_{1D}/\hbar^2 n_{1D}$, where n_{1D} is atomic density. For $\gamma \ll 1$ the gas is in the mean-field regime, while for $\gamma \gg 1$ in a strongly interacting regime [151, 153–155, 157].

4.1.3 Lieb-Liniger model

The simplest nontrivial model of interacting bosons in the continuum is the one introduced by Lieb and Liniger [151]. This model describes a system of N identical bosons in 1D, which interact through a δ-function potential of strength g_{1D}. For the Lieb-Liniger model, the Hamiltonian is given by

$$H = -\frac{\hbar^2}{2m}\sum_{i=1}^{N}\frac{\partial^2}{\partial x_i^2} + g_{1D}\sum_{i<j}^{N}\delta(x_i - x_j). \tag{4.3}$$

We can parametrize the interaction strength in this model using the interaction parameter $c = mg_{1D}/\hbar^2$. Therefore, $c = 0$ corresponds to free bosons, while $c \to +\infty$ is the hard-core or Tonks-Girardeau limit [150]. As shown by Lieb and Liniger [151], the model can be solved for all values of interaction strength c by employing the Bethe ansatz. One can see the Bethe's wavefunction as the factorization of the scattering of the N particles in the gas into a series of two particle scattering events. A set of quasimomenta determine the eigenstates. If one sets periodic boundary conditions, the behavior of quasimomenta is governed by a set of transcendental Bethe equations. Its eigenfunctions are of the form

$$\psi_B(x_1, \ldots, x_N) = \sum_P A(P)e^{i\sum_n k_{P(n)}x_n},$$

or $x_1 < x_2 < \cdots < x_N$ where the P's are the $N!$ possible permutations of the set $\{1,\ldots,N\}$, k_n are momenta and $A(P)$ are coefficients. A broader review of the Lieb-Liniger model, which is beyond the scope of this dissertation, can be found in Ref. [171]. Our research deals with two regimes of the Lieb-Liniger model - Tonks-Girardeau limit ($c \to +\infty$) and weakly interacting limit $c \ll 1$ described by the Gross-Pitaevskii theory. In the following we review these models.

4.1.4 Tonks-Girardeau model

The Tonks-Girardeau model describes impenetrable 1D Bose gas, corresponding to the limit $c \to +\infty$. We study a system of N identical Bose particles in 1D geometry. The system is exposed to an external potential $V(x)$. The infinitely strong contact repulsion between the bosons imposes a constraint that the bosonic many-body wave function must vanish when the two particles are in contact. As first pointed out by Girardeau [150], this constraint can be implemented by writing the wave function as follows

$$\psi_B(x_1, x_2, \ldots, x_N, t) = 0 \quad \text{if} \quad x_i = x_j, \quad 1 \le i < j \le N. \tag{4.4}$$

Furthermore, the wave function ψ_B should satisfy the Schrödinger equation

$$i\hbar \frac{\partial \psi_B}{\partial t} = \sum_{j=1}^{N} \left[-\frac{\hbar^2}{2m} \frac{\partial^2}{\partial x_j^2} + V(x_j) \right] \psi_B. \tag{4.5}$$

Fermi-Bose mapping connects the Tonks-Girardeau bosonic wave function ψ_B and an antisymmetric many-body wave function ψ_F, which describes a gas of noninteracting spinless fermions in 1D. Let us consider a solution of Eq. (4.5) $\psi_F(x_1, x_2, \ldots, x_N, t)$, which is antisymmetric when two coordinates x_i and x_j are exchanged. Unit antisymmetric function is defined as

$$S(x_1, x_2, \ldots, x_N) = \prod_{1 \le i < j \le N} \mathrm{sgn}(x_i - x_j),$$

where $\mathrm{sgn}(x)$ is the algebraic sign of the coordinate difference $x = x_i - x_j$, i.e., it is $+1(-1)$ if $x > 0 (x < 0)$. In Fermi-Bose mapping, the wave function

$$\psi_B(x_1, x_2, \ldots, x_N, t) = S(x_1, x_2, \ldots, x_N) \psi_F(x_1, x_2, \ldots, x_N, t) \tag{4.6}$$

satisfies Eq. (4.5), hard-core constraint in Eq. (4.4), and has Bose symmetry since the function $S(x_1, \ldots)$ compensates the sign change of $\psi_F(x_1, \ldots)$ when any two particles are exchanged. Therefore, it represents a solution of the Tonks-Girardeau model in arbitrary external potential $V(x)$, which is a sum of one-body external potentials.

This can be proved in the following way. We consider the $N-$dimensional configuration space. The surfaces $x_i = x_j$ divide the configuration space into $N!$ disjoint regions. In every

permutation sector, the function S is constant, and equal to either +1 or -1. As a result ψ_B satisfies the Schrödinger equation throughout the allowed portion of configuration space [all $|x_i - x_j| > 0 (i \neq j)$], if ψ_F obeys it. The boundary condition is satisfied because of the Pauli exclusion principle set on ψ_F. The Bose symmetry of ψ_B is provided by an antisymmetric function S. Thus, we conclude that ψ_B is a solution of the Schrödinger equation satisfying Bose statistics, having the same energy as ψ_F, and satisfying the same boundary condition.

Very often the fermionic wave function ψ_F can be constructed as the Slater determinant,

$$\psi_F(x_1, \ldots, x_N, t) = \frac{1}{\sqrt{N!}} \det_{m,j=1}^{N} \left(\psi_m(x_j, t) \right), \tag{4.7}$$

where $\psi_m(x, t)$ are N orthonormal single-particle wave functions satisfying a set of uncoupled single-particle Schrödinger equations.

$$i\hbar \frac{\partial \psi_m}{\partial t} = \left[-\frac{\hbar^2}{2m} \frac{\partial^2}{\partial x^2} + V(x) \right] \psi_m(x, t), \quad m = 1, \ldots, N. \tag{4.8}$$

As a result, because of the Fermi-Bose mapping, the many-body problem of strongly interacting bosons in 1D is equivalent to solving the single-particle equations (4.8). We point out that the above proof cannot be generalized to systems of particles which move in higher dimensions. Namely, it is not possible to construct generalization of the function S in more than one dimension since one cannot separate the configuration space into disjoint regions by hyperplanes $x_i = x_j$. In two or more dimensions one can hold all particles but one fixed and move the remaining particle about throughout the box containing the system without encountering any of the fixed particles. On the contrary, in one dimension the motion of one particle is blocked by the presence of other particles.

The construction of the many-body wave function through the Fermi-Bose mapping in Eq. (4.6) may also be used in the eigenvalue equation

$$\sum_{j=1}^{N} \left[-\frac{\hbar^2}{2m} \frac{\partial^2}{\partial x_j^2} + V(x_j) \right] \psi_B = E \psi_B,$$

where E denotes the energy of an eigenstate.

Due to the property $|S(x_1, \ldots, x_N)|^2 = 1$, single-particle density of two systems is the same since $|\psi_B|^2 = |\psi_F|^2$. It is important to notice that Fermi-Bose mapping gives exact solutions for an arbitrary external potential $V(x)$. On the other hand, for the Lieb-Liniger model [151] it gives exact solutions when there is no external potential, i.e., when it is zero in the region with atoms (infinite line, half-infinite line, infinitely deep box [172]). The only exception is the linear potential [173].

4.1.5 Gross-Pitaevskii equation

In the regime of weak interaction, i.e., when $c \ll 1$, the wave function of the system described by the Hamiltonian should not differ greatly from the case when there is no interaction, i.e., from noninteracting bosonic 1D gas. At temperature $T \approx 0$ K noninteracting 1D bosonic gas is in the state of Bose-Einstein condensate (BEC) [161]. For a fully condensed system, all particles are in the same single particle state. We assume that in the case of weak interactions all atoms occupy the same state and we use a Hartree or mean-field approach [161]. Atoms are placed on the x-axis and this system is described by the Hamiltonian in Eq. (4.3). The wave function is a symmetrized product of the single-particle wave functions $\phi(x)$ and we write the wave function of the N-particle system as

$$\psi_B(x_1, x_2, \ldots, x_N) = \prod_{i=1}^{N} \phi(x_i). \tag{4.9}$$

The normalization of the wave function $\phi(x)$ is given as $\int dx |\phi(x)|^2 = 1$. Now we use a variational approach and assume that the condensate wave function is $\psi(x) = \sqrt{N}\phi(x)$, and the according particle density $n(x) = |\psi(x)|^2$. We can neglect terms of the order of $1/N$ what is valid for large atom numbers, and find the energy functional for the N-particle wave function

$$E(\psi, \psi^*) = \int dx \left(\frac{\hbar^2}{2m} |\frac{d}{dx}\psi(x)|^2 + V(x)|\psi(x)|^2 + \frac{1}{2}g_{1D}|\psi(x)|^4 \right).$$

A solution for the wave function can be found by minimizing the energy functional under variations of ψ with the constraint that the total number of particles $\int dx |\psi(x)|^2 = N$ stays constant [174]. This is achieved with the Lagrange multiplier μ, which is the chemical potential ensuring constancy of the particle number. One writes $\delta E - \mu \delta N = 0$, and this gives

$$\left(-\frac{\hbar^2}{2m}\frac{d^2}{dx^2} + V(x) + g_{1D}|\psi(x)|^2 \right) \psi(x) = \mu \psi(x).$$

This equation is called Gross-Pitaevskii equation (GPE). It is a type of nonlinear Schrödinger equation, where the total potential consists of the external potential $V(x)$ and a non-linear term $g_{1D}|\psi(x)|^2$ which describes the mean-field potential of the other atoms. Here, one can notice that the eigenvalue is the chemical potential μ, and not the mean energy per particle E/N, what would be the case for linear equation. It has been shown that the GPE is very successful in describing the behaviour of BEC [174].

4.1.6 Synthetic gauge fields with ultracold atoms

Atoms as electrically neutral particles are not able to directly create magnetic phenomena. However, the core of many interesting phenomena, such as the gauge invariance, or the quantum

Hall and Aharonov-Bohm effects, is the coupling of charged particles to the electromagnetic fields. Moreover, it has been shown that magnetism is an important direction in the search for intriguing topologically ordered phases [175]. Therefore, it is of great interest to look for strategies how to create synthetic gauge fields for neutral atoms. The first synthetic magnetic fields were achieved in rapidly rotating BECs. Here, the Coriolis force mimics the Lorentz force. [176, 177]. Another idea is to put the atomic gas in a specially tailored laser field. Because of the atomic interactions with light, laser field behaves as an artificial magnetic field for neutral atoms [145, 147]. The root of this method is the analogy between the Aharonov-Bohm phase [140] and the Berry phase [87] acquired when an atom undergoes adiabatically a closed loop in the tailored laser field [145]. Furthermore, synthetic magnetic fields can also be created in optical lattices. Such methods engineer the complex tunneling matrix elements between lattice sites [178–180], where the nontrivial phases of the complex tunneling parameters are described as Peierls phases. These methods involve shaking of the optical lattice [178], laser assisted tunneling which realizes the Harper Hamiltonian in tilted lattices [179–181] or periodical modulation of optical honeycomb lattice which realizes the Haldane model [182].

4.2 Berry phase for a Bose gas on a 1D ring

The developments of synthetic gauge fields for ultracold atoms have opened the way for investigating topological states of matter in these systems [145, 147, 176–183]. The single-particle topological phenomena are well understood [147, 183]. However, strongly interacting quantum systems coupled to gauge fields can yield intriguing correlated topological states of matter, which are difficult to understand [175]. It is natural to ask whether exactly solvable models coupled to gauge fields can provide some insight. We are interested in 1D quantum particles on a ring, which is pierced with a synthetic magnetic flux-tube (in this geometry the pertinent gauge field cannot be gauged out), and explore the Berry phase [87] as the quantum gas is stirred around the ring with an external local potential. This geometry is readily found in atomtronics - emerging field in quantum technology seeking for ultracold-gas analogs of electronic devices and circuits [184]. An important example of an atomtronic circuit is provided by a Bose-Einstein condensate flowing in a ring-shaped trapping potential, which can be realized using different methods [185–190]. Such systems interrupted by one or several weak barriers and pierced by an effective magnetic flux, have been studied in analogy with the superconducting quantum interference devices (SQUIDs) [186, 191–199]. In particular, in system with weak barriers and weak atom-atom interaction, hysteresis effects have been evidenced [193]. The persistent current phenomenon has been theoretically characterized for 1D bosons in this geometry, for all interaction and barrier strengths [200]. Studies of the Aharonov-Bohm (AB) effect [20] for the density excitations propagated through the ring predicted the absence of the AB oscillations for all interaction regimes [194, 195, 201]. The presence of disorder leads to

crossover from AB to Al'tshuler-Aronov-Spivak oscillations, investigated in the presence of bosonic interaction [202]. This configuration can also serve to study the dynamics of vortices in a quantum fluid [196]. For stronger interactions and higher barriers, Bose gas confined to a ring shaped lattice, has shown the emergence of the effective two-level system of current states, suggesting it to be a cold-atom analog of qubit [197, 198]. Moreover, the study of bosonic Josephson effect in this geometry, has shown that strongly correlated 1D bosonic system exhibits the damping of the particle-current oscillations [199, 203].

In this section we study a system of strongly interacting one-dimensional (1D) bosons on a ring pierced by a synthetic magnetic flux tube. By the Fermi-Bose mapping, this system is related to the system of spin-polarized non-interacting electrons confined on a ring and pierced by a solenoid (magnetic flux tube). On the ring there is an external localized delta-function potential barrier $V(\phi) = g\delta(\phi - \phi_0)$. We study the Berry phase associated to the adiabatic motion of delta-function barrier around the ring as a function of the strength of the potential g and the number of particles N. The behavior of the Berry phase can be explained via quantum mechanical reflection and tunneling through the moving barrier which pushes the particles around the ring. The barrier produces a cusp in the density to which one can associate a missing charge Δq (missing density) for the case of electrons (bosons, respectively). We show that the Berry phase (i.e., the Aharonov-Bohm phase) cannot be identified with the quantity $\Delta q/\hbar \oint \mathbf{A} \cdot d\mathbf{l}$. This means that the missing charge cannot be identified as a (quasi)hole. We point out to the connection of this result and our studies of synthetic anyons in noninteracting systems. In addition, for bosons we study the weakly-interacting regime, which is related to the strongly interacting electrons via Fermi-Bose duality in 1D systems.

4.2.1 Berry phase for one particle on a ring

We start by considering a particle confined on a ring of radius R, containing a localized delta-function potential barrier somewhere on the ring. This particle can be a boson of a synthetic charge q subjected to a synthetic gauge field of a solenoid carrying flux Φ placed in the center of a ring, or an electron of electric charge q coupled with a vector potential of a solenoid with a magnetic flux Φ. In the rest of the paper we will refer to q and Φ as to charge and flux, and we will not distinguish the electric (i.e., real) from the artificial charge and flux which can be engineered in ultracold atomic gases. This system is described by the Hamiltonian

$$H = \frac{1}{2m} \left(-\frac{i\hbar}{R}\frac{\partial}{\partial \phi} - \frac{q\Phi}{2\pi R} \right)^2 + \bar{g}\delta(\phi - \phi_0), \tag{4.10}$$

where $\phi \in [-\pi, \pi]$. In order to simplify calculation, we introduce the dimensionless parameters $\alpha = q\Phi/h$, $g = (2mR^2/\hbar^2)\bar{g} > 0$, and dimensionless energy $\varepsilon = (2mR^2/\hbar^2)E$. Our task is to

solve time-independent dimensionless Schrödinger equation

$$-\left[\left(\frac{\partial}{\partial \phi} - i\alpha\right)^2 - g\delta(\phi - \phi_0)\right]\psi = \varepsilon\psi. \tag{4.11}$$

For $\phi \neq \phi_0$, the delta term vanishes. Thus, for $\phi \in [-\pi, \phi_0\rangle$ we have

$$\psi_l = Ae^{+i(\sqrt{\varepsilon}+\alpha)\phi} + Be^{-i(\sqrt{\varepsilon}+\alpha)\phi},$$

and for $\phi \in \langle\phi_0, \pi]$,

$$\psi_r = Ce^{+i(\sqrt{\varepsilon}+\alpha)\phi} + De^{-i(\sqrt{\varepsilon}-\alpha)\phi}.$$

For the whole domain we write

$$\psi = \theta(\phi_0 - \phi)\psi_l + \theta(\phi - \phi_0)\psi_r. \tag{4.12}$$

Next, we impose boundary conditions: continuity of the wave function $\psi_l(-\pi) = \psi_r(+\pi)$, continuity of its derivative $\psi_l'(-\pi) = \psi_r'(+\pi)$, and continuity of the wave function at ϕ_0. This leads us to the result

$$\begin{aligned}\psi_l = \mathcal{N}e^{i\alpha(\phi+\pi)}\big(&e^{+i\sqrt{\varepsilon}(\phi+\pi-\phi_0)}\sin[\pi(\sqrt{\varepsilon}-\alpha)] \\ &+ e^{-i\sqrt{\varepsilon}(\phi+\pi-\phi_0)}\sin[\pi(\sqrt{\varepsilon}+\alpha)]\big),\end{aligned}$$

and

$$\begin{aligned}\psi_r = \mathcal{N}e^{i\alpha(\phi-\pi)}\big(&e^{+i\sqrt{\varepsilon}(\phi-\pi-\phi_0)}\sin[\pi(\sqrt{\varepsilon}-\alpha)] \\ &+ e^{-i\sqrt{\varepsilon}(\phi-\pi-\phi_0)}\sin[\pi(\sqrt{\varepsilon}+\alpha)]\big),\end{aligned}$$

where $\mathcal{N}$ is the normalization constant:

$$\begin{aligned}\mathcal{N} = \big[2\pi\big(1 &- \cos 2\pi\alpha \cos 2\pi\sqrt{\varepsilon} \\ &+ \frac{\sin 2\pi\sqrt{\varepsilon}}{2\pi\sqrt{\varepsilon}}(\cos 2\pi\alpha - \cos 2\pi\sqrt{\varepsilon}))\big]^{-1/2}.\end{aligned} \tag{4.13}$$

The energy ε can be found by integrating Eq. (4.11) around ϕ_0, which yields $\psi_r'(\phi_0) - \psi_l'(\phi_0) = g\psi(\phi_0)$, i.e., an implicit equation for the energy:

$$\cos 2\pi\alpha - \cos 2\pi\sqrt{\varepsilon} = g\frac{\sin 2\pi\sqrt{\varepsilon}}{2\sqrt{\varepsilon}}. \tag{4.14}$$

Note that for $\alpha = 0, 1, 2, \ldots$ the energy spectrum is mapped onto itself, which means that these cases are related by a simple gauge. Therefore it is sufficient to consider flux in the domain $\alpha \in [0, 1]$.

We are interested in the Berry phase [87] γ when the delta-function travels adiabatically

around the ring: $\phi_0 \to \phi_0 + 2\pi$. The Berry phase is

$$\gamma = \Delta + i \int_{-\pi}^{+\pi} d\phi_0 \int_{-\pi}^{+\pi} d\phi \, \psi^* \frac{\partial}{\partial \phi_0} \psi, \tag{4.15}$$

where Δ denotes the phase difference of the wave function when parameter ϕ_0 is at the endpoints of a closed path [87, 205]. Namely, the wave function is a single-valued function of the variable ϕ, but multivalued in the parameter ϕ_0. The phases of the wave function at endpoints $\pm\pi$ differ as

$$\frac{\psi(\phi_0 = +\pi)}{\psi(\phi_0 = -\pi)} = e^{2\pi i \alpha},$$

i.e., $\Delta = 2\pi\alpha$. By calculating the derivatives, we obtain

$$\gamma = 2\pi\alpha - (2\pi\mathcal{N})^2 \sqrt{\varepsilon} \sin 2\pi\alpha \sin 2\pi\sqrt{\varepsilon}. \tag{4.16}$$
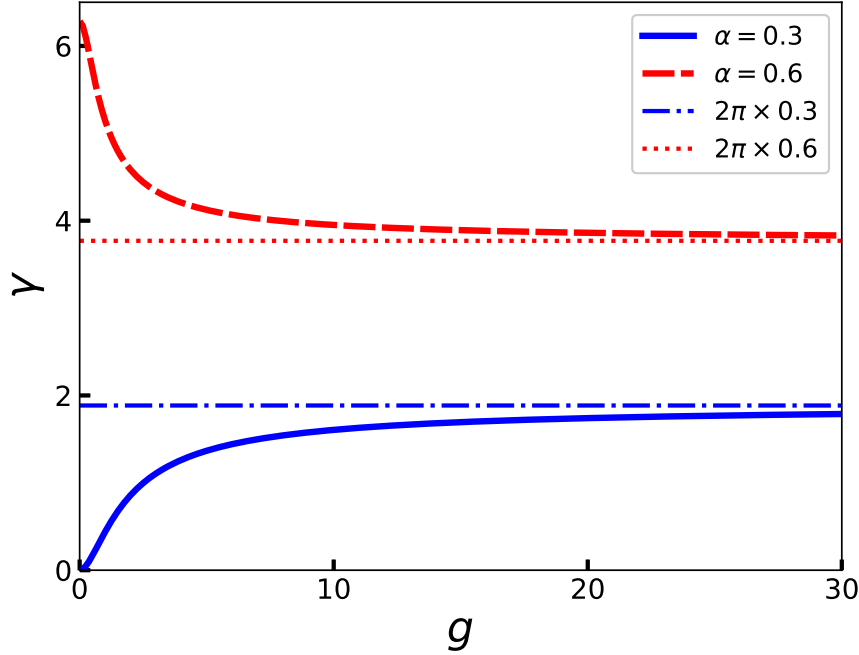
Figure 4.1: The Berry phase as a function of the barrier height g for one particle on a ring. The parameter α describing the flux through the ring is $\alpha = 0.3$ and $\alpha = 0.6$. Horizontal lines denote the asymptotic value of the Berry phase $q\Phi/\hbar = 2\pi\alpha$ for $g \to \infty$.

The dependence of the Berry phase on the height of the potential barrier is shown in Fig. 4.1. For the vanishing barrier, Eq. (4.14) and Eq. (4.16) give $\gamma = 0$ when $\alpha < 0.5$, and $\gamma = 2\pi$ when $\alpha > 0.5$. Both results describe vanishing Berry phase, as expected. As the potential barrier becomes stronger, the Berry phase increases (decreases) for $\alpha < 0.5$ ($\alpha > 0.5$, respectively). In the limit of infinitely strong potential barrier $g \to \infty$, the Berry phase saturates at the value $\gamma = 2\pi\alpha = q\Phi/\hbar$. This result is equal to the Aharonov-Bohm (AB) phase [140] acquired when *one* particle of charge q circles around the solenoid carrying flux Φ.

Results shown in Fig. 4.1 can be explained through the phenomena of quantum-mechanical tunneling and reflection. As the barrier moves, in the classical sense it pushes the particle; the particle can tunnel through, or be reflected from the barrier. Thus, the whole probability density (i.e., the whole charge of the particle) will generally not make a full circle around the ring, but only a part of it. The Berry phase is the AB phase acquired by the amount of probability density that encircled the flux tube. The particle probability density reflected from the moving barrier, also moves around the flux tube and acquires the AB phase. In contrast, the probability density that tunneled through the barrier does not contribute to the AB phase. For the infinite barrier there is total reflection, i.e., one particle of charge q moved around the flux Φ, resulting in the phase $q\Phi/\hbar$.

Finally, we generalize our result and consider a situation where the solenoid of flux Φ is inside the ring, but at the distance $r < R$ from the center of the ring. It can be shown that the wave function ψ_R for a displaced solenoid is related to the wave function ψ by a gauge transformation,

$$\psi_R = \psi \exp\left\{ i\alpha \left[\arctan\left(\frac{R+r}{R-r} \tan\frac{\phi}{2} \right) - \frac{\phi}{2} \right] \right\}.$$

Energy remains the same as in Eq. (4.14); the Berry phase in Eq. (4.16) is also unchanged since the additional gauge factor does not depend on ϕ_0. Thus, our previous analysis is generally valid for a particle on ring threaded by a flux tube anywhere inside the ring.

4.2.2 Berry phase for strongly interacting bosons on a ring

Now we consider a system of N indistinguishable bosons interacting via point-like interactions in the same configuration, described by the Lieb-Liniger model [151] with an additional gauge term:

$$H = \sum_{i=1}^{N} \left[\frac{1}{2m} \left(-\frac{i\hbar}{R} \frac{\partial}{\partial \phi_i} - \frac{q\Phi}{2\pi R} \right)^2 + \bar{g}\delta(\phi_i - \phi_0) \right] + c_{1D} \sum_{1 \leq i < j \leq N} \delta(\phi_i - \phi_j). \tag{4.17}$$

Here c_{1D} is the effective 1D interaction strength. By varying c_{1D}, the system can be tuned from the weakly interacting regime described by the mean field theory, up to the strongly interacting TG regime with infinitely repulsive contact interactions $c_{1D} \to \infty$. In the TG limit, the interaction term of the Hamiltonian can be replaced by a boundary condition on the many-body wave function [150, 156]

$$\Psi_{TG}(\phi_1, \phi_2, ..., \phi_N, t) = 0 \quad \text{if} \quad \phi_i = \phi_j$$

for any $i \neq j$. Now, the Hamiltonian becomes

$$H = \sum_{i=1}^{N} \left[\frac{1}{2m} \left(-\frac{i\hbar}{R} \frac{\partial}{\partial \phi_i} - \frac{q\Phi}{2\pi R} \right)^2 + \bar{g}\delta(\phi_i - \phi_0) \right].$$

The bosonic wave function Ψ_{TG} satisfying the boundary condition and the Schrödinger equation is related to the fermionic wave function Ψ_F, which describes a system of N noninteracting spinless fermions through the Fermi-Bose mapping [150]:

$$\Psi_{TG} = \prod_{1 \leq j < l \leq N} \text{sgn}(\phi_j - \phi_l)\Psi_F. \tag{4.18}$$

Here, Ψ_F is given by the Slater determinant,

$$\Psi_F = \frac{1}{\sqrt{N!}} \det[\psi_k(\phi_j, t)],$$

where $\psi_k(\phi, t)$ denote N orthonormal single-particle wave functions obeying a set of uncoupled single-particle Schrödinger equations

$$i\hbar \frac{\partial \psi_k}{\partial t} = \left[\frac{1}{2m} \left(-\frac{i\hbar}{R} \frac{\partial}{\partial \phi} - \frac{q\Phi}{2\pi R} \right)^2 + \bar{g}\delta(\phi - \phi_0) \right] \psi_k. \tag{4.19}$$

The eigenfunctions of the single-particle Schrödinger equation are given in Eq. (4.12) with normalization constant in Eq. (4.13). The energies of the single-particle states are given by Eq. (4.14); bosons in the TG gas occupy states from the lowest energy state up to the N-th energy state.

We study now the Berry phase arising when the barrier potential is set into adiabatic anticlockwise rotation around the ring. The Berry phase is

$$\gamma = \Delta + i \int_{-\pi}^{+\pi} d\phi_0 \langle \Psi_{TG} | \frac{\partial}{\partial \phi_0} | \Psi_{TG} \rangle, \tag{4.20}$$

where Δ is the phase difference of the wave function at the endpoints [?, 205], which is for N particles given by

$$\Delta = N2\pi\alpha.$$

The second term in Eq. (4.20) is calculated by using the fact that

$$\langle \Psi_{TG} | \partial/\partial\phi_0 | \Psi_{TG} \rangle = \langle \Psi_F | \partial/\partial\phi_0 | \Psi_F \rangle,$$

i.e., one has to calculate the Berry phase for the Slater determinant wave function. This problem was studied in detail in [206, 207], where it was shown that the Berry phase is a sum over the
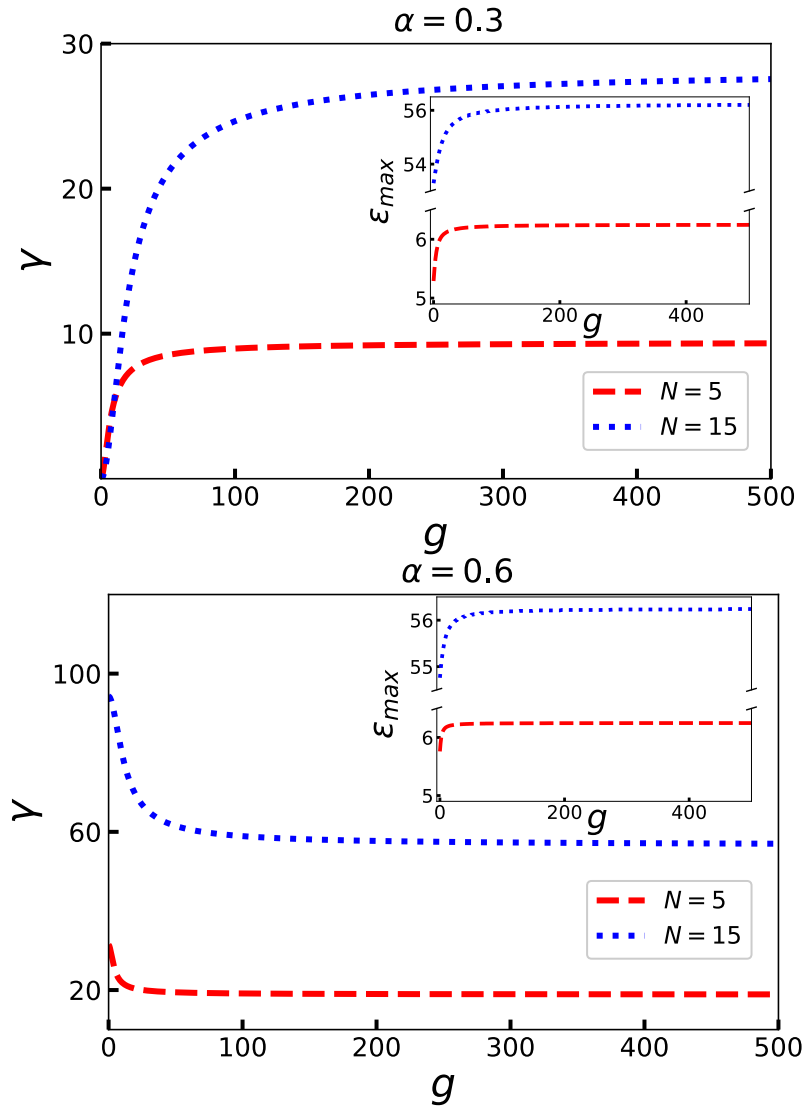
Figure 4.2: Berry phase for N Tonks-Girardeau bosons as a function of the strength of the barrier g for $\alpha = 0.3$ (upper plot) and $\alpha = 0.6$ (lower plot). The insets show the energy of the highest occupied single-particle state as a function of g.

Berry phases of single-particle states

$$\gamma = \Delta + i \sum_{n=1}^{N} \int_{-\pi}^{+\pi} d\phi_0 \langle \psi_n | \frac{\partial}{\partial \phi_0} | \psi_n \rangle.$$

In the previous section, we have already solved the one particle case in Eq. (4.16), which leads to

$$\gamma = N2\pi\alpha - \sum_{n=1}^{N} (2\pi \mathcal{N}_n)^2 \sqrt{\varepsilon_n} \sin 2\pi\alpha \sin 2\pi \sqrt{\varepsilon_n}. \tag{4.21}$$

The dependence of the Berry phase in Eq. (4.21) on the strength of the potential barrier g is illustrated in Fig. 4.2, for different N and α. We do not plot the phase modulo 2π for clearer view. For $g = 0$, the Berry phase is zero or an integer of 2π. By increasing the barrier strength, the Berry phase monotonically increases for $\alpha = 0.3$ (decreases for $\alpha = 0.6$), and saturates at the value

$$\gamma = N2\pi\alpha = Nq\Phi/\hbar \tag{4.22}$$

in the limit $g \to \infty$. This is the AB phase collected when N particles of charge q circle around the solenoid with flux Φ. Results in Fig. 4.2 can again be interpreted through the tunneling and reflection of the particle density from the moving barrier, in the same fashion as for a single-particle.

Here we take into account that single-particle states that contribute to the Berry phase (4.21) have different energies, and consequently different transmission probabilities. In the inset of Fig. 4.2 we plot the highest single-particle energy contributing to the Berry phase. For large g this energy saturates, confirming the behavior of the Berry phase on the plot.

4.2.3 Missing density (missing charge) is not an emergent quasiparticle

The single-particle density of TG gas described by Eq. (4.18) is given as $n(\phi) = \sum_{k=1}^{N} |\psi_k|^2$ [150]. In Fig. 4.3 we show the single-particle density when an impenetrable delta barrier is placed at $\phi_0 = 0$. At the position of the barrier, there is a cusp in the density. For a sufficiently large number of particles, one can define a missing synthetic charge Δq for the system of TG bosons, or the missing electric charge Δq for noninteracting electrons on the Fermi side of the mapping.

We calculate the missing charge in the thermodynamic limit, $N \to \infty$, $R \to \infty$, $N/2\pi R = \tilde{n}_0$. The coordinate space is now $x = R\phi \in \langle -\infty, \infty \rangle$. If there is no barrier, the particle density is uniform and equal to $\tilde{n}_0$. For simplicity, suppose that we insert an impenetrable barrier with $g \to \infty$ at $x = 0$. In this limit, it is straightforward to calculate the single particle density,

$$\tilde{n}(x) = \tilde{n}_0 - \frac{\sin(2\pi\tilde{n}_0 x)}{2\pi x}. \tag{4.23}$$

The missing charge is

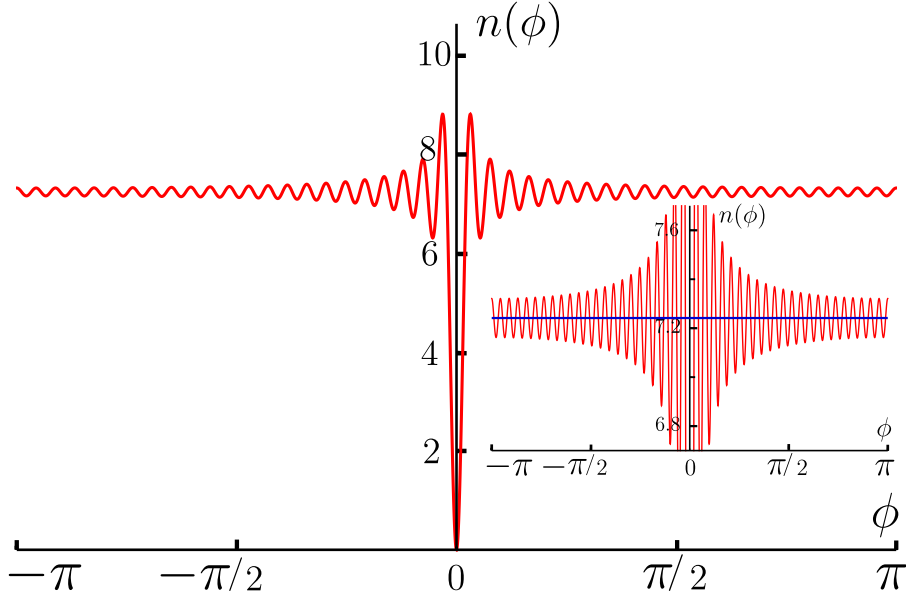$$\Delta q = q \int_{-\infty}^{\infty} [\tilde{n}(x) - \tilde{n}_0] dx = -\frac{q}{2}. \tag{4.24}$$

Figure 4.3: Single-particle density for $\alpha = 0.3$, $N = 45$ particles and infinite barrier $g = \infty$. Inset shows magnified view of single-particle density and horizontal blue line at $(N+1/2)/2\pi$.

Thus, the barrier induces density fluctuations which carry fractional charge $-q/2$.

In order to shed more light onto this result, we return to the geometry of the (finite) ring. For N particles on the ring, in the absence of the barrier, the angular density is $n_0 = N/2\pi$. We then insert an impenetrable barrier at $\phi_0 = 0$. The energy of the k-th single-particle state for $g = \infty$ is $\varepsilon = k^2/4$, $k = 1, 2, \ldots$, and the single particle density is

$$
\begin{aligned}
n(\phi) &= \sum_{k=1}^{N} |\psi_k|^2 = \sum_{k=1}^{N} \frac{1}{2\pi}(1 - \cos k\phi) \\
&= \frac{N+1/2}{2\pi} - \frac{1}{4\pi}\left(\frac{\sin(N\phi)}{\tan(\phi/2)} + \cos(N\phi)\right).
\end{aligned} \tag{4.25}
$$

The density $n(\phi)$ integrated over the ring gives N particles, i.e., the number of particles on the ring is unchanged after we insert the delta barrier. The first term in Eq. (4.25), i.e., $(N+1/2)/2\pi$, corresponds to the uniform density of $N+1/2$ particles, and the second term gives density fluctuations of the missing $(-1/2)$ charge, in agreement with the fact that the number of particles does not change after insertion of the barrier. This is supported with the inset in Fig. 4.3, where we show the single-particle density $n(\phi)$, and the horizontal line at $(N+1/2)/2\pi$, which goes through the center of the density oscillations away from the barrier.

Note that we cannot use a formula analogous to (4.24) to calculate the missing charge on the ring, simply because $\int_{-\pi}^{\pi}[n(\phi) - n_0]d\phi = 0$, i.e., the number of particles does not change as we insert the delta barrier. One could try to resort to a formula such as $\int_{-\phi^*}^{\phi^*}[n(\phi) - n_0]d\phi = 0$, i.e., to integrate over a region around the density dip induced by the barrier, but it is difficult to unambiguously define the region of integration $[-\phi^*, \phi^*]$ because the decay of the density oscillations is algebraic, i.e., without a scale. However, the thermodynamic limit allows for

an unambiguous calculation of the missing charge via Eq. (4.24), because in this limit $(N + 1/2)/2\pi R = N/2\pi R = \tilde{n}_0$.

It may be tempting to interpret the obtained missing fractional charge as a fractional quasiparticle. When the delta barrier moves around the ring, one may consider the Berry phase (or Aharonov-Bohm phase for electrons) as the phase acquired by the motion of the missing charge. If the missing charge was caused by a quasiparticle excitation, this picture would be correct, however, this is not the case. The Berry phase acquired for a barrier with $g = \infty$ is $Nq\Phi/\hbar$. On the other hand, the AB phase acquired by the motion of the missing charge around the ring is $\Delta q\Phi/\hbar$. Since $\Delta q\Phi/\hbar \neq Nq\Phi/\hbar$ modulo 2π, we conclude that one cannot interpret the Berry phase as the motion of the missing charge, but rather as the movement of the particles reflected from the barrier as it pushes them around the solenoid. The cusp in the density cannot be considered as a quasiparticle.

While this conclusion seems clear and perhaps obvious in this 1D system, we find that it provides insight into studies of braiding of fractional fluxes in 2D electron gases in magnetic fields [67, 204]. More specifically, consider a 2D electron gas in a magnetic field in the IQH state. When this system is pierced with flux-tubes carrying fractional fluxes, it can be shown that braiding of fractional fluxes has anyonic properties [204]. One can ask whether the missing charge around these fluxes behaves as a quasiparticle [67] or not [204]. We have found, in consistency with this report, that the missing charge around these fluxes cannot be considered as a quasiparticle [204].

4.2.4 Berry phase for weakly interacting bosons on a ring

Now we turn to the weakly interacting regime described by the Gross-Pitaevskii theory (e.g., see Ref. [174]). The GP equation for our problem is given by

$$
\begin{aligned}
\frac{1}{2m} \left(-\frac{i\hbar}{R}\frac{\partial}{\partial \phi} - \frac{q\Phi}{2\pi R} \right)^2 \psi + \bar{g}\delta(\phi - \phi_0)\psi \\
+ c_{1D}N|\psi|^2\psi = \mu\psi(\phi;\phi_0),
\end{aligned}
\tag{4.26}
$$

where μ is the chemical potential. Without loss of generality, we assumed that the solenoid is placed in the center of the ring. The effect of interactions is contained in a non-linear mean field term. We are interested in the behavior of the Berry phase in dependence of the strength of the mean field interaction $c_{1D}N$. We calculate the Berry phase numerically following Ref. [205]. The delta barrier is approximated as a rectangular potential barrier. The evolution parameter, angle ϕ_0, is discretized to obtain a set of T equidistant points denoted by $\phi_0(t)$. The wave function $\psi(\phi;\phi_0(t))$, corresponding to the barrier position at $\phi_0(t)$, is the lowest single-particle eigenstate found by diagonalization of Eq. (4.26). The overlap at two

different points is $M(k,l) = \langle \psi(\phi;\phi_0(k)) | \psi(\phi;\phi_0(l)) \rangle$, and the product

$$U = M(0,1)M(1,2)...M(T,0)$$

gives the Berry phase

$$\gamma_0 = -\arg(U).$$

Note that γ_0 is the Berry phase per particle since we discuss now the mean field regime. The mean-field many-body wave function is given by $\prod_{i=1}^{N} \psi(\phi_i;\phi_0)$, from which we find the Berry phase $\gamma = N\gamma_0$.
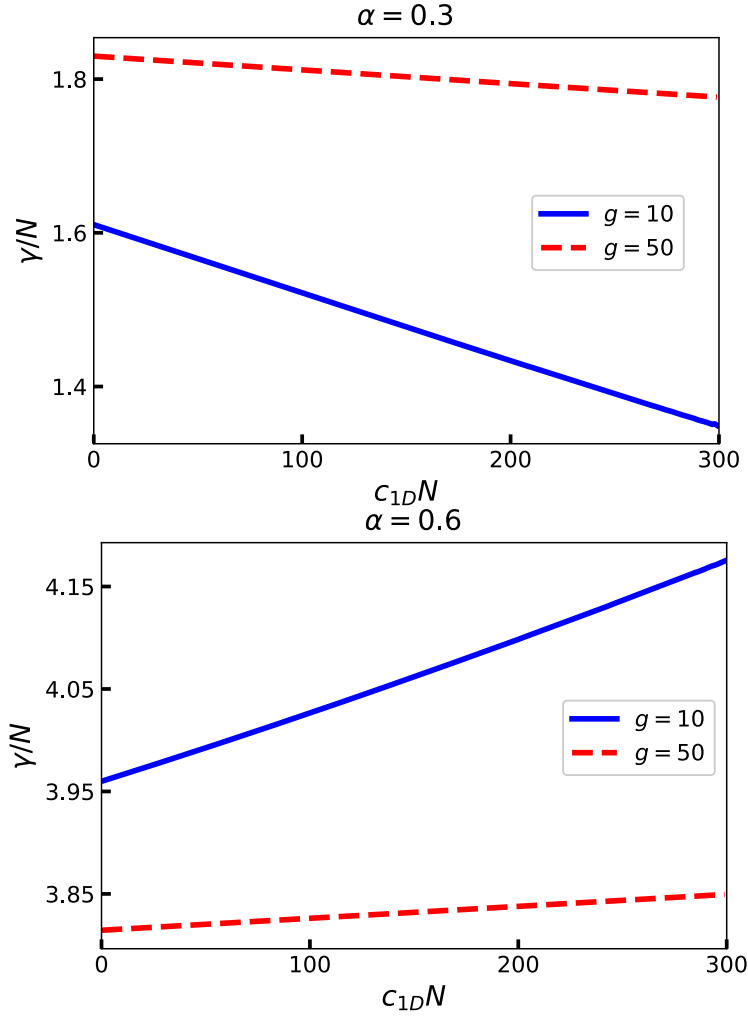
Figure 4.4: Berry phase per particle as a function of $c_{1D}N$ calculated in the mean field regime. Results are shown for two values of the flux: $\alpha = 0.3$ and $\alpha = 0.6$, and two different barriers corresponding to $g = 10$ and $g = 50$.

In Fig. 4.4 we show the dependence of the Berry phase per particle on the strength of the effective potential $c_{1D}N$, for different barrier strengths. With the increase of $c_{1D}N$, the chemical potential increases as well. This means that, effectively, increase of $c_{1D}N$ should lead to the same trend in the behavior of the Berry phase as the decrease of the barrier strength g, since the

states with higher energy tunnel more easily through the barrier. We see that this is indeed the case by comparing Fig. 4.1 and Fig. 4.4. For $\alpha = 0.3$ ($\alpha < 0.5$), the Berry phase per particle γ/N decreases with the increase of $c_{1D}N$; the same trend occurs when g is decreased for a single particle at $\alpha = 0.3$ as depicted in Fig. 4.1. For $\alpha = 0.6$ ($\alpha > 0.5$), we see that γ/N increases with the increase of $c_{1D}N$; the same trend occurs when g is decreased for a single particle at $\alpha = 0.6$. This is consistent with the interpretation of the Berry phase via reflection and transmission of the particles through the moving barrier.

$$\sim$$

In conclusion, we have studied the Berry phase in a system of interacting 1D bosons on a ring, with an external localized delta-function potential on the ring, and a synthetic solenoid threading the ring. We have calculated the Berry phase associated to the adiabatic motion of the delta-function potential around the ring. Results are shown for a single particle, for the impenetrable Tonks-Girardeau bosons (where identical results hold for noninteracting spinless electrons via Fermi-Bose mapping), and interacting bosons in the Gross-Pitaevskii mean field regime. The behavior of the Berry phase can be explained via quantum mechanical reflection and tunneling through the moving barrier which pushes the particles around the ring. For an impenetrable barrier, the Berry phase is given by $Nq\Phi/\hbar$, where q is the synthetic charge of one particle, Φ is the flux through the solenoid, and N is the number of particles. These results provide insight into systems of BECs in toroidal traps used in the context of atomtronics. In addition, our results provide insight into the interpretation of the Berry phase obtained when fractional fluxes piercing a 2D electron gas in the IQH state are braided [204]. An infinite barrier expels the particle density away from itself, leading to a cusp in the density profile, to which one can associate a missing density, i.e., a missing charge Δq. We have shown that the Berry phase cannot be identified with the quantity $\Delta q/\hbar \oint \mathbf{A} \cdot d\mathbf{l}$, which shows that the missing density (charge) cannot be identified as a (quasi)hole.

Chapter 5

Conclusions

In three spatial dimensions particles are classified into bosons and fermions depending on whether they obey the Bose-Einstein or the Fermi-Dirac statistics. The many-body wave function is symmetric under permutations of identical bosons, but antisymmetric under permutations of identical fermions. According to the spin-statistics connection, bosons are particles with integer spin, while fermions are particles with half-integer spin.

In 2D systems, new possibilities for statistics and spin arise. The quantum statistics is not limited to the Bose-Einstein and the Fermi-Dirac cases, but rather it is a continuous interpolation between bosons and fermions. Particles with any statistics in between are called *anyons* [3–5]. They are characterized by a fractional spin, or more generally by fractional quantum numbers. The emergence of anyons arises from the peculiar topological properties of the configuration space of collections of identical 2D particles [6].

The paradigmatic realization of anyons is found in the FQHE [23, 25] where localized quasiparticle excitations have a fractional elementary charge [25] and statistics [26, 27]. Other systems realizing anyons are spin systems (quantum spin-liquids) which realize the Kitaev model [8] and systems supporting Majorana zero-modes [62, 63]. Apart from the fundamental motivation for exploring anyons, non-Abelian anyonic excitations hold potential for technological advances, since they could be used for robust topological quantum computation [7, 8]. A lot of work needs to be done before experiments will be able to efficiently detect and manipulate anyons, especially for fault tolerant quantum computing [7].

In the present thesis we contribute to the study of less traditional schemes for realizing and manipulating anyons. We have proposed an experimental realization of the original Wilczek's model for anyons in 2D electron gas placed in a perpendicular magnetic field, which gives rise to the IQHE. Moreover, we have presented exact solutions of a model for synthetic anyons in a non-interacting quantum many-body system, which was considered in [67, 68]. We have shown that synthetic anyons cannot be considered as emergent quasiparticles. Following this research, we have studied a system of strongly interacting bosons placed on a 1D ring pierced by a synthetic magnetic flux tube. On the ring there is an external localized delta-function

potential barrier and we have explored the Berry phase associated to its motion. The barrier produces a cusp in the density and we have shown that the corresponding missing charge cannot be identified as a quasihole.

In Chapter 1, we have reviewed the quantum statistics and introduced the concept of fractional statistics and anyons. We have explained topological properties of the configuration space of collections of identical particles, showing a crucial difference between 2D and 3D. The fundamental group of this space in 2D is the braid group, which is the root of anyonic statistics. The braid group governs the exchange statistics of anyons. We have explained Abelian and non-Abelian anyons and fusion of anyons. After the behaviour of a charged particle in an electromagnetic field and Aharonov-Bohm phase has been described, we have presented the prototype of anyons, Wilczek's charge-flux-tube composite. We have reviewed different physical realizations of anyons and described topological quantum computation, an approach to fault-tolerant quantum computation.

In Chapter 2, we have reviewed the Quantum Hall Effect, which is the most prominent system hosting anyons. First, we have explained the concept of the geometric phase and derived the Berry phase when a time-dependent set of parameters is moving align a certain closed path in the parameter space. We have interpreted Aharonov-Bohm effect in the light of the Berry phase and defined the Berry's phase as an important example of holonomy. Afterwards, we have described the Quantum Hall Effect, both integer and fractional, and explained the quasiparticles emerging in the FHQ state which behave as Abelian or non-Abelian anyons.

In Chapter 3 we have considered new mechanisms for the realization and signatures of anyons in non-interacting systems. We have proposed an experimental realization of the original Wilczek's model for Abelian anyons, composites formed from charged particles and magnetic flux tubes. First, we have proposed a scheme for realizing charged flux tubes, in which a charged object with an intrinsic magnetic dipole moment is placed between two semi-infinite blocks of a high-permeability μ_r material, and the images of the magnetic moment create an effective flux tube. A 2D electron gas (2DEG) is placed in a perpendicular uniform magnetic field, which gives rise to the IQHE. Then we have sandwiched the 2DEG between two semi-infinite blocks of high-μ_r material, assumed to have a fast temporal response. For this system, we have found the exact many-body wave function. We have discussed possible implementations of the proposed system, the obstacles, and possible ways to overcome them. We have shown that the signature of anyons is a slight shift of the Hall conductance which can be experimentally measured. Afterwards, we have presented exact solutions of a model for synthetic anyons in a non-interacting quantum many-body system, which was considered in [67, 68]. This model is represented by the Hamiltonian for non-interacting electrons in 2D, in a uniform magnetic field, pierced with solenoids with a magnetic flux that is a fraction of the flux quantum. We have found analytically and numerically the ground state of the model when only the LLL states are occupied. We have calculated the statistical parameter using the Berry phase and we have shown that the ground state is anyonic in the coordinates of the probes. We have shown

that these synthetic anyons cannot be considered as emergent quasiparticles.

Chapter 4 focuses on a system of 1D bosons coupled to synthetic gauge fields. Namely, strongly interacting quantum systems coupled to gauge fields can yield intriguing correlated topological states of matter which are difficult to understand. In this light, we asked whether exactly solvable 1D quantum many body models coupled to gauge fields can provide some insight into strongly correlated states. In particular, the research presented in this chapter is aimed at deeper understanding of synthetic anyons in noninteracting systems. We have begun by reviewing the physics of 1D interacting bosonic systems. We have explained experimental techniques for realization of 1D models in ultracold atomic systems and how such systems can be theoretically described using the Lieb-Liniger model, Tonks-Girardeau model and Gross-Pitaevskii equation. We have discussed how synthetic gauge fields can be achieved in ultracold atomic systems. Then, we have investigated a particular system of strongly interacting bosons placed on a 1D ring pierced by a synthetic magnetic flux tube. An external localized delta-function potential barrier has been placed on the ring. We have studied the Berry phase associated to the adiabatic motion of the delta-function barrier around the ring as a function of the strength of the potential and the number of particles. The system of strongly interacting bosons has been related to the system of noninteracting spinless fermions. We have shown that the quantum mechanical reflection and tunneling through the moving barrier explains the behavior of the Berry phase. Finally, we have shown that the barrier produces a cusp in the density to which we have associated a missing charge Δq (missing density) for the case of electrons (bosons). One might interpret the obtained missing fractional charge as a fractional quasiparticle. However, we have shown that the missing charge cannot be identified as a (quasi)hole. We point out that this result is related to the studies of synthetic anyons in noninteracting systems [204], where we have shown that local perturbations in the density around the flux tubes cannot be identified as emergent quasiparticles.

Poglavlje 6

Prošireni sažetak

6.1   Uvod

Kvantna statistika ima fundamentalnu teorijsku važnost u kvantno-mehaničkom pogledu na svijet. Naime, fizikalno ponašanje skupine identičnih čestica nije određeno samo interakcijama, već i statistikom čestica. Identične čestice su one čestice čiji je hamiltonijan simetričan prilikom zamjene čestica uz pretpostavku da čestice imaju ista intrinzična svojstva [1]. U kvantnoj mehanici identične su čestice neraspoznatljive. Ta činjenica uvodi određene simetrijske zahtjeve na ukupnu višečestičnu valnu funkciju koja opisuje sustav mnoštva identičnih čestica prilikom zamjene bilo koje dvije čestice. U tri prostorne i jednoj vremenskoj dimenziji [(3+1)D] postoje samo dvije moguće simetrije i čestice su klasificirane kao bozoni i fermioni ovisno o tome prate li Bose-Einsteinovu ili Fermi-Diracovu statistiku [1]. Višečestična valna funkcija jest simetrična prilikom permutacije identičnih bozona te antisimetrična prilikom permutacije identičnih fermiona. Značajno je da su simetrijski zahtjevi blisko povezani sa spinom čestica. Prema teoremu spina i statistike, bozoni su čestice s cjelobrojnim spinom, dok su fermioni čestice s polucjelobrojnim spinom [2]. Dugo vremena smatralo se da su bozoni i fermioni jedine mogućnosti statistike. To vrijedi za čestice koje se gibaju u najmanje tri dimenzije (3D), ali u dvije dimenzije (2D) situacija postaje zanimljivija. Naime, kvantna statistika postaje neprekidna interpolacija između Bose-Einsteinova i Fermi-Diracova slučaja. Čestice koje slijede necjelobrojnu statistiku koja se javlja između ta dva slučaja zovu se *anyoni* i tema su ove disertacije [3–5]. Primjenom teorema o spinu i statistici, može se zaključiti da su anyoni karakterizirani necjelobrojnim spinom, ili općenitije, necjelobrojnim kvantnim brojevima. Nove mogućnosti spina i statistike objasnili su Leinaas i Myrheim koji su prepoznali podrijetlo koncepta necjelobrojne statistike u neobičnim topološkim svojstvima konfiguracijskog prostora skupine identičnih čestica [6]. Veliki interes za anyonima dolazi od činjenice da ne-Abelove anyonske kvazičestice topoloških stanja materije mogu postati građevni elementi topoloških kvantnih računala koji su otporni na greške (*fault-tolerant*) [7, 8]. Kvantna informacija bi u ovakvim sustavima bila topološki zaštićena i otporna na perturbacije iz okoline. Napominjemo da se pojam statistike na zamjenu

odnosi na fazu koju višečestična valna funkcija koja opisuje identične čestice dobije kad su bilo koje dvije čestice adijabatski pomaknute i pritom zamijenjene [9].

Statistika se može proučiti s formalne točke gledišta [12]. Neka M_N^d označava konfiguracijski prostor skupine N identičnih neprobojnih čestica u d-dimenzionalnom euklidskom prostoru $\mathbb{R}^d$. Konfiguracijski prostor ovog sustava jest

$$M_N^d = \frac{(\mathbb{R}^d)^N - \Delta}{S_N}. \tag{6.1}$$

Dvije su petlje ekvivalentne ili homotopne ako se jedna može dobiti iz druge kontinuiranom deformacijom. Jedna klasa sastoji se od svih homotopnih petlji, a skup svih takvih klasa zove se fundamentalna grupa π_1. Petlje koje pripadaju dvama različitim elementima $\pi_1(M_N^d)$ ne mogu biti povezane kontinuiranim transformacijama. S točke gledišta *path* integrala u kvantnoj mehanici, može se pokazati da amplituda propagatora postaje suma doprinosa pojedinih klasa, pri čemu doprinosi imaju različite težine. Težinski faktori parcijalnih amplituda tvore jednodimenzionalnu (1D) unitarnu reprezentaciju fundamentalne grupe $\pi_1(M_N^d)$ [11]. Potraga za fundamentalnom grupom tog prostora predstavlja standardni problem u algebarskoj topologiji [13, 14], a citirani je rezultat

$$\pi_1(M_N^d) = \begin{cases} S_N, & \text{ako} \quad d \geq 3 \\ B_N, & \text{ako} \quad d = 2, \end{cases} \tag{6.2}$$

pri čemu S_N označava permutacijsku grupu, a B_N *braid* grupu N objekata.

Braid grupa B_N može se algebarski predstaviti preko generatora σ_i, gdje je $1 \leq i \leq N-1$. Generatori zadovoljavaju dvije definirajuće relacije σ_i *braid* grupe $\sigma_i \sigma_{i+1} \sigma_i = \sigma_{i+1} \sigma_i \sigma_{i+1}$ za $i = 1, \ldots, N-2$ i $\sigma_i \sigma_j = \sigma_j \sigma_i$ za $|i-j| \geq 2$. Inverz σ_i označava se s σ_i^{-1}, element identiteta je 1, a centar B_N generiran je s $(\sigma_1 \ldots \sigma_{N-1})^N$. Bitno je napomenuti da općenito vrijedi $\sigma_i^2 \neq 1$.

Braid grupa B_N predstavlja grupu neekvivalentnih krivulja koje se javljaju u adijabatskom transportu N čestica. Topološke klase krivulja koje vode ove čestice of početnih položaja $R_1, \ldots, R_N$ u vremenu t_i do konačnih položaja $R_1, \ldots, R_N$ u vremenu t_f jednoznačno se podudaraju s elementima *braid* grupe B_N. Stoga se dijagrami braid brupe mogu interpretirati kao opis vremenske evolucije identičnih čestica. Da bismo definirali kvantnu evoluciju sustava, promotrimo kako *braid* grupa djeluje na stanja kvantnog sustava. Najjednostavniji mogući slučaj je 1D reprezentacija povezana sa skalarnom kvantnom mehanikom, koja je dana kao

$$\chi(\sigma_i) = e^{i\theta}$$

za sve $i = 1, \ldots, N-1$, gdje je faza θ realni parametar poistovjećen sa statistikom. Kako općenito vrijedi $\sigma_I^2 \neq 1$, θ je bilo koji (eng. *any*) proizvoljni broj. Stoga se čestice s bilo kojom statistikom zamjene definiranom braid grupom nazivaju *anyoni*. Ako u elementarnom pokretu

σ_i jedna čestica napravi zatvorenu petlju oko druge, valna funkcija dobiva fazu 2θ. Posebni slučajevi anyona, $\theta = 0, \pi$ predstavljaju bozone i fermione. 1D reprezentacija je Abelova jer redoslijed operacija nije važan. Ako je statistika zamjene opisana višedimenzionalnim ireducibilnim reprezentacijama *braid* grupe, imamo ne-Abelove anyone i ne-Abelovu *braiding* statistiku. Takve se reprezentacije javljaju kad su valne funkcije multipleti, odnosno postoji degenerirani skup l kvantnih stanja. Element braid grupe predstavljen je sa $l \times l$ unitarnom matricom.

6.2 Realizacije anyona

Ciklička evolucija vanjskih parametara u fizikalnom sustavu vodi na ukupnu evoluciju koja uključuje fazu, a ovisi jedino o geometriji puta koji se prelazi u parametarskom prostoru, tj. faza je neovisna o brzini prelaska različitih dijelova puta. Stoga se ova faza zove geometrijska faza [81–83]. Koncept kvantne geometrijske faze generalizirao je Michael Berry 1984. godine [87]. U bilo kojem kvantnom sustavu sa sporo varirajućim vanjskim parametrima koji je podvrgnut cikličkoj adijabatskoj evoluciji, valna funkcija nakuplja netrivijalnu geometrijsku fazu koja ovisi o detaljima evolucijskog puta, a naziva se *Berryjeva faza*. Berryjeva faza predstavlja važan primjer holonomije u kvantnoj mehanici [92]. Aharonov-Bohm efekt predstavlja fenomen u kojem vektorski potencijal ima fizikalno značenje iako odgovara iščezavajućem elektromagnetskom polju [20]. U tom efektu valna funkcija kvantne čestice naboja q koja se giba duž krivulje $\mathscr{C}$ na kojoj magnetsko polje iščezava, no vektorski potencijal $\mathbf{A} \neq 0$, poprima fazni pomak $\phi = \frac{q}{\hbar} \int_{\mathscr{C}} \mathbf{A} \cdot d\mathbf{r}$ [1]. U radu [87] Berry je pokazao da Aharonov-Bohm faza predstavlja manifestaciju Berryjeve geometrijske faze.

Frank Wilczek uveo je prototip anyona, objekt koji se sastoji od nabijene čestice koja interagira s beskonačno dugom zavojnicom (solenoidom) [3–5]. Kad je gibanje duž solenoida zanemareno, dinamika se odvija u ravnini i sustav je podvrgnut zakonima 2D svijeta. Razmotrimo nerelativističku česticu bez spina, mase m i električnog naboja q koja se giba u magnetskom polju $\mathbf{B}$ beskonačno duge, tanke, cilindrično simetrične zavojnice koja prolazi kroz ishodište i usmjerena je duž z-osi, a Φ je tok kroz zavojnicu. Da bi se odredila statistička svojstva tog kompozita, proučavamo kvantnu mehaniku sustava takvih dviju čestica koji je opisan jednoznačnom, simetričnom valnom funkcijom ψ. Postupnim pomicanjem jednog kompozita oko drugog po punoj petlji, prema Aharonov-Bohm efektu [20], ukupna faza koju valna funkcija ψ nakupi prilikom rotacije od 2π iznosi $\exp(-2iq\Phi/\hbar)$.

Može se pokazati da postoji ekvivalentan opis necjelobrojne statistike gdje je efektivna interakcija zamijenjena kompliciranim rubnim uvjetima. Da bi se eliminirao dugodosežni vektorski potencijal između anyona, provodi se singularna baždarna transformacija tako da je $\mathbf{A}' = \mathbf{A} - \nabla\Lambda(r, \varphi) = 0$. Hamiltonijan postaje hamiltonijan slobodnih čestica, a transformirana valna funkcija je $\psi' = \exp(-iq\Phi\varphi_{12}/\pi\hbar)\psi$, gdje je φ_{12} azimutalni kut relativnog vektora $\mathbf{r}_1 - \mathbf{r}_2$. Valna funkcija ψ' je višeznačna i zadovoljava rubni uvjet $\psi'(\mathbf{r}_2, \mathbf{r}_1) = \exp(-iq\Phi/\hbar)\psi'(\mathbf{r}_1, \mathbf{r}_2)$.

Iz ovog se može vidjeti da ψ' ima Abelovu reprezentaciju *braid* grupe, te predstavlja anyonsku valnu funkciju.

Cjelobrojni kvantni Hallov efekt IQHE [97, 98] i FQHE [23, 25] otkriveni su u posebnom kontekstu poluvodičkih heterostruktura (IQHE u Si MOSFET [97] i FQHE u GaAs-AlGaAs [23] heterospoju), koji se nalazi u jakim magnetskim poljima($\sim$ 10T) i niskim temperaturama($\sim$ mK). Sloj elektrona zatočen je na plohi između dvaju poluvodiča, tj. heterospoju, ili između poluvodiča i izolatora. Niska temperatura i jako magnetsko polje zamrznu gibanje duž smjera okomitog na sloj te se bitna dinamika odvija se u ravnini. Elektroni se u tom sloju mogu idealizirati kao 2D elektronski plin (2DEG) s Coulombovom interakcijom. Osnovno opažanje QHE jest to da dok se magnetsko polje mijenja na fiksnoj elektronskoj gustoći, Hallov otpor ostaje konstantan na konačnim intervalima - platoima. Platoi su razdvojeni intervalima kontinuiranog ponašanja. Vrijednost Hallove vodljivost σ_{xy} na platoima jest

$$\sigma_{xy} = \nu \frac{e^2}{h},\qquad(6.3)$$

gdje je kvantni broj ν cijeli broj za IQHE [97, 98] ili razlomak za FQHE [23, 25]. Pokazuje se da ν odgovara faktoru popunjenja Landauova nivoa. Na platoima je tenzor vodljivosti nedijagonalan, što upućuje na nedisipativan transverzalni tok kao odgovor na primijenjeno električno polje. Hallov koeficijent izražen je preko fundamentalnih fizikalnih veličina i pokazano je da je kvantizacijsko pravilo za QHE topološka kvantizacija [99–102]. Ova relacija eksperimentalno je opažena s iznimno visokom preciznošću, relativna nepouzdanost je 10^{-10} [103].

Postoji nekoliko kandidata za fizikalnu realizaciju čestica s anyonskim svojstvima. Najvažniji fizikalni objekti koji se mogu opisati kao anyoni su kvazielektronska i kvazišupljinska pobuđenja 2D sustava elektrona u jakom magnetskom polju koji pokazuje FQHE [23–25]. Platoi kvantiziranog otpora pokazuju gdje se 2DEG ponaša kao nekompresibilni fluid, što znači da sva nabijena pobuđenja imaju konačni energijski procjep. Kod FQHE, za faktor popunjenja $\nu = 1/m$ za neparan m, za naboj kvazielektrona ili kvazišupljine pokazuje se da je $e^* = 1/m$, dok je statistika ovih Abelovih anyona $\theta = 1/m$ [26–28]. Općenitije, na $\nu = n/(2pn \pm 1)$ vrijednost naboja je $|e^*| = \nu e = e/(2pn \pm 1)$ [94, 106]. Teorija predviđa da se ne-Abelovi anyoni pojavljuju u FQH na posebnim frakcijama popunjenja [29–40], pri čemu je prvo otkriće originalno napravljeno za $\nu = 5/2$ stanje [29]. U ultrahladnim atomskim plinovima napravljeni su teorijski prijedlozi anyona temeljeni na oponašanju FQHE [41, 42]. Drugi primjer sustava koji mogu imati anyonsku statistiku jest Kitaevljev model definiran na 2D spinskoj rešetki [8, 46] gdje niskoenergijska pobuđenja Hamiltonijana mogu biti Abelove ili ne-Abelove kvazičestice. Ovaj model predstavlja platformu za izvođenje topološkog kvantnog računanja. Nadalje, sljedeći primjer anyonskih sustava uključuje Majorana *zero modove*. Ne-Abelovi anyoni imena Isingovi anyoni [62–64] pojavljuju se kao kvazičestice ili defekti koji podržavaju Majorana *zero mod*.

Posljednjih godina javio se veliki interes za anyonima zbog mogućnosti korištenja takvih

objekata u topološkom kvantnom računanju [7, 62, 80]. Naime, Kitaev je pokazao ideju da bi se Hilbertov prostor ne-Abelovih anyona trebao promatrati kao skup kubita, pri čemu su operacije na ne-Abelovim anyonima unitarne operacije koje se ponašaju kao kvantna vrata [8]. U ovoj shemi informacija nije pohranjena lokalno, te je nelokalni prostor stanja neprobojan na lokalne perturbacije, što kubit čini topološki zaštićenim od pogrešaka. Ovaj pristup kvantnom računanju otpornom na greške (*fault tolerant*) pri čemu se unitarna kvantna vrata dobiju iz *braiding* operacija ne-Abelovih anyona poznato je kao topološko kvantno računanje [7, 62, 80].

6.3 Prijedlozi realizacije anyona

Rad predstavljen u ovom odjeljku objavljen je u sljedećim radovima:

- M. Todorić, D. Jukić, D. Radić, M. Soljačić, and H. Buljan, *Quantum Hall Effect with Composites of Magnetic Flux Tubes and Charged Particles*, Phys. Rev. Lett. **120**, 267201 (2018).

- F. Lunić, M. Todorić, B. Klajn, T. Dubček, D. Jukić, H. Buljan, *Exact solutions of a model for synthetic anyons in noninteracting systems*, Phys. Rev. B **101**, 115139 (2020).

U potrazi za fizikalnom realizacijom anyona, kvazičestična pobuđenja u 2D interagirajućim višečestičnim sustavima igraju glavnu ulogu [7]. Primjer kvazičestica s necjelobrojnom statistikom su pobuđenja u FQHE [23–28]. Ključni sastojci u FQHE su 2D elektroni u jakom jednolikom magnetskom polju [23] i Coulombove interakcije [24, 25]. S druge strane, Coulombove interakcije nisu potrebne za objašnjenje IQHE [97, 98]. Neki noviji primjeri realizacije anyona uključuju spinske sustave [8, 46, 51, 56] i Majorana *zero modove* [62, 63]. Zanimljivi su i eksperimenti u polju kondenzirane materije u slabom ili neinteragirajućem sustavu [67–69]. Međutim, dug je put prije nego će eksperimenti biti u mogućnosti učinkovito detektirati i manipulirati anyonima, posebno za kvantno računanje otporno na greške [7, 62]. Stoga postoji interes za istraživanjem nekih manje tradicionalnih shema za realizaciju i manipulaciju anyonima.

Motivirani IQHE, ovdje razmatramo nove mehanizme realizacije i potpisa anyona u neinteragirajućim sustavima. Prvo predlažemo eksperimentalnu realizaciju originalnog Wilczekova modela anyona u 2DEG smještenom u okomitom magnetskom polju koji pokazuje IQHE. Pokazujemo da je potpis anyona blagi pomak Hallova otpora. Nadalje predstavljamo egzaktna rješenja modela sintetičkih anyona u neinteragirajućem kvantnom višečestičnom sustavu, koji je razmatran u [67, 68]. Pokazujemo da je osnovno stanje anyonsko u koordinatama proba.

6.3.1 Kvantni Hallov efekt s kompozitima zavojnica i nabijenih čestica

U ovom radu predlažemo eksperimentalnu realizaciju originalnog Wilczekova modela Abelovih anyona, kompozita nabijenih čestica i cijevi određenog magnetskog toka [3–5]. Prvo predlažemo shemu realizacije nabijenih zavojnica, u kojoj je nabijeni objekt s intrinzičnim magnet-

skim dipolnim momentom smješten između dvaju polubeskonačnih blokova materijala s visokom permeabilnosti (μ_r), a slike magnetskog momenta stvaraju efektivnu magnetsku cijev. Ova shema dalje se koristi u određenom fizikalnom sustavu kako bi se dobio prijedlog realizacije Wilczekovih anyona. Polazišna točka jest 2D elektronski plin (2DEG) smješten u okomito jednoliko magnetsko polje koji pokazuje IQHE [97, 98]. Pretpostavimo da smjestimo 2DEG između dvaju polubeskonačnih blokova magnetskih materijala s velikom permeabilnošću μ_r, za koje se pretpostavlja da imaju brz vremenski odgovor (u području ciklotronske i Larmorove frekvencije). Elektronski spinovi (tj. magnetski dipolni momenti) bit će poravnati zbog Zeemanova efekta, dok će materijal s velikom permeabilnošću μ_r inducirati magnetsku cijev pridruženu svakom elektronu. Za ovaj sustav koristimo egzaktnu mnogočestičnu valnu funkciju. Pronalazimo potpis prisutnosti anyona u ovom sustavu - Hallovu vodljivost. Hallov otpor na platou IQHE, koji služi kao standard električnog otpora [97, 103, 104], bit će blago pomaknut. Diskutiramo moguće implementacije predloženog sustava, prepreke, i moguće načine da ih prevladamo. U ovom radu potraga za materijalima s velikim μ_r na visokim frekvencijama koja je u tijeku u polju metamaterijala i potraga za anyonima nalaze se na istom putu.

6.3.2 Egzaktna rješenja modela sintetičkih anyona u neinteragirajućem sustavu

U kontekstu manje tradicionalnih shema realizacije i manipulacije anyona, vrijedi istaknuti nekoliko primjera eksperimenata u kondenziranoj materiji, gdje je predložena sintetizacija anyona vezanjem slabo interagirajućih (ili neinteragirajućih) elektrona na topološki netrivijalnu pozadinu (ili topološki netrivijalne vanjske perturbacije) [67–69]. U ovom radu proučavamo teorijski model sintetičkih anyona u neinteragirajućem kvantnom višečestičnom sustavu. Predstavljamo egzaktna rješenja modela sintetičkih anyona, koja su razmotrena u [67, 68]. Sintetički anyoni mogu se javiti u neinteragirajućem sustavu kad je perturbiran posebno skrojenim lokaliziranim probama, koje daju traženu netrivijalnu topologiju sustava. Ovaj model predstavljen je Hamiltonijanom neinteragirajućih elektrona u 2D, u jednolikom magnetskom polju, kojeg probadaju zavojnice s magnetskim tokom koji je razlomak kvanta toka. U potencijalnoj eksperimentalnoj realizaciji modela, trebao bi postojati mehanizam koji fiksira tok u svim probama na identičnu vrijednost za ove perturbacije da bi predstavljale sintetičke anyone. Tražimo analitički osnovno stanje modela kad su popunjena samo stanja najnižeg Landauova nivoa. Računamo statistički parametar koristeći Berryjevu fazu i pokazujemo da je osnovno stanje anyonsko u koordinatama proba. Ovi rezultati potvrđeni su numerički. Iz rješenja nalazimo da se oko svake probe nalazi nedostatak elektronskog naboja Δq. Pokazujemo da se ovaj nedostatak naboja ne može identificirati s konceptom kvazičestica tako što pokazujemo da $\frac{\Delta q}{\hbar} \oint \mathbf{A} \cdot d\mathbf{l}$ ne odgovara Aharonov-Bohm fazi nakupljenoj kad proba prelazi petlju u prostoru. Kao posljedica toga što se sintetički anyoni ne mogu smatrati kvazičesticama, diskutirana su fuzijska pravila za različite mikroskopske realizacije fuzijskih procesa.

6.4 Berryjeva faza za Boseov plin na jednodimenzionalnom prstenu

Rad predstavljen u ovom poglavlju objavljen je u sljedećem radu

- M. Todorić, B. Klajn, D. Jukić, and H. Buljan, *Berry phase for a Bose gas on a one-dimensional ring*, Phys. Rev. A **102**, 013322 (2020).

1D kvantni višečestični sustavi područje su interesa matematičara i fizičara već čitavo stoljeće. Bethe je odredio egzaktno rješenje za 1D Heisenbergov model spina $\frac{1}{2}$ koristeći pretpostavku za valnu funkciju [149]. Nakon toga uslijedila su mnoga egzaktna rješenja drugih teorijskih 1D modela, uključujući rješenje Girardeaua koje opisuje neprobojni Boseov plin [150]. Jednostavni 1D modeli čija se rješenja ne mogu naći egzaktno detaljno su istraženi učinkovitim pristupima posebno prilagođenima jednoj dimenziji. Bitan primjer je model koji su uveli Lieb i Liniger, a koji opisuje sustav identičnih Boseovih čestica u 1D koje interagiraju preko interakcija oblika δ- funkcije jakosti c. Ova rješenja nisu smatrana ničim više od matematičke znatiželje koja nije važna za stvarni 3D svijet. Međutim, nedavni tehnološki napredak u zatočenju ultrahladnih atomskih plinova vodio je do eksperimentalne realizacije mnogih kvazi-1D modela, što je oživjelo zanimanje za proučavanje teorijskih 1D modela [152–155] (za pregled polja vidi [156]).

U eksperimentima, ultrahladni atomi stavljaju se u uske, transverzalno zatočene, efektivno 1D atomske valovode, gdje su transverzalna pobuđenja jako potisnuta [152–155]. Ovi atomski plinovi karakterizirani su Lieb-Liniger modelom [151] kontaktnih interakcija proizvoljne snage c. U slučaju beskonačne snage interakcije ($c \to \infty$), takve se bozonske čestice mogu opisati Tonks-Girardeau modelom [150]. Fermi-Boseovo mapiranje povezuje Tonks-Girardeau bozonsku valnu funkciju s antisimetričnom višečestičnom valnom funkcijom koja opisuje plin neinteragirajućih fermiona bez spina u 1D. Tonks-Girardeau režim eksperimentalno je postignut [153–155] s atomima na niskoj temperaturi i linearnim gustoćama, te s jakim efektivnim interakcijama [157–159]. U granici slabe interakcije, LL model može se opisati Gross-Pitaevskii teorijom [160].

Atomi kao neutralne čestice ne mogu izravno proizvesti magnetske fenomene, no srž mnogih zanimljivih fenomena, uključujući baždarnu invarijantnost ili kvantni Hallov efekt, jest vezanje nabijenih čestica i elektromagnetskih polja. Zanimljivo je, stoga, istražiti strategije stvaranja sintetičkih baždarnih polja za neutralne atome. Prva sintetička magnetska polja postignuta su u brzo rotirajućim Bose-Einsteinovim kondenzatima, gdje Coriolisova sila igra ulogu Lorentzove sile [176, 177]. Druga ideja je smještanje atomskog plina u posebno skrojeno lasersko polje, gdje se zbog atomskih interakcija sa svjetlom, lasersko polje ponaša kao umjetno magnetsko polje za neutralne atome [145, 147]. Nadalje, sintetička magnetska polja mogu se postići u optičkim rešetkama, gdje se kreiraju kompleksni matrični elementi tuneliranja između stranica rešetke [178–182].

Razvoj sintetičkih baždarnih polja otvorio je put istraživanju topoloških stanja materije u ultrahladnim atomskim sustavima [145, 147, 176–183]. Jednočestični topološki fenomeni dobro su objašnjeni [147, 183], međutim, jako interagirajući kvantni sustavi vezani za baždarna polja mogu voditi na zanimljiva korelirana topološka stanja materije koja je teško razumjeti [175]. Prirodno je stoga pitati mogu li egzaktno rješivi modeli vezani za baždarna polja dati neki dublji uvid u takva stanja.

6.4.1 Berryjeva faza za Boseov plin na 1D prstenu

U ovom radu proučavamo sustav jako interagirajućih 1D bozona na prstenu koji probada sintetička zavojnica. Preko Fermi-Bose mapiranja, ovaj sustav povezan je sa sustavom neinteragirajućih elektrona polariziranog spina zatočenih na prstenu koji probada zavojnica. Na prstenu postoji vanjska lokalizirana potencijalna barijera oblika delta funkcije $V(\phi) = g\delta(\phi - \phi_0)$. Proučavamo Berryjevu fazu pridruženu adijabatskom gibanju barijere delta funkcije oko prstena kao funkciju jakosti potencijala g i broja čestica N. Ponašanje Berryjeve faze može se objasniti preko kvantno mehaničkog reflektiranja i tuneliranja kroz barijeru koja se giba i gura čestice oko prstena.

Barijera proizvodi nedostatak u gustoći kojem se može pridružiti nedostatak naboja Δq (nedostatak gustoće) za slučaj elektrona (bozona). Pokazujemo da se Berryjeva faza (tj. Aharonov-Bohm faza) ne može poistovjetiti s veličinom $\Delta q/\hbar \oint \mathbf{A} \cdot d\mathbf{l}$. Ovo znači da se nedostatak naboja ne može identificirati kao (kvazi)šupljina. Ukazujemo na poveznicu ovog rezultata i istraživanja sintetičkih anyona u neinteragirajućim sustavima. Konačno, za bozone proučavamo slabo interagirajući režim, koji je povezan s jako interagirajućim elektronima preko Fermi-Bose dualnosti u 1D sustavima.

6.5 Zaključak

U tri prostorne dimenzije čestice se klasificiraju kao bozoni i fermioni ovisno o tome slijede li Bose-Einsteinovu ili Fermi-Diracovu statistiku. Prema vezi spina i statistike, bozoni su čestice cjelobrojnog spina, dok su fermioni čestice polucjelobrojnog spina. U dvije dimenzije kvantna statistika može biti neprekidna interpolacija između bozonske i fermionske, a čestice s takvom statistikom zovu se *anyoni* [3–5]. Karakterizirani su necjelobrojnim spinom. Mogućnost postojanja anyona posljedica je neobičnih topoloških svojstava konfiguracijskog prostora skupine identičnih 2D čestica [6]. Važnu fizikalnu realizaciju anyona predstavljaju lokalizirana kvazičestična pobuđenja u FQHE [23, 25]. Druge realizacije anyona uključuju spinske sustave koji podržavaju Kitaevljev model [8] i sustave koji podržavaju Majorana *zero* modove [62, 63]. Pored fundamentalne motivacije istraživanja anyona, ne-Abelova anyonska pobuđenja mogu se koristiti za robusno topološko kvantno računanje [7, 8].

Ova disertacija proučava nove sheme realizacije i manipulacije anyona. U prvom dijelu

predloženi su novi mehanizmi realizacije i potpisa anyona u neinteragirajućim sustavima. Prvi prijedlog jest eksperimentalna realizacija originalnog Wilczekova modela Abelovih anyona, kompozita tvorenih od nabijenih čestica i magnetskih zavojnica u 2D elektronskom plinu koji je smješten u okomitom magnetskom polju te pokazuje IQHE. Realizacija kompozita temelji se na tome da je nabijeni objekt s intrinzičnim magnetskim dipolnim momentom smješten između dva polubeskonačna bloka magnetskog materijala velike permeabilnosti, pri čemu slike magnetskog momenta stvaraju efektivnu zavojnicu. Pokazali smo da je potpis anyona blagi pomak Hallove vodljivosti koji se može eksperimentalno mjeriti. Drugi prijedlog prezentira egzakta rješenja modela sintetičkih anyona u neinteragirajućem kvantnom višečestičnom sustavu, koji je razmatran u [67, 68]. Ovaj model predstavljen je hamiltonijanom sustava neinteragirajućih elektrona u dvije dimenzije u jednolikom magnetskom polju, koji probadaju zavojnice s magnetskim tokom koji je razlomak kvanta magnetskog toka. Pronašli smo analitički i numerički osnovno stanje modela, a korištenjem Berryjeve faze izračunali smo statistički parametar i pokazali da je osnovno stanje anyonsko u koordinatama proba. Pokazano je da se sintetički anyoni ne mogu smatrati kvazičesticama.

Drugi dio usmjeren je na 1D sustav bozona vezanih za sintetička baždarna polja. Motivacija jest u tome što jako interagirajući kvantni sustavi vezani na baždarna polja mogu voditi do zanimljivih koreliranih topoloških stanja materije koja je teško razumjeti. Pitanje je stoga mogu li egzaktno rješivi 1D kvantni višečestični modeli vezani za baždarna polja dati neki uvid u jako korelirana stanja. Točnije, ovdje nas zanima dublje razumijevanje sintetičkih anyona u neinteragirajućim sustavima. Proučili smo sustav jako interagirajućih bozona smještenih na 1D prstenu koji je proboden sintetičkom zavojnicom. Na prstenu postoji vanjska lokalizirana barijera oblika δ-funkcije. Istražena je Berryjeva faza koja se javlja zbog gibanja barijere. Barijera stvara nedostatak naboja u gustoći, a pokazano je da se odgovarajući nedostatak naboja ne može poistovjetiti s kvazišupljinom. Taj rezultat povezan je s proučavanjem sintetičkih anyona u neinteragirajućim sustavima za koje je pokazano da se ne mogu smatrati kvazičesticama [204].

Bibliography

[1] G. Auletta, M. Fortunato, and G. Parisi, *Quantum Mechanics* (University Press, Cambridge, 2009).

[2] R. F. Streater and A. S. Wightman *PCT, Spin and Statistics, and All That*, (Princeton University Press, Princeton, 2000).

[3] F. Wilczek, Phys. Rev. Lett. **48**, 114 (1982).

[4] F. Wilczek, Phys. Rev. Lett. **49**, 957 (1982).

[5] F. Wilczek, *Fractional Statistics and Anyon Superconductivity*, (World Scientific, Singapore, 1990).

[6] J. Leinaas and J. Myrheim, Nuovo Cimento B **37**, 1 (1977).

[7] C. Nayak, S. H. Simon, A. Stern, M. Freedman, and S. Das Sarma, Rev. Mod. Phys. **80**, 1083 (2008).

[8] A. Kitaev, Ann. Phys. **303**, 2 (2003).

[9] A. Lerda, *Anyons: quantum mechanics of particles with fractional statistics*, (Springer-Verlag, Berlin Heidelberg, 1992).

[10] R. P. Feynman, Rev. Mod. Phys. **20**, 367 (1948).

[11] M. G. G. Laidlaw, C. M. DeWitt, Phys. Rev. D **3**, 1375 (1971).

[12] Y.-S. Wu, Phys. Rev. Lett. **52**, 2103 (1984).

[13] E. Fadell, L. Neuwirth, Math. Scand. **10**, 111 (1962).

[14] R. Fox, L. Neuwirth, Math. Scand. **10**, 119 (1962).

[15] E. Artin, Abh. Math. Sem. Hamburg **4**, 47 (1926).

[16] E. Artin, Annals of Math. **48**, 101 (1947).

[17] G. A. Goldin, R. Menikoff, D. H. Sharp, Phys. Rev. Lett. **54** 603 (1985).

[18] D. Tong, Lectures on the Quantum Hall Effect, http://www. damtp.cam.ac.uk/user/tong/qhe.html.

[19] J. D. Jackson, *Classical Electrodynamics* (John Wiley & Sons, New York, 1999).

[20] Y. Aharonov and D. Bohm, Phys. Rev. **115**, 485 (1959).

[21] A. S. Goldhaber, Phys. Rev. Lett. **36**, 1122 (1976), *ibid.* **49**, 905 (1982).

[22] Y.-S. Wu, Phys. Rev. Lett. **53**, 111 (1984).

[23] D. C. Tsui, H. L. Stormer, and A. C. Gossard, Phys. Rev. Lett. **48**, 1559 (1982).

[24] R. B. Laughlin, Phys. Rev. B **27**, 3383 (1983).

[25] R. B. Laughlin, Phys. Rev. Lett. **50**, 1395 (1983).

[26] B. I. Halperin, Phys. Rev. Lett. **52**, 1583 (1984).

[27] D. Arovas, J. R. Schrieffer, and F. Wilczek, Phys. Rev. Lett. **53**, 722 (1984).

[28] F. E. Camino, W. Zhou, and V. J. Goldman, Phys. Rev. B **72**, 075342 (2005).

[29] G. Moore and N. Read, Nucl. Phys. B **360**, 362 (1991).

[30] N. Read and E. Rezayi, Phys. Rev. B **59**, 8084 (1999).

[31] E. Ardonne and K. Schoutens, Phys. Rev. Lett. **82**, 5096 (1999).

[32] E. Ardonne, N. Read, E. Rezayi, K. Schoutens, Nucl. Phys. B **607**, 549 (2001).

[33] S. H. Simon, E. H. Rezayi, N. R. Cooper, and I. Berdnikov, Phys. Rev. B **75**, 075317 (2007).

[34] R. H. Morf, Phys. Rev. Lett. **80**, 1505 (1998).

[35] E. H. Rezayi, F. D. M. Haldane, Phys. Rev. Lett. **84**, 4685 (2000).

[36] C. Nayak, F. Wilczek, Nucl. Phys. B **479**, 529 (1996).

[37] J. K. Slingerland, F. A. Bais, Nucl. Phys. B **612**, 229 (2001).

[38] N. Read, D. Green, Phys. Rev. B **61**, 10267 (2000).

[39] D. A. Ivanov, Phys. Rev. Lett. **86**, 268 (2001).

[40] A. Stern, F. von Oppen, E. Mariani, Phys. Rev. B **70**, 205338 (2004).

[41] B. Paredes, P. Fedichev, J. I. Cirac, and P. Zoller, Phys. Rev. Lett. **87**, 010402 (2001).

[42] Y. Zhang, G. J. Sreejith, N. D. Gemelke, and J. K. Jain, Phys. Rev. Lett. **113**, 160404 (2014).

[43] M. Burrello and A. Trombettoni, Phys. Rev. Lett. **105**, 125304 (2010).

[44] E. Kapit, M. Hafezi, and S. H. Simon, Phys. Rev. X **4**, 031039 (2014).

[45] R. O. Umucalilar and I. Carusotto, Phys. Rev. A **96**, 053808 (2017).

[46] A. Y. Kitaev, Ann. Phys. (NY) **321**, 2 (2006).

[47] L.M. Duan, E. Demler, and M.D. Lukin, Phys. Rev. Lett. **91**, 090402 (2003).

[48] K. J. Pachos, Int. J. Quant. Inf. **4**, 947–954 (2006).

[49] L. Jiang, G. K. Brennen, A. V. Gorshkov, K. Hammerer, M. Hafezi, E. Demler, M. D. Lukin, and P. Zoller, Nat. Phys. **4**, 482 (2008).

[50] A. Micheli, G. K. Brennen, and P. Zoller, Nat. Phys. **2**, 341 (2006).

[51] H.-N. Dai, B. Yang, A. Reingruber, H. Sun, X.-F. Xu, Y.-A. Chen, Z.-S. Yuan, and J.-W. Pan, Nat. Phys. **13**, 1195 (2017).

[52] J. T. Barreiro, M. Müller, P. Schindler, D. Nigg, T. Monz, M. Chwalla, M. Hennrich, C. F. Roos, P. Zoller, and R. Blatt, Nature, **470**, 486 (2011).

[53] C.-Y. Lu, W.-B. Gao, O. Guhne, X.-Q. Zhou, Z.-B. Chen, and J.-W. Pan, Phys. Rev. Lett. **102**, 030502 (2009).

[54] J. K. Pachos, W. Wieczorek, C. Schmid, N. Kiesel, R. Pohlner, and H. Weinfurter, New J. Phys. **11**, 083010 (2009).

[55] Y.-P. Zhong, D. Xu, P. Wang, C. Song, Q.-J. Guo, W.-X. Liu, K. Xu, B.-X. Xia, C.-Y. Lu, S. Han, J.-W. Pan, and H. Wang, Phys. Rev. Lett. **117**, 110501 (2016).

[56] N. Janša, A. Zorko, M. Gomilšek, M. Pregelj, K. W. Krämer, D. Biner, A. Biffin, Ch. Rüegg, and M. Klanjšek, Nature Physics **14**, 786 (2018).

[57] M.H. Freedman, K. Shtengel, K. Walker, and Z. Wang, Ann. Phys. **310**, 428 (2004).

[58] P. Fendley, E. Fradkin, Phys. Rev. B **72**, 024412 (2005).

[59] M. A. Levin, and X.-G. Wen, Rev. Mod. Phys. **77**, 871 (2005).

[60] M. A. Levin, and X.-G. Wen, Phys. Rev. B **71**, 045110 (2005).

[61] K. Li, Y. Wan, L.-Y. Hung, T. Lan, G. Long, D. Lu, B. Zeng, and R. Laflamme, Phys. Rev. Lett. **118**, 080502 (2017).

[62] S. Das Sarma, M. Freedman, and C. Nayak, npj Quantum Information **1**, 15001 (2015).

[63] V. Mourik, K. Zuo, S. M. Frolov, S. R. Plissard, E. P. A. M. Bakkers, and L. P. Kouwenhoven, Science **336**, 1003 (2012).

[64] M. A. Baranov: Majorana fermions in atomic wire networks as non-Abelian anyons

[65] P. Etingof, D. Nikshych, V. Ostrik, **1** 209 2010.

[66] M. Barkeshli, P. Bonderson, M. Cheng, Z. Wang, Phys. Rev. X **4** 041035 (2014).

[67] C.Weeks, G. Rosenberg, B. Seradjeh, and M. Franz, Nat. Phys. **3**, 796 (2007).

[68] G. Rosenberg, B. Seradjeh, C.Weeks, and M. Franz, Phys. Rev. B **79**, 205102 (2009).

[69] A. Rahmani, R. A. Muniz, and I. Martin, Phys. Rev. X **3**, 031008 (2013).

[70] B. Seradjeh and M. Franz, Phys. Rev. Lett. **101**, 146401 (2008).

[71] M. T. Batchelor, X.-W. Guan, and N. Oelkers, Phys. Rev. Lett. **96**, 210402 (2006).

[72] O. Patu, V. E. Korepin, and D. V. Averin, J. Phys. A **40**, 14963 (2007).

[73] R. Santachiara and P. Calabrese, J. Stat. Mech. P06005 (2008).

[74] A. del Campo, Phys. Rev. A **78**, 045602 (2008).

[75] Y. Hao, Y. Zhang, and S. Chen, Phys. Rev. A **78**, 023631 (2008).

[76] T. Keilmann, S. Lanzmich, I. McCulloch, and M. Roncaglia, Nat. Commun. **2**, 361 (2011).

[77] G. Tang, S. Eggert, and A. Pelster, New J. Phys. **17**, 123016 (2015).

[78] S. Greschner and L. Santos,Phys. Rev. Lett. **115**, 053002 (2015).

[79] C. Sträter, S. C. L. Srivastava, and A. Eckardt, Phys. Rev. Lett. **117**, 205303 (2016).

[80] V. Lahtinen, J. K. Pachos, SciPost Phys. **3**, 021 (2017).

[81] A. Shapere, F. Wilczek, *Geometric phases in physics*, World Scientific, Singapore (1989).

[82] E. Cohen, H. Larocque, F. Bouchard, F. Nejadsattari, Y. Gefen, and E. Karimi, Nat. Rev. Phys. **1**, 437 (2019).

[83] T. Stanescu, *Introduction to Topological Quantum Matter and Quantum Computation* (CRC Press, Boca Raton, 2016).

[84] M. Berry, Phys. Today **43**, 34 (1990).

[85] S. Pancharatnam, Proc. Indian Acad. Sci. A **44**, 247 (1956).

[86] H. C. Longuet-Higgins, U.Öpik, M. H. L. Pryce,and R. A. Sack, Proc. R. Soc. Lond. A **244**, 1 (1958).

[87] M. V. Berry, Proc. R. Soc. A **392**, 45 (1984).

[88] F. Wilczek, A. Zee, Phys. Rev. Lett. **52**, 2111 (1984).

[89] Y. Aharonov, J. Anandan, Phys. Rev. Lett. **58**, 1593 (1987).

[90] J. Samuel, R. Bhandari, Phys. Rev. Lett. **60**, 2339 (1988).

[91] J. H. Hannay, J. H., J. Phys. A **18**, 221 (1985).

[92] B. Simon, Phys. Rev. Lett. **51**, 2167 (1983).

[93] M. Nakahara, *Geometry, topology, and physics* (Institute of Physics Pub, 2003).

[94] R. E. Prange, S. M. Girvin (Eds.), *The Quantum Hall effect*, (Springer-Verlag, Berlin, 1990).

[95] S. Das Sarma, A. Pinczek, *Perspectives in quantum Hall effects: Novel quantum liquids in low-dimensional semiconductor structures*, (Wiley, New York, 1997).

[96] J. P. Eisenstein, H. L. Stormer, Science **248**, 1510 (1990).

[97] K. v. Klitzing, G. Dorda, and M. Pepper, Phys. Rev. Lett. **45**, 494 (1980).

[98] R. B. Laughlin, Phys. Rev. B **23**, 5632 (1981).

[99] D. J. Thouless, M. Kohmoto, M. P. Nightingale, and M. den Nijs, Phys. Rev. Lett. **49**, 405 (1982).

[100] J. E. Avron, R. Seiler, and B. Simon Phys. Rev. Lett. **51**, 51 (1983).

[101] Q. Niu, D. J. Thouless, and Y.-S. Wu, Phys. Rev. B **31**, 3372 (1985).

[102] M. Kohmoto, Ann. Phys. (NY) **160**, 343 (1985).

[103] http://physics.nist.gov/cgi-bin/cuu/Value?rk

[104] B. Jeckelmann and B. Jeanneret, Rep. Prog. Phys. **64**, 1603 (2001).

[105] J. K. Jain, Phys. Rev. Lett. **63**, 199 (1989).

[106] J. K. Jain, *Composite Fermions* (Cambridge University Press, Cambridge, 2007).

[107] A. Lopez and E. Fradkin, Phys. Rev. B **44**, 5246 (1991).

[108] B. I. Halperin, P. A. Lee, and N. Read, Phys. Rev. B **47**, 7312 (1993).

[109] S. M. Girvin, *Introduction to the Fractional Quantum Hall Effect*, B. Douçot, V. Pasquier, B. Duplantier, and V. Rivasseau (eds), *The Quantum Hall Effect*, Progress in Mathematical Physics **45**, (Birkhäuser Basel, 2005).

[110] V. J. Goldman, B. Su, Science, **267**, 1010 (1995).

[111] L. Saminadayar, D. C. Glattli, Y. Jin, B. and Etienne, Phys. Rev. Lett. **79**, 2526 (1997).

[112] V. J. Goldman, J. Liu, A. Zaslavsky, Phys. Rev. B **71**, 153303 (2005).

[113] M. D. Johnson and G. S. Canright, Phys. Rev. B **41**, 6870 (1990).

[114] M. Greiter and F. Wilczek, Mod. Phys. Lett. B **4**, 1063 (1990); M. Greiter and F. Wilczek, Nucl. Phys. B **370**, 577 (1992).

[115] J. Grundberg, T. H. Hansson, A. Karlhede, and E. Westerberg, Phys. Rev. B **44**, 8373(R) (1991).

[116] G. V. Dunne, A. Lerda, and C. A. Trugenberger, Mod. Phys. Lett. A **6**, 2891 (1991); G. V. Dunne, A. Lerda, S. Sciuto, and C. A. Trugenberger, Nucl. Phys. **B37O**, 601 (1992).

[117] A. Khare, J. McCabe, and S. Ouvry, Phys. Rev. D **46**, 2714 (1992); A. Dasnières de Veigy and S. Ouvry, Phys. Rev. Lett. **72**, 600 (1994); S. Mashkevich and S. Ouvry, Phys. Lett. A **310**, 85 (2003).

[118] C. W. J. Beenakker and H. van Houten, Solid State Physics **44**, 1 (1991).

[119] Y.-S. Wu, Phys. Rev. Lett. **53**, 111 (1984).

[120] A. Cappelli, C. A. Trugenberger, and G. R. Zemba, Phys. Lett. B **306**, 100 (1993).

[121] V. Pasquier, *Some Remarks on the Quantum Hall Effect*, K. Iohara, S. Morier-Genoud, and B. Rèmy (eds), *Symmetries, Integrable Systems and Representations* (Springer, London, 2013).

[122] P. Schattschneider, T. Schachinger, M. Stöger-Pollach, S. Löffler, A. Steiger-Thirsfeld, K. Y. Bliokh, and F. Nori, Nat. Commun. **5**, 4586 (2014).

[123] Ikai Lo, W. C. Mitchel, R. E. Perrin, R. L. Messham, and M. Y. Yen, Phys. Rev. B **43**, 11787 (1991).

[124] J. B. Pendry, A. J. Holden, D. J. Robbins, and W. J. Stewart, IEEE Trans. Microw. Theory Tech. **47**, 2075 (1999).

[125] T. J. Yen, W. J. Padilla, N. Fang, D. C. Vier, D. R. Smith, J. B. Pendry, D. N. Basov, and X. Zhang, Science **303**, 5663 (2004).

[126] R. Merlin, Proc. Natl. Acad. Sci. USA **106**, 1693 (2009).

[127] I. Liberal, A. M. Mahmoud, Y. Li, B. Edwards, and N. Engheta, Science **355**, 1058 (2017).

[128] S. Z. Butler, S. M. Hollen, L. Cao, Y. Cui, J. A. Gupta, H. R. Gutierrez, T. F. Heinz, S. S. Hong, J. Huang, A. F. Ismach, E. Johnston-Halperin, M. Kuno, V. V. Plashnitsa, R. D. Robinson, R. S. Ruoff, S. Salahuddin, J. Shan, L. Shi, M. G. Spencer, M. Terrones, W. Windl, and J. E. Goldberger, ACS Nano **7**, 2898 (2013).

[129] G. L. Doll, J. S. Speck, G. Dresselhaus, M. S. Dresselhaus, K. Nakamura, and S.I. Tanuma, J. Appl. Phys. **66**, 2554 (1989).

[130] A. Sumiyoshi, H. Hyodo, K. Kimura, J. Phys. Chem. Solids **71**, 569 (2010).

[131] I. Lončarić, Z. Rukelj, V. M. Silkin, and V. Despoja, npj 2D Mater. Appl. **2**, 33 (2018).

[132] M. S. Dresselhaus, G. Dresselhaus, Adv. Phys. **51**, 1 (2002).

[133] T. Eknapakul, I. Fongkaew, S. Siriroj, R. Vidyasagar, J. D. Denlinger, L. Bawden, S.-K. Mo, P. D. C. King, H. Takagi, S. Limpijumnong, and W. Meevasana, Phys. Rev. B **94**, 201121 (2016).

[134] K. S. Novoselov, A. K. Geim, S. V. Morozov, D. Jiang, M. I. Katsnelson, I. V. Grigorieva, S. V. Dubonos, and A. A. Firsov, Nature **197**, 201 (2005).

[135] Y. Zhang, Y.-W. Tan, H. L. Stormer, and P. Kim, Nature **438**, 201 (2005).

[136] A. H. Castro Neto, F. Guinea, N. M. R. Peres, K. S. Novoselov, and A. K. Geim, Rev. Mod. Phys. **81**, 109 (2009).

[137] C. Si, Z. Suna, and F. Liu, Nanoscale **8**, 3207 (2016).

[138] S. Longhi and G. della Valle, Opt. Lett. **37**, 11 (2012).

[139] F. Wilczek, Phys. Rev. Lett. **49**, 957 (1982).

[140] Y. Aharonov and D. Bohm, Phys. Rev. **115**, 485 (1959).

[141] N. Mukunda and R. Simon, Ann. Phys. (NY) **228**, 205 (1993).

[142] I. Bloch, J. Dalibard, and W. Zwerger, Rev. Mod. Phys. **80**, 885 (2008).

[143] Z. Hadzibabic, P. Kruger, M. Cheneau, B. Battelier, and J. Dalibard, Nature (London) **441**, 1118 (2006).

[144] Y.-J. Lin and I. B. Spielman, J. Phys. B **49**, 183001 (2016).

[145] J. Dalibard, F. Gerbier, G. Juzeliunas, and P. Öhberg, Rev. Mod. Phys. **83**, 1523 (2011).

[146] I. Bloch, J. Dalibard, and S. Nascimbene, Nat. Phys. **8**, 267 (2012).

[147] N. Goldman, G. Juzeliunas, P. Ohberg, and I. B. Spielman, Rep. Prog. Phys. **77**, 126401 (2014).

[148] E. Jajtic, Synthetic magnetism for ultracold atomic gases, Master's thesis, University of Zagreb, 2018.

[149] H. A. Bethe, Z. Phys. **71**, 205 (1931).

[150] M. Girardeau, J. Math. Phys. **1**, 516 (1960).

[151] E. Lieb and W. Liniger, Phys. Rev. **130**, 1605 (1963); E. Lieb, Phys. Rev. **130**, 1616 (1963).

[152] F. Schreck, L. Khaykovich, K. L. Corwin, G. Ferrari, T. Bourdel, J. Cubizolles, and C. Salomon, Phys. Rev. Lett. **87**, 080403 (2001); A. Görlitz, J. M. Vogels, A. E. Leanhardt, C. Raman, T. L. Gustavson, J. R. Abo-Shaeer, A. P. Chikkatur, S. Gupta, S. Inouye, T. Rosenband, and W. Ketterle, Phys. Rev. Lett. **87**, 130402 (2001); H. Moritz, T. Stöferle, M. Kohl, and T. Esslinger, Phys. Rev. Lett. **91**, 250402 (2003); B. Laburthe Tolra, K. M. O'Hara, J. H. Huckans, W. D. Phillips, S. L. Rolston, and J. V. Porto, Phys. Rev. Lett. **92**, 190401 (2004); T. Stöferle, H. Moritz, C. Schori, M. Kohl, and T. Esslinger, Phys. Rev. Lett. **92**, 130403 (2004).

[153] T. Kinoshita, T. Wenger, and D. S. Weiss, Science **305**, 1125 (2004).

[154] B. Paredes, A. Widera, V. Murg, O. Mandel, S. Fölling, I. Cirac, G. V. Shlyapnikov, T. W. Hänsch, and I. Bloch, Nature (London) **429**, 277 (2004).

[155] T. Kinoshita, T. Wenger, and D. S. Weiss, Nature (London) **440**, 900 (2006).

[156] M. A. Cazalilla, R. Citro, T. Giamarchi, E. Orignac, M. Rigol, Rev. Mod. Phys. **83**, 1405 (2011).

[157] M. Olshanii, Phys. Rev. Lett. **81**, 938 (1998).

[158] D. S. Petrov, G. V. Shlyapnikov, and J. T. M. Walraven, Phys. Rev. Lett. **85**, 3745 (2000).

[159] V. Dunjko, V. Lorent, and M. Olshanii, Phys. Rev. Lett. **86**, 5413 (2001).

[160] L. P. Pitaevskii, Zh. Eksp. Teor. Fiz. **40**, 646 (1961) [Sov. Phys.–JETP **13**, 451 (1961)]; E. P. Gross, Nuovo Cimento **20**, 454 (1961); J. Math. Phys. **4**, 195 (1963).

[161] C. Pethick and H. Smith, Bose-Einstein Condensation in Dilute Gases (University Press, Cambridge, 2004).

[162] M. H. Anderson, J. R. Enscher, M. R. Matthews, C. E. Wieman, and E. A. Cornell, Science **269**, 198 (1995).

[163] C. C. Bradley, C. A. Sackett, J. J. Tollet, and R. G. Hulet, Phys. Rev. Lett. **75**, 1687 (1995).

[164] K. B. Davis, M.-O. Mewes, M. R. Andrews, N. J. van Druten, D. S. Durfee, D. M. Kurn, and W. Ketterle, Phys. Rev. Lett. **75**, 3969 (1995).

[165] M. Greiner, I. Bloch, O. Mandel, T.W. Hänsch, and T. Esslinger, Phys. Rev. Lett. **87**, 160405 (2001).

[166] M. Greiner, O. Mandel, T. Esslinger, T.W. Hänsch, and I. Bloch, Nature **415**, 39 (2002).

[167] M. Greiner, O. Mandel, T.W. Hänsch, and I. Bloch, Nature **419**, 51 (2002).

[168] I. Bloch, Nature Phys. **1**, 23 (2005).

[169] R. Folman, P. Krüger, J. Schmiedmayer, J. Denschlag, and C. Henkel, Adv. At. Mol. Opt. Phys. **48**, 263 (2002).

[170] J. Fortagh, S. Kraft, A. Günther, P. Trück, P. Wicke, and C. Zimmermann, Opt. Commun. **243**, 45 (2004).

[171] B. Sutherland, *Beautiful models: 70 years of exactly solved quantum many-body problems*, World Scientific Press, (2004).

[172] M. Gaudin, Phys. Rev. A **4**, 386 (1971).

[173] D. Jukić, S. Galić, R. Pezer, and H. Buljan, Phys. Rev. A, **82**, 023606 (2010).

[174] F. Dalfovo, S. Giorgini, L. P. Pitaevskii, and S. Stringari, Rev. Mod. Phys. **71**, 463 (1999).

[175] X.-G. Wen, ISRN Cond. Matt. Phys., **2013**, 198710 (2013).

[176] J. R. Abo-Shaeer, C. Raman, J. M. Vogels, and W. Ketterle, Science **292**, 476 (2001).

[177] V. Schweikhard, I. Coddington, P. Engels, V. P. Mogendorff, and E. A. Cornell, Phys. Rev. Lett. **92**, 040404 (2004).

[178] J. Struck, C. Ölschläger, M. Weinberg, P. Hauke, J. Simonet, A. Eckardt, M. Lewenstein, K. Sengstock, and P. Windpassinger, Phys. Rev. Lett. **108**, 225304 (2012).

[179] H. Miyake, G. A. Siviloglou, C. J. Kennedy, W. C. Burton, and W. Ketterle, Phys. Rev. Lett. **111**, 185302 (2013).

[180] M. Aidelsburger, M. Atala, M. Lohse, J. T. Barreiro, B. Paredes, and I. Bloch, Phys. Rev. Lett. **111**, 185301 (2013).

[181] C. J. Kennedy, W. C. Burton, W. C. Chung, W. Ketterle, Nat. Phys. **11**, 859 (2015).

[182] G. Jotzu, M. Messer, R. Desbuquois, M. Lebrat, T. Uehlinger, D. Greif, and T. Esslinger, Nature **515**, 237 (2014).

[183] N. R. Cooper, J. Dalibard, I. B. Spielman, Rev. Mod. Phys. **91**, 015005 (2019).

[184] B. T. Seaman, M. Krämer, D. Z. Anderson, and M. J. Holland, Phys. Rev. A **75**, 023615 (2007).

[185] C. Ryu, M. F. Andersen, P. Clade, V. Natarajan, K. Helmerson, and W. D. Phillips, Phys. Rev. Lett. **99**, 260401 (2007).

[186] A. Ramanathan, K. C. Wright, S. R. Muniz, M. Zelan, W. T. Hill, C. J. Lobb, K. Helmerson, W. D. Phillips, and G. K. Campbell, Phys. Rev. Lett. **106**, 130401 (2011).

[187] S. Moulder, S. Beattie, R. P. Smith, N. Tammuz, and Z. Hadzibabic, Phys. Rev. A **86**, 013629 (2012).

[188] G. E. Marti, R. Olf, and D. M. Stamper-Kurn, Phys. Rev. A **91**, 013602 (2015).

[189] K. Henderson, C. Ryu, C. MacCormick, and M. G. Boshier, New J. Phys. **11**, 043030 (2009).

[190] B. M. Garraway and H. Perrin, J. Phys. B At. Mol. Opt. Phys. **49**, 172001 (2016).

[191] K. C. Wright, R. B. Blakestad, C. J. Lobb, W. D. Phillips, and G. K. Campbell, Phys. Rev. Lett. **110**, 025302 (2013).

[192] C. Ryu, P. W. Blackburn, A. A. Blinova, and M. G. Boshier, Phys. Rev. Lett. **111**, 205301 (2013).

[193] S. Eckel, J. G. Lee, F. Jendrzejewski, N. Murray, C. W. Clark, C. J. Lobb, W. D. Phillips, M. Edwards, and G. K. Campbell, Nature (London) **506**, 200 (2014).

[194] T. Haug, H. Heimonen, R. Dumke, L. C. Kwek, and L. Amico, Phys. Rev. A **100**, 041601(R) (2019).

[195] T. Haug, R. Dumke, L. C. Kwek, and L. Amico, Quantum Sci. Technol. **4**, 045001 (2019).

[196] A. I. Yakimenko, Y. M. Bidasyuk, M. Weyrauch, Y. I. Kuriatnikov, and S. I. Vilchinskii, Phys. Rev. A **91**, 033607 (2015).

[197] D. Aghamalyan, M. Cominotti, M. Rizzi, D.Rossini, F. Hekking, A. Minguzzi, L. C. Kwek, and L. Amico, New J. Phys. **17**, 045023 (2015).

[198] D. Aghamalyan, N. Nguyen, F. Auksztol, K. Gan, M. M. Valado, P. Condylis, L. C. Kwek, R. Dumke, and L. Amico, New J. Phys. **18**, 075013 (2016).

[199] C. Schenke, A. Minguzzi, and F. W. J. Hekking, Phys. Rev. A **84**, 053636 (2011).

[200] M. Cominotti, D. Rossini, M. Rizzi, F. Hekking, and A. Minguzzi, Phys. Rev. Lett. **113**, 025301 (2014).

[201] A. Tokuno, M. Oshikawa, and E. Demler, Phys. Rev. Lett. **100**, 140402 (2008).

[202] R. Chrétien, J. Rammensee, J. Dujardin, C. Petitjean, and P. Schlagheck, Phys. Rev. A **100**, 033606 (2019).

[203] J. Polo, V. Ahufinger, F. W. J. Hekking, and A. Minguzzi, Phys. Rev. Lett. **121**, 090404 (2018).

[204] F. Lunić, M. Todorić, B. Klajn, T. Dubček, D. Jukić, and H. Buljan, Phys. Rev. B **101**, 115139 (2020).

[205] N. Mukunda and R. Simon, Ann. Phys. (N. Y.) **228**, 205 (1993).

[206] R. Resta, Rev. Mod. Phys. **66**, 899 (1994).

[207] R. Resta, J. Phys.: Condens. Matter. **12**, R107 (2000).

Chapter 7

Curriculum vitae

Marija Todorić was born on March 26th, 1993 in Split (Croatia). In 2016, she obtained her Master's degree in Physics from the Department of Physics, Faculty of Science, University of Zagreb. Since 2016 she stayed to work as a research and teaching assistant, in the group of Hrvoje Buljan. She co-authored 3 papers in journals cited in the Web of Science, being the first author on two of them. She presented her work at 7 international scientific conferences and workshops. She received the state scholarship from The Ministry of Science and Education (2012-2013) and scholarship from The Adris Foundation (2014-2016) for gifted and talented students. In 2019 the Society of University Teachers, Scholars and Other Scientists honoured her with the Annual Award for Young Scientists and Artists.

List of publications

- M. Todorić, D. Jukić, D. Radić, M. Soljačić, and H. Buljan, *Quantum Hall Effect with Composites of Magnetic Flux Tubes and Charged Particles*, Phys. Rev. Lett. **120**, 267201 (2018).

- F. Lunić, M. Todorić, B. Klajn, T. Dubček, D. Jukić, and H. Buljan, *Exact solutions of a model for synthetic anyons in noninteracting systems*, Phys. Rev. B **101**, 115139 (2020).

- M. Todorić, B. Klajn, D. Jukić, and H. Buljan, *Berry phase for a Bose gas on a one-dimensional ring*, Phys. Rev. A **102**, 013322 (2020).

Hrvoje Buljan is a Professor at the Department of Physics at the University of Zagreb. His main research interests are in optics and photonics, graphene plasmonics and ultracold atomic gases. He is a co-author of more than 70 publications, and he has been invited to give more than 40 invited talks at conferences, workshops, scientific institutes and universities around the world. He mentored more than 30 diploma theses, four defended PhD theses, and currently mentors three PhD theses. He lead grants 5MEUR project funded by the European Structural and Investment Funds (2017), Scientific Center of Excellence for Quantum and Complex Systems and Representations of the Lie Algebra (2015), Pseudomagnetic forces and fields for atoms and photons funded by the Unity through Knowledge Fund (2013), Nonlinear phenomena and wave dynamics in photonic systems funded by the Ministry of Science in Croatia (2007), and participated in others. In 1995, he was awarded Rector's Award by the Rector of the University of Zagreb. He co-authored the most cited Phys. Rev. B paper published in 2009. He is the recipient of the Annual State Award for Science, awarded by the Croatian parliament (2010).

Dario Jukić is an Assistant Professor of Physics at the Faculty of Civil Engineering at the University of Zagreb. The topics of his research include nonequilibrium dynamics of low-dimensional many-body systems, light-matter interaction in cold atomic gases, nonlinear optics, and photonics. He authored and co-authored 17 publications. He is the recipient of the Award by the Faculty of Science, University of Zagreb, for exceptional success as a student (2007). In 2009, he received annual award 'Znanost' by National Science Foundation for the best student paper in natural science.